Doctoral Dissertations   Graduate School

5-2014

Dynamic Simulations and Data Mining of Single-Leg Jump Landing: Implications for Anterior Cruciate Ligament Injury Prevention

Kristin Denise Morgan
University of Tennessee - Knoxville, kmorga12@utk.edu

To the Graduate Council:

I am submitting herewith a dissertation written by Kristin Denise Morgan entitled "Dynamic Simulations and Data Mining of Single-Leg Jump Landing: Implications for Anterior Cruciate Ligament Injury Prevention." I have examined the final electronic copy of this dissertation for form and content and recommend that it be accepted in partial fulfillment of the requirements for the degree of Doctor of Philosophy, with a major in Biomedical Engineering.

Jeffrey A. Reinbolt, Major Professor

We have read this dissertation and recommend its acceptance:

William R. Hamel, J. A. M. Boulet, Songning Zhang

Accepted for the Council:

Carolyn R. Hodges

Vice Provost and Dean of the Graduate School

(Original signatures are on file with official student records.)

Dynamic Simulations and Data Mining of Single-Leg Jump Landing: Implications for Anterior Cruciate Ligament Injury Prevention

A Dissertation Presented for the
Doctor of Philosophy
Degree
The University of Tennessee, Knoxville

Kristin Denise Morgan
May 2014

DEDICATION

To my parents

Drs. Morris and Carolyn Morgan

And my brother

Eric Morgan

ACKNOWLEDGEMENTS

ABSTRACT

It is estimated that 400,000 anterior cruciate ligament (ACL) injuries occur in the United States each year with the cost of ACL reconstruction surgery and rehabilitation exceeding $1 billion annually. The majority of ACL injuries are non-contact injuries occurring during cutting and jump landing movements. Because the majority of the injuries are non-contact injuries there is the potential to develop programs to reduce the risk of injury. Given our understanding of the joint kinematics and kinetics that place an individual at high risk for ACL, researchers have developed neuromuscular training programs that focus on improving muscle function in order to help the muscles support and stabilize the knee during the dynamic movements that increase the strain on the ACL. Yet, despite the implementation of these neuromuscular-based ACL injury training intervention programs ACL rates continue to rise. Thus the objective of this dissertation is to determine the cause and effect relationship between joint biomechanics and muscle function with respect ACL injury.

There are four studies in this dissertation. The first two studies rely heavily on the development of subject-specific musculoskeletal models to analyze muscle contribution during single-leg jump landing. These studies will generate forward dynamic simulations to estimate muscle force production and contribution to movement. The results of these studies will aid in the development of muscle-targeted ACL injury training intervention programs. The last two studies will employ data mining techniques; such as, principal component analysis (PCA) and wavelet analysis along with stability methods from control theory, to evaluate an individual's risk of ACL injury and determine how muscle function differs for individuals at varying levels of injury risk. The goal will be to use this information to develop a more robust ACL injury prescreening tool.

The use of both dynamic simulations and data mining techniques provides a unique approach to investigating the relationship between joint biomechanics and muscle function with respect to ACL injury. And this approach has the potential to gain much needed insight about the underlying mechanism of ACL injury and help progress ACL research forward.

PREFACE

This dissertation presents four studies conducted using dynamic simulations, data mining and wavelet analyses to develop more effective ACL injury intervention and prescreening programs. Each chapter is writing as a separate technical paper and an overview of the goals and methods employed in each study are provided. Additionally, each chapter provides an in-depth discussion of the study findings and how these findings were used to answer the questions posed. Chapter 6 provides a summary of the results of the four studies in the dissertation and delineates how they were applied to develop better protocols for identifying individuals at risk for ACL injury.

TABLE OF CONTENTS

LIST OF TABLES

LIST OF FIGURES

xiii

CHAPTER I

INTRODUCTION

1.1 Literature Review

1.1.1 Defining the Function of the Anterior Cruciate Ligament

The anterior cruciate ligament (ACL) is one of four ligaments in the knee. The three additional ligaments are the posterior cruciate ligament (PCL), medial collateral ligament (MCL) and the lateral collateral ligament (LCL). Together these ligaments function to stabilize the knee. The MCL and LCL are aligned along the outside of the knee with the ACL and PCL crisscrossing each other in the knee joint. The ACL connects the medial portion of the lateral femoral condyle to the distal portion of the midtibial plateau (Whiting et al., 2008) (Fig. 1). This orientation allows the ACL to resist anterior translation of the tibia with respect to the femur and maintain rotational joint stability (Whiting et al., 2008). Thus, when the ACL tears, joint (specifically rotational) stability is lost. ACL tears occur when the force/loads applied to the ACL exceeds the ligament strength (tolerance) (Donnelly et al. 2012). It was the work of previous researchers that determined the orientation and movements that placed the greatest forces/loads on the ACL and increased its risk for injury.
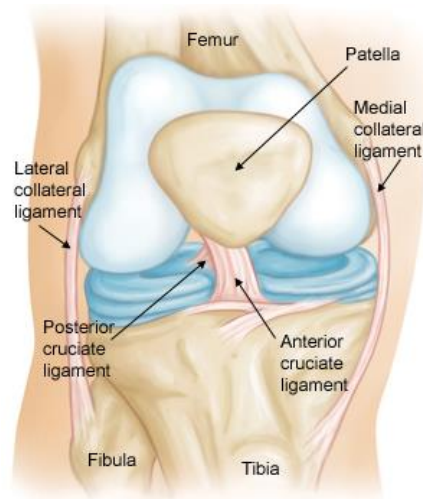
Figure 1. Front view of knee including the anterior cruciate ligament (ACL), posterior cruciate ligament (PCL), lateral collateral ligament (LCL) and medial collateral ligament (MCL). (American Academy of Orthopaedic Surgeons)

1.1.2 Cadaveric and In-vivo Analysis of ACL Strain

Cadaveric and in-vivo research provide researchers with the ability to directly measure ACL strain (forces) under a variety of loading conditions. Such research specifies the combinations of forces, torques, and moments that are applied to the ACL in the sagittal, frontal and transverse planes that increase the risk for injury (Fleming et al., 2001). Based on the ability of the ACL to resist anterior tibial translation (occurring in the sagittal plane) and tibial rotation (occurring in the transverse plane) researchers were able to evaluate loading in each plane. With respect to the sagittal plane researchers concentrated on knee flexion-extension angles, varus and valgus moments in the frontal plane and internal and external rotation torques/moments in the transverse plane. When applied in isolation, ACL strain increased when the knee is near full extension or hyperextended and experiencing valgus moments and internal rotation torques (Fleming et al., 2001; Markolf et al., 1990). Examining various loading conditions in isolation is important for determining which state has the greatest influence on ACL strain; yet, the knee

2

motion that leads to ACL injuries does not occur solely in one plane, thus researchers analyzed the effect of combined loadings on the ACL in all three planes.

Such studies analyzed the combined effect knee flexion-extension angles and knee valgus moments under compression; the combination of externally applied anterior-posterior shear force, internal-external torques and varus-valgus moments during (20° of) flexion; and the combination of anterior tibial force, varus-valgus moments and internal-external torques (Fleming et al., 2001; Markolf et al., 1995; Withrow et al., 2006). The results of these studies found that ACL strain increased nonlinearly with increasing anterior tibial force as the knee neared full extension and the force in the ACL increased 30% when under the combined effect of knee flexion and valgus loading than during flexion alone (Markolf et al., 1995; Withrow et al., 2006). Fleming et al. (2001) observed an increase in ACL strain during small flexion angles and valgus loading. The ACL force increased to 300N for the combined loading of internal rotation and anterior tibial force when the knee was hyperextended, which was twice the force under the same conditions for external tibial rotation. All of these studies showed that the ACL is under increased strain and force when the knee is near full extension and experiencing valgus (abduction) and internal rotation loading.

Cadaveric and in-vivo studies set the ground work for assessing load conditions that lead to elevated ACL strain. However, cadaveric studies are limited by their inability to measure strain in its natural environment surrounded by live, supporting musculature and in-vivo studies are limited by the number of willing participants. Thus researchers were unable to directly measure ACL strain during dynamic movements. They did nevertheless use the knowledge that ACL strain increased during increasing valgus (abduction) and internal rotation moments when

the knee was hyperflexed or near full extension to investigate during which dynamic movements (tasks) the knee was in these orientations and the ACL was greater risk of injury.

1.1.3 Kinematics and Kinetics: Biomechanical Assessment of ACL Injury Risk

Sports; such as, basketball, soccer, volleyball, Australian Rules Football, report high incidences of ACL injury (Arendt et al., 1995; Cochrane et al., 2007; DeMorat 2004). During these sports, running, cutting, sidestepping and landing are typical movements that all involve rapid transition and/or decelerations of the body (Cochrane et al., 2007; DeMorat 2004). Thus biomechanical researchers investigated joint kinematics and kinetics during these movements to determine which were more likely to place elevated strain on the ACL. A comparison of running, cutting and sidestepping tasks discovered that knee valgus and internal rotation moments were larger during cutting and sidestepping tasks than running (Besier et al., 2001). Studies of single-leg jump landing also reported increased valgus and internal rotation moments during the movement (Chappell et al., 2007; Dempsey et al., 2012; Fagenbaum et al., 2003; Ford et al., 2003). These results indicate that the sidestepping, cutting and single-leg jump landings may place the ACL under greater loading (strain, forces) than the other sports tasks. To validate if the biomechanical measurements assessed during these studies were indicative of increased ACL injury risk, researchers compared joint biomechanics between individuals who had and had not suffered an ACL injury and between female and male athletes, as females are more likely to tear their ACLs than men (Arendt et al., 1995; Hewett et al., 1999; Hewett et al., 2005). Researchers found that ACL sufferers exhibited significantly larger knee abduction angles 8° than non ACL injury sufferers and significant higher knee abduction moments (45.3±28.5Nm) than non-sufferers (18.5±15.6Nm) (Hewett et al., 2005). An investigation of female and male kinematics and kinetics during sidestepping and jump landing tasks again observed higher knee abduction

4

angles and moments in females than males (Ford et al., 2003; Ford et al., 2010;, McLean et al., 2005). One study found knee abduction moments in females (21.9±13.5Nm) were nearly twice as large as in males (13.0±12.0Nm). These and other studies indicated that sidestepping and jump landing tasks could place elevated strain on the ACL and it was also found that knee valgus/abduction moments were a strong predictor of ACL injury in individuals (Hewett et al., 2005; McLean et al. 2005).

With knee valgus/abduction moments identified as strong predictors of ACL injury and the fact that elevated knee abduction moments in combination with internal rotation moments and small knee flexion angles further increase strain on the ACL, Besier et al. (2001) decided to analyze when during the movements these biomechanical variables were the largest. Besier et al. (2001) divided the ground reaction force (GRF) profile measured during the sidestepping task into three phases: weight acceptance (WA), peak push off (PPO) and finale push off (FPO). The WA phase is defined as the time from the heel strike to the first trough, PPO is the time from 10% before and after peak GRF and the FPO is the last 15% of stance (Fig. 2) (Besier et al., 2001). Peak knee valgus moments were significantly larger during the WA and FPO phases of cutting and sidestepping than running and peak internal rotation moments were significantly larger during the WA phase for sidestepping and cutting than running. Since peak knee valgus and internal rotation moments are associated with increased ACL strain, it is possible to infer that ACL injury is more likely to occur during the WA phase of movement.
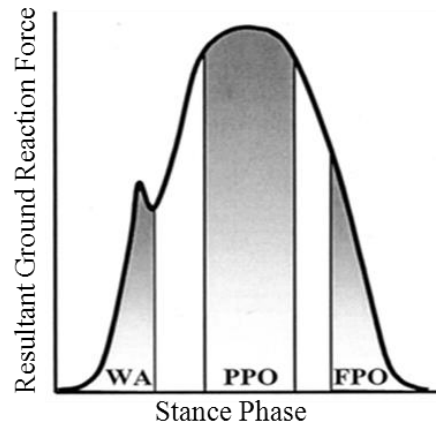
Figure 2. Schematic of the three stages of stance phase determined using the resultant ground reaction force (GRF). WA, weight acceptance; PPO, peak push off; FPO, final push off. (Besier et al., 2001)

The assessment of biomechanical variables determined that sidestepping, cutting and jump landing tasks placed individuals at higher risk for injury as the elevated knee valgus/abduction measured during the WA phase of movement these tasks were strongly correlated with ACL injury risk. Since we have determined the tasks, predictors and timing associated with ACL injury the remaining step centers on determining the role muscles play in protecting the ACL against elevated knee valgus and internal rotation moments during these tasks.

1.1.4 Electromyography (EMG): Bridging the Gap between Kinematics and Kinetics and Muscle Function

Electromyography (EMG) is utilized to gain insight into muscle function during movement. EMG studies measure muscle activity during movements associated with ACL injury to better understand how muscles support/protect the knee under dangerous loading (Lloyd et al., 2001; McLean et al., 2010; Podraza et al., 2010; Wikstrom et al., 2008). Muscle activity/function is assessed via muscle activation magnitude/amplitude, timing and co-contraction indices (CCI).

6

Muscle activation amplitude and timing relate muscle excitation coordination (temporal) patterns to movement while CCI assesses the contribution of muscle groups to see how muscle groups activate and co-contract to balance each other and stabilize the knee. How muscles function during movement, such as landing, is important because muscles and ligaments are responsible for the distribution of forces across the articular surface, which in this case is the knee (Lloyd et al., 2001). Thus increased muscle force contribution could reduce the forces (taken up by) exerted on the ligament and mitigate injury risk. Given that anterior tibial translation, small knee flexion angles, elevated knee valgus/abduction and internal rotation moments are all associated with ACL injury, researchers investigated muscle activation under these conditions to ascertain how muscles function to support and stabilize the knee during these movements (dangerous loading). Together the aforementioned metrics can be used to determine muscle contribution to movement via muscle activation measurement(s).

Besier et al. (2003) and Wikstrom et al. (2008) investigated selective muscle activation patterns during running, cutting, sidestepping and single-leg jump landing tasks. Besier et al. (2003) observed that when grouping the muscles by function (i.e. knee flexor and extensor, medial and lateral and internal-external rotators), an increase in their muscle activation was correlated with an increase in valgus and internal rotation moments during the pre-planned as opposed to unanticipated cutting and sidestepping tasks. This finding was believed to indicate that muscles selectively activate to properly execute the task and protect the knee against dangerous loadings. Wikstrom et al. (2008) examined how muscle activation patterns differ during successful and failed jump landings. EMG data was collected for the vastus medialis, semimbranosus, lateral gastrocnemius and tibialis anterior muscles 200 milliseconds (ms) pre through 200ms post landing. The results showed that muscles activated earlier and exhibited

stronger preparatory and reactive amplitudes for successful landings as opposed to failed landings. Additionally, muscles were found to activate in a different order for successful and failed landings with muscles activating in the following order for successful landings: vastus medialis, semimbranosus, lateral gastrocnemius and then the tibialis anterior muscle. The vastus medialis and semimbranosus represent the quadriceps and hamstring muscles in this study. An analysis of those two muscles showed that the vastus medialis activated 3ms before the semimbranosus and that post landing the vastus medialis was slightly more activated than the semimbranosus at 0.40 and 0.34, respectively. However, for the failed landings the semimbranosus muscle activated 16ms before the vastus medialis and there was a slightly larger discrepancy in reactive muscle activation amplitude with the vastus medialis producing 0.35 while the semimbranosus produced 0.27. This study like prior investigations highlighted that the quadriceps and hamstring muscles are critical to supporting the knee during landing. And that to successfully support the knee increased activation of the hamstring muscles could help counterbalance the increased activation of the quadriceps muscles.

Previous cadaveric studies also indicated that strong quadriceps loading was found to cause increased anterior tibial translation with respect to the femur and in turn contributed to increased ACL injury (DeMorat 2004). This result focused attention on the relationship between the quadriceps and hamstring muscles during different tasks to assess the relationship between joint biomechanics and muscle activation (Malinzak et al., 2001). Analysis of muscle activation during such events revealed that in populations at greater risk for ACL injury, individuals displayed greater quadriceps muscle activation (Malinzak et al., 2001; Wojtys et al., 2002). The greater the level of muscle activation of the quadriceps relative to the hamstrings leads to enhanced knee joint instability (Malinzak et al., 2001). A more balanced co-contraction of these

muscles reduced anterior tibial translation and helped support the knee during valgus loading (Lloyd et al., 2001; Wojyts et al., 2002). The balanced co-contraction during tasks typically indicates an increase in hamstring muscle activity to counter the strongly activated quadriceps muscles during tasks associated with ACL injury. Fujii et al. (2012) found that this increased hamstring muscle activation was correlated with smaller peak internal tibial rotation angle during single-leg jump landing. While studies have shown quadriceps-hamstring co-contraction are the main contributors to stabilizing the knee during dynamic sports tasks associated with ACL injury; Podraza et al. (2010) found that other muscles surrounding the knee may also function to stabilize the knee and improve joint stiffness. Podraza et al. (2010) evaluated muscle activation during single-leg landing task and concluded that in response to the dominant activation of the quadriceps that it is possible that the soleus and gastrocnemius muscles may play a more prominent role in countering the quadriceps activation than the hamstrings during landing. This result suggests that greater concentration should be paid to the function of all of the muscles surrounding the knee not just the quadriceps and hamstrings.

EMG is effective in evaluating muscle activity during dynamic movements but does not yield information about a muscle's relative contribution to movement, but computer simulations may provide additional insights (Anderson et al., 2006). For example, algorithms (e.g., computed muscle control) can estimate muscle forces required for the desired movement given kinematic and kinetic data (Thelen et al., 2003). To determine individual muscles contribution to movement, computational modeling that incorporates mathematical algorithms has and continues to be used to analyze muscle function during dynamic movement (Hatze et al., 1976; Thelen et al., 2003).

1.1.5 Computational Modeling: Utilizing Simulations to Assess Cause-Effect Relationship in Human Movement

Computational modeling of human movement is used to relate various aspects of the human biological system to movement. In previous decades, biomechanical models were simplistic 1- and 2- dimensional models containing fewer body segments, degrees of freedom and muscles for their analysis (Hatze et al., 1976; Hatze 1984; Hoy et al., 1990; Winter 1980). The advancements in computer technology have led to the development of more complex biomechanical models and more computationally efficient analyses (Pandy 2001).

Through computational modeling, researchers are able to develop subject-specific simulations that relate joint kinematics and kinetics to muscle force production and function. Unlike EMG analysis where muscle activation is linearly related to muscle force, simulations are able to account for the musculotendon properties; such as, muscle activation and contraction dynamics, force-length and force-velocity relationships and moment arms analysis to appropriately model non-linear relationships between muscle activation and force production. Such simulations are utilized to investigate the cause-and-effect relationship between joint motion and muscle function (Dorn et al., 2012; Hamner et al., 2010; Liu et al., 2008; Thelen et al., 2003;Thelen et al., 2006)

1.2 OpenSim and Musculoskeletal Modeling Software

Musculoskeletal modeling software programs allow users to select from a bank of models and create subject-specific simulations to explore a variety of research questions. OpenSim is such a software program that provides users with a mathematical and computational modeling framework to analyze everything from designing prosthetic devices, to studying how they will function in the body and assessing the outcomes of surgical procedures like tendon lengthening

in cerebral palsy patients. It is unique in that it is user friendly but also allows the user to increase model complexity to answer difficult problems related to human movement.

This dissertation will use high quality experimental motion capture data of individuals performing a single-leg jump landing protocol to conduct and evaluate simulation based research of muscle contribution during these jump landings. This research is divided into four studies introduced in the following section.

1.3 Overview and Specific Studies

Over 400,000 anterior cruciate ligament (ACL) injuries occur every year (Utturkar et al. 2013) in the United States costing $1.5 billion annually in ACL reconstruction and treatment (Boden et al., 2000; Kao et al., 1995). Approximately 80% of ACL injuries are non-contact injuries (Noyes et al., 1983), the majority of which occur during single-leg landings when the knee is near full extension and externally valgus loaded (Cochrane et al., 2007; Koga et al., 2010; Krosshaug et al., 2007). While clinical and experimental studies have well defined these kinematic and kinetic characteristics of ACL injury, the mechanism behind ACL injury is not well understood. Despite the implementation of ACL injury prevention programs, there has been a 50% increase in ACL injuries reported over the last decade (Donnelly et al., 2012), Such programs are aimed at altering muscle force and activation patterns to circumvent the ACL injury mechanism; however, they are limited by their inability to assess individual muscle function (e.g. force, activation) to resist excessive knee loading during movement. Our long-term goal is to determine individual muscle function during jump landing in order to dramatically reduce the rate of ACL injury through the implementation of muscle-targeted prevention programs.

Musculoskeletal models and dynamic simulations have been used to determine individual muscle contributions to pedaling, walking and running (Liu et al., 2006; Liu et al., 2008; Hamner et al., 2010; Thelen et al., 2003); yet, none have assessed individual muscle contributions to jump landing. Here muscle-actuated dynamic simulations will be used to determine the joint accelerations induced by individual muscles, to identify the muscles that resist excessive knee abduction moments in individuals at high risk of ACL injury. We hypothesize that increased force generation of the quadriceps and medial and lateral gastrocnemius muscles will serve to resist excessive knee abduction moments during single-leg jump landing and help mitigate ACL injury risk after proposed muscle-targeted training intervention programs. The findings from the dynamic simulations will be integrated with the findings from the data mining techniques to identify individuals at risk for ACL injury. All of this information will then be utilized to design muscle-targeted training intervention programs to reduce excessive knee abduction moments.

Each of the next four chapters of the dissertation will present four distinct studies conducted using dynamic simulations, data mining and wavelet analyses to develop a protocol to identify and train individuals at risk for ACL injury as highlighted above. Each chapter is written as a separate technical paper and an overview of the goals and methods employed in each study are provided below. In addition, each chapter includes an in-depth discussion of the proposed methods and findings of each study and demonstrated how they were used to answer the questions posed. Chapter 6 gives a summary of the results of the four studies in the dissertation and delineates how they were applied to develop better protocols for identifying individuals at risk for ACL injury.

1.3.1 Study 1: Elevated Gastrocnemius Forces Compensate for Decreased Hamstrings Forces during the Weight-Acceptance Phase of Single-Leg Jump Landing: Implications for ACL

Goal: The purpose is to answer the following questions:

1) What are the individual muscle forces generated to successfully perform a single-leg jump landing?

2) Which muscles serve as the main contributors for supporting the knee during landing?

Methods: To accomplish this study, subject-specific muscle-actuated simulations will reproduce experimentally measured landing kinematics and kinetics of seven subjects. For each simulation, individual muscles forces will be estimated using a computed muscle control (CMC) during single-leg jump landing.

Significance: This investigation will clarify how individual muscles generate force to dynamically support the knee during single-leg jump landing.

1.3.2 Study 2: Assess How Individual Muscles Resist Elevated Knee Abduction Moment during Single-Leg Jump Landing.

Goal: The purpose is to address the questions:

1) Which muscle(s) produce the greatest acceleration to resist elevated knee abduction moment?

Methods: The subject-specific muscle-actuated simulations and resulting muscle force data from generated from CMC will serve as inputs for induced acceleration analysis to quantify which muscles function to resist knee abduction moment during jump landing.

Significance: This work will enable researchers to determine which individual muscles are specifically responsible for resisting knee abduction moment during single-leg jump landing and how they can potentially reduce ACL injury risk.

1.3.3 Study 3: Dynamic Knee Stability and Principal Component Analysis: Methodology for Assessing Anterior Cruciate Ligament Injury Risk.

Goal: The purpose is to address these questions:

1) What is dynamic knee stability?

2) What underlying muscle activation patterns are common amongst individuals at elevated risk for ACL injury?

Methods: We will utilize Nyquist and Bode stability criterions, in conjunction with principal component analysis, to explore the experimentally measured kinematic, kinetic and surface EMG data for critical features and underlying muscle activation patterns that may be associated with individuals at-risk for injury.

Significance: This work will provide us with ability to develop new metrics to identify individuals at-risk for ACL injury and design muscle-targeted training programs.

1.3.4 Study 4: Utilizing Stability and Wavelet Analyses to Detect Muscle Activation Patterns Associated with ACL Injury Risk.

Goal: The purpose of Study 4 is to answer the following questions:

1) What are unstable joint biomechanics?

2) What underlying muscle activation patterns are common amongst individuals at elevated risk for ACL injury?

Methods: Stability and wavelet analysis will be employed to explore the experimentally measured kinematic, kinetic and surface EMG data for critical features and underlying muscle activation patterns that may be correlated with individuals at-risk for injury.

Significance: This work will identify muscle activation patterns specific to individuals at-risk for ACL injury.

Together, these studies will determine the roles muscles play in supporting the knee and direct future research for designing more effective training protocols. The mechanisms behind ACL injury are exceptionally complex; yet, by isolating critical features and muscle activation patterns common amongst individuals at elevated risk for ACL injury via principal component and wavelet analysis it may indicate how muscles function differently to support the knee in individuals at-risk for ACL injury. This knowledge is an important and necessary step toward both understanding and designing muscle-targeted training protocols that reduce ACL injury risk.

1.4 References

Anderson, F.C., Arnold, A. S., Pandy, M. G., Goldberg, S. R., Delp S. L., 2006. Simulations in Walking. 3 ed, Wilkins.

Jolliffe, I.T., 2002. Principal Component Analysis, 2nd Ed Springer, New York.

Arendt, E., Dick, R., 1995. Knee injury patterns among men and women in collegiate basketball and soccer NCAA data and review of literature. The American Journal of Sports Medicine 23, 694-701.

Besier, T. F., Lloyd, D. G., Cochrane, J. L., Ackland, T. R. 2001. External loading of the knee joint during running and cutting maneuvers. *Medicine and Science in Sports and Exercise*, *33*(7), 1168-1175.

Besier, T.F., Lloyd, D.G., Ackland, T.R., 2003. Muscle activation strategies at the knee during running and cutting maneuvers. Med. Sci. Sports Exerc. 35, 119-127.

Boden, B.P., Griffin, L.Y., Garrett, W.E., 2000. Etiology and prevention of noncontact ACL injury Physician Sportsmed. 28, 53-60.

Chappell, J.D., Creighton, R.A., Giuliani, C., Yu, B., Garrett, W.E., 2007. Kinematics and electromyography of landing preparation in vertical stop-jump: risks for noncontact anterior cruciate ligament injury. Am. J. Sports Med. 35, 235-241.

Cochrane, J.L., Lloyd, D.G., Buttfield, A., Seward, H., McGivern, J., 2007. Characteristics of anterior cruciate ligament injuries in Australian football. J. Sci. Med. Sport 10, 96-104.

DeMorat, G., 2004. Aggressive Quadriceps Loading Can Induce Noncontact Anterior Cruciate Ligament Injury. Am. J. Sports Med. 32, 477-483.

Dempsey, A.R., Elliott, B.C., Munro, B.J., Steele, J.R., Lloyd, D.G., 2012. Whole body kinematics and knee moments that occur during an overhead catch and landing task in sport. Clin. Biomech. (Bristol, Avon) 27, 466-474.

Donnelly, C.J., Elliott, B.C., Ackland, T.R., Doyle, T.L., Beiser, T.F., Finch, C.F., Cochrane, J.L., Dempsey, A.R., Lloyd, D.G., 2012. An anterior cruciate ligament injury prevention framework: incorporating the recent evidence. Res. Sports Med. 20, 239-262.

Dorn, T.W., Y.C. Lin, and M.G. Pandy, 2012. Estimates of muscle function in human gait depend on how foot-ground contact is modelled. Comput Methods Biomech Biomed Engin. 15(6), 657-68.

Fagenbaum, R., Darling, W.G., 2003. Jump landing strategies in male and female college athletes and the implications of such strategies for anterior cruciate ligament injury. Am. J. Sports Med. 31, 233-240.

Fleming, B. C., Renstrom, P. A., Beynnon, B. D., Engstrom, B., Peura, G. D., Badger, G. J., Johnson, R. J., 2001.The effect of weightbearing and external loading on anterior cruciate ligament strain. Journal of Biomechanics. 34, 163-170.

Ford, K. R., Shapiro, R., Myer, G. D., Van Den Bogert, A. J., & Hewett, T. E., 2010. Longitudinal sex differences during landing in knee abduction in young athletes. Med Sci Sports Exerc. 42(10),1923-31.

Ford, K.R., G.D. Myer, T.E. Hewett, 2003. Valgus knee motion during landing in high school female and male basketball players. Med Sci Sports Exerc. 35(10), 1745-50.

Fujii, M., H. Sato, N. Takahira, 2012. Muscle activity response to external moment during single-leg drop landing in young basketball players: The importance of biceps femoris in reducing internal rotation of knee during landing. Journal of Sports Science & Medicine. 11, 255-259.

Hamner, S.R., Seth, A., Delp, S.L., 2010. Muscle contributions to propulsion and support during running. J. Biomech. 43, 2709-2716.

Hatze, H., 1976. The Complete Optimization of Human Motion. Mathematical Biosciences. 28, 99-135.

Hatze, H.,1984. Quantitative Analysis, Synthesis and Optimization of Human Motion. Human Movement Science. 3, 5-25.

Hewett, T.E., Myer, G.D., Ford, K.R., Heidt, R.S., Jr., Colosimo, A.J., McLean, S.G., van den Bogert, A.J., Paterno, M.V., Succop, P., 2005. Biomechanical measures of neuromuscular control and valgus loading of the knee predict anterior cruciate ligament injury risk in female athletes: a prospective study. Am. J. Sports Med. 33, 492-501.

Hewett, T. E., Lindenfeld, T. N., Riccobene, J. V., & Noyes, F. R. (1999). The Effect of Neuromuscular Training on the Incidence of Knee Injury in Female Athletes A Prospective Study. The American Journal of Sports Medicine, 27(6), 699-706.

Hoy, M.G., F.E. Zajac, M.E. Gordon, 1990. A musculoskeletal model of the human lower extremity: the effect of muscle, tendon, and moment arm on the moment-angle relationship of musculotendon actuators at the hip, knee, and ankle. J. Biomech. 23(2), 157-69.

Kao, J. T., Giangarra, C. E., Singer, G., Martin, S., 1995. A comparison of outpatient and inpatient anterior cruciate ligament reconstruction surgery. Arthroscopy: The Journal of Arthroscopic & Related Surgery, 11(2), 151-156.

Koga, H., Nakamae, A., Shima, Y., Iwasa, J., Myklebust, G., Engebretsen, L., Bahr, R., Krosshaug, T., 2010. Mechanisms for noncontact anterior cruciate ligament injuries: knee joint kinematics in 10 injury situations from female team handball and basketball. Am. J. Sports Med. 38, 2218-2225.

Krosshaug, T., Nakamae, A., Boden, B.P., Engebretsen, L., Smith, G., Slauterbeck, J.R., Hewett, T.E., Bahr, R., 2007. Mechanisms of anterior cruciate ligament injury in basketball: video analysis of 39 cases. Am. J. Sports Med. 35, 359-367.

Liu, M. Q., Anderson, F. C., Schwartz, M. H., Delp, S. L., 2008. Muscle contributions to support and progression over a range of walking speeds. J. Biomech, 41(15), 3243-3252.

Liu, M. Q., Anderson, F. C., Pandy, M. G., Delp, S. L., 2006. Muscles that support the body also modulate forward progression during walking. J. Biomech, 39(14), 2623-2630.

Lloyd, D.G., Buchanan, T.S., 2001. Strategies of muscular support of varus and valgus isometric loads at the human knee. J. Biomech. 34, 1257-1267.

Malinzak, R. A., Colby, S. M., Kirkendall, D. T., Yu, B., Garrett, W. E., 200. A comparison of knee joint motion patterns between men and women in selected athletic tasks. Clin Biomechanics, 16(5), 438-445.

Markolf, K. L., Burchfield, D. M., Shapiro, M. M., Shepard, M. F., Finerman, G. A., Slauterbeck, J. L., 1995. Combined knee loading states that generate high anterior cruciate ligament forces. Journal of Orthopaedic Research, 13(6), 930-935.

Markolf, K. L., Gorek, J. F., Kabo, J. M., Shapiro, M. S.,1990. Direct measurement of resultant forces in the anterior cruciate ligament. An in vitro study performed with a new experimental technique. The Journal of Bone & Joint Surgery, 72(4), 557-567.

McLean, S.G., Huang, X., van den Bogert, A.J., 2005. Association between lower extremity posture at contact and peak knee valgus moment during sidestepping: implications for ACL injury. Clin. Biomech. (Bristol, Avon) 20, 863-870.

McLean, S.G., B. Borotikar, and S.M. Lucey, 2010. Lower limb muscle pre-motor time measures during a choice reaction task associate with knee abduction loads during dynamic single leg landings. Clin Biomech (Bristol, Avon). 25(6), 563-9.

Noyes, F. R., Matthews, D. S., Mooar, P. A., Grood, E. S., 1983. The symptomatic anterior cruciate-deficient knee. Part II: the results of rehabilitation, activity modification, and counseling on functional disability. The Journal of bone and joint surgery. American volume, 65(2), 163.

Onyshko, S., and Winter, D. A., 1980. A mathematical model for the dynamics of human locomotion. J. Biomech. 13(4), 361-368.

Pandy, M.G., 2001. Computer modeling and simulation of human movement. Annu Rev Biomed Eng. 3, 245-73.

Podraza, J.T., White, S.C., 2010. Effect of knee flexion angle on ground reaction forces, knee moments and muscle co-contraction during an impact-like deceleration landing: implications for the non-contact mechanism of ACL injury. Knee 17, 291-295.

Thelen, D.G., Anderson, F.C., Delp, S.L., 2003. Generating dynamic simulations of movement using computed muscle control. J. Biomech. 36, 321-328.

Thelen, D.G., Anderson, F.C., 2006. Using computed muscle control to generate forward dynamic simulations of human walking from experimental data. J. Biomech. 39, 1107-1115.

Utturkar, G. M., Irribarra, L. A., Taylor, K. A., Spritzer, C. E., Taylor, D. C., Garrett, W. E., and DeFrate, L. E., 2013. The effects of a valgus collapse knee position on in vivo ACL elongation. Annals of biomedical engineering, 41(1), 123-130.

Whiting, W.C. and R.F. Zernicke, *Biomechanics of Musculoskeletal Injury*. 2008, United States of America: Human Kinetics.

Wikstrom, E.A., Tillman, M.D., Schenker, S., Borsa, P.A., 2008. Failed jump landing trials: deficits in neuromuscular control. Scand. J. Med. Sci. Sports 18, 55-61.

Withrow, T. J., Huston, L. J., Wojtys, E. M., & Ashton-Miller, J. A., 2006. The effect of an impulsive knee valgus moment on in vitro relative ACL strain during simulated jump landing. Clin. Biomech. (Bristol, Avon), 21(9), 977-983.

Wojtys, E.M., Ashton-Miller, J.A., Huston, L.J., 2002. A gender-related difference in the contribution of the knee musculature to sagittal-plane shear stiffness in subjects with similar knee laxity. J. Bone Joint Surg. Am. 84-A, 10-16.

CHAPTER II

ELEVATED GASTROCNEMIUS FORCES COMPENSATE FOR DECREASED HAMSTRINGS FORCES DURING THE WEIGHT-ACCEPTANCE PHASE OF SINGLE-LEG JUMP LANDING: IMPLICATIONS FOR ACL INJURY RISK

2.1 Abstract

Approximately 320,000 anterior cruciate ligament (ACL) injuries in the U.S. each year are non-contact injuries, with most occurring during a single-leg jump landing or sidestepping sports tasks when the knee is near full extension. To reduce ACL injury risk, one option deserving further investigation is to improve muscle strength and/or activation patterns to support the knee under elevated external loading. This study's purpose was to characterize the relative force production of muscles supporting the knee during the weight-acceptance (WA) phase of single-leg jump landing and investigate the gastrocnemii forces compared to the hamstring forces. Amateur male Western Australian Rules Football players completed a single-leg jump landing protocol and seven participants were randomly chosen for further modeling and simulation. A three-dimensional, 14-segment, 37 degree-of-freedom, 92 muscle-tendon actuated model was created for each participant in OpenSim 1.9.1. Computed muscle control was used to generate 14 muscle-driven simulations, 2 trials per participant, of the WA phase of single-leg jump landing. A one-way ANOVA and Tukey post-hoc analysis showed both the quadriceps and gastrocnemii muscle force estimates were significantly greater than the hamstrings ($p < 0.001$). Elevated quadriceps and gastrocnemii forces during landing may represent a generalized muscle support strategy to: 1) produce a support moment in the stance limb and 2) increase knee joint stiffness, protecting the knee and ACL from external knee loading and injury risk. These results not only contribute to our understanding of muscle function during single-leg jump landing, but also serve as the foundation for novel muscle-targeted training intervention programs to reduce ACL injuries.

2.2 Introduction

Over 400,000 anterior cruciate ligament (ACL) injuries occur annually in the U.S. (Utturkar et al., 2013) despite decades of research and development of injury prevention protocols (Donnelly et al., 2012a). ACL healthcare costs the U.S. approximately $1.5 billion annually (Boden et al., 2000; Kao et al., 1995). Approximately 80% of ACL injuries are non-contact, with most occurring during single-leg jump landing or sidestepping sports tasks (Cochrane et al., 2007; Koga et al., 2010; Krosshaug et al., 2007). During a single-leg jump landing with the knee near full extension, the application of externally applied translational forces coupled with valgus and internal rotation knee moments elevates the forces on the ACL to injurious thresholds (>2000 N) greater than when these loads are applied in isolation (Hagood et al., 1990; Markolf et al., 1995; Markolf et al., 1998; McLean et al., 2004; McLean et al., 2005, 2008; Podraza and White, 2010; Walla et al., 1985, Woo et al., 1991). There are effectively two avenues to reduce ACL injury risk: 1) change an athlete's technique to reduce joint loading and/or 2) improve muscle strength and/or activation patterns to stabilize and support the knee (Donnelly et al., 2012a). Most preventative training protocols focus on reducing externally applied knee loads and/or increasing support of muscles crossing the knee when loading is elevated to mitigate ACL strain and injury risk. With ACL injury rates increasing 50% over the past decade (Donnelly et al., 2012a), it appears prevention research is not effectively translating into injury prevention practice among heterogeneous community-level athletic populations (Donnelly et al., 2012a).

The roles muscles play in stabilizing the knee during landing are not well understood. A byproduct of the primary motor control task goal, which is to generate a support moment keeping the center of mass (CoM) upright, is the co-contraction of the quadriceps and hamstrings

muscles, which is believed to be essential to stabilizing the knee during dynamic movements, specifically with regard to ACL injury. However, recent literature has shown that the gastrocnemii muscles may play an increased role in stabilizing the knee during landing (Mokhtarzadeh et al., 2013; Podraza and White, 2010). In addition to small knee flexion angles and elevated valgus and internal rotation moments, increased anterior tibial translation is also associated with increased ACL injury risk (Hewett et al., 2007; Pflum et al., 2004; Podraza and White, 2010). While increased quadriceps force increases anterior tibial translation, it has been shown that hamstrings as well as the gastrocnemii and soleus muscles can reduce anterior tibial translation and potentially reduce ACL injury risk (Fleming et al., 2001; Hewett et al., 2007; Pflum et al., 2004; Podraza and White, 2010, Sherbondy et al., 2003). Furthermore, moderate hamstrings activation compared to quadriceps activation has been linked to elevated knee valgus and internal rotation moments which are often predictors of ACL injury risk (Donnelly et al., 2012a; Hewett et al., 2006; Hewett et al., 2005; Wojtys et al., 2002). Thus, it is possible that elevated gastrocnemii force could function to replace and/or work in conjunction with the hamstrings to reduce harmful knee flexor-extensor imbalance and potential ACL injury risk.

There are limitations to using electromyography alone to determine biomechanical factors elevating ACL injury risk. Surface electromyography (sEMG) has been used to estimate muscle activation, where muscle force and function during sports tasks is then inferred (Besier et al., 2003; Lloyd and Buchanan, 2001; Wikstrom et al., 2008). As the joint kinematics change during these tasks, so does the force and moment generating capacity of the muscles to help support the knee and ACL from external loading. Yet, sEMG measurements do not account for muscle architecture, force-length-velocity relationships or muscle moment arm geometry during dynamic movements. A gap exists in estimating muscle forces, and more importantly functions,

22

during these tasks. Muscle-actuated, forward dynamic simulation is an *in-silico* computational tool bridging this gap, providing valuable insights into the roles individual muscles play during dynamic movements (Seth et al., 2011; Thelen and Anderson, 2006; Thelen et al., 2003). This tool has been used to analyze muscle contributions during dynamic movements such as walking, cycling, running, sidestep cutting and landing tasks and, in combination with sEMG, may be used to investigate single-leg jump landing (Arnold et al., 2007; Hamner et al., 2010; Laughlin et al., 2011; Thelen et al., 2003; Weinhandl et al., 2013).

This study used dynamic simulation, in combination with motion capture data, to investigate the important role lower limb muscles crossing the knee play in mitigating ACL injury risk during single-leg jump landing. The objective of this work was to characterize the force production of the muscles supporting the knee during the weight-acceptance (WA) phase of single-leg jump landing. It is hypothesized that the gastrocnemii will produce forces comparable to that of the hamstrings to counteract the quadriceps muscle forces to help support and stabilize the knee. With this information, our understanding of muscle function in single-leg jump landing will increase so researchers/clinicians may effectively target these muscles in developing preventative training protocols to reduce ACL injury risk and see ACL focused research translated into injury prevention practice.

2.3 Methodology

2.3.1 Experimental Protocol and Data Collection

Thirty-four Amateur male Western Australian Rules Football players were recruited to perform a single-leg jump landing experimental protocol (Donnelly et al., 2012c). Seven participants (age 20.7 ± 1.8 years; height 1.9 ± 0.1m; mass 87.8 ± 5.1 kg) were randomly selected from the cohort and two trials per participant for a total of 14 experimental trials were chosen for

further subject-specific modeling and dynamic simulation analysis. Participants were instructed to jump from their preferred leg (the right leg for participants presented here) and, while in flight, grab an Australian rules football randomly swung medially, laterally or held central relative to the participants approach direction (Dempsey et al., 2012). The ball height was approximately 90% of each participant's maximal vertical jump height. Participants were instructed to land with the same leg from which they jumped upon a force platform. Of the 14 jump landing trials analyzed in this study, 9 trials were assessed when the ball was swung laterally, 3 medially and 2 where the ball remained in the center. All experimental procedures were approved by the Human Research Ethics Committee and all participants provided their informed written consent prior to data collection.

Fifty-six upper- and lower-body retro-reflective markers were utilized to capture kinematic trajectories (Donnelly et al., 2012b). Marker trajectories were recorded at 250 Hz using a 12-camera Vicon MX motion capture system (VICON Peak, Oxford Metrics Ltd., UK) (Dempsey et al., 2007; Donnelly et al., 2012c). GRF data were synchronously recorded at 2,000 Hz using an AMTI (Advanced Mechanical Technology Inc., Watertown, MA) 1.2 x 1.2m force platform. Both the kinematic and GRF data were low-pass filtered using a zero phase-shift, 4th-order Butterworth filter with a cutoff frequency of 20 Hz in Workstation (ViconPeak, Oxford Metrics Ltd., UK). The sEMG data were synchronously collected at 2,000 Hz for six muscles: vastus medialis, vastus lateralis, medial and lateral gastrocnemii and medial and lateral hamstrings. The raw experimental sEMG data were band-pass filtered using a zero phase-shift, 4th-order Butterworth filter with a band-pass filter at cutoff frequencies of 30 and 500 Hz, full wave rectified and then low-pass filtered using a zero phase-shift, 4th-order Butterworth filter at a cutoff frequency of 6 Hz to create linear envelopes. Following linear enveloping, peak muscle

activation from each muscle recorded during the protocol was used to normalize each muscle's sEMG signal.

2.3.2 Subject-Specific Models and Simulations

Seven three-dimensional, 14-segment, 37 degree-of-freedom (DoF), 92 muscle-tendon actuated subject-specific models were created in OpenSim 1.9.1 to generate simulations of each participant performing the single-leg jump landing task (Fig. 3). The details of this model have been described previously (Donnelly et al., 2012c). The 92 muscle-tendon units actuated the lower extremity and lower back joint, while the arms were actuated by torque actuators instead of muscle-tendon actuators also described previously (Hamner et al., 2010). The maximum isometric force of each muscle was increased by 60% compared to the model provided in OpenSim (Delp et al., 1990) based on research by Arnold et al. (2010). The model included a 3 DoF knee actuated by muscles and ideal torque actuators (±50Nm) which were used to provide the resistance supplied by the knee ligaments and articular surface that help stabilize the knee in the frontal plane. These values are consistent with previous literature (Seedhom et al., 1972; Zhao et al., 2007). Subject-specific joint centers were derived using functional knee and hip joint methods (Besier et al., 2003), custom biomechanical models in MATLAB (MATLAB 7.8, The MathWorks, Inc., Natick Massachusetts, USA) and Vicon Bodybuilder (Dempsey et al., 2007). The resulting joint centers, marker trajectories and GRF data were then exported to OpenSim 1.9.1. Segment lengths were scaled to each participant's specific joint centers and segment masses to each participant's total body mass (detailed in Appendix 2.7.1). Inverse kinematics (IK) was used to derive simulated joint angles from the experimental marker data recorded during the jump landing (detailed in Appendix 2.7.2). Residual reduction analysis (RRA) was used to create simulations that were dynamically consistent with the experimentally recorded ground reaction

forces (Delp et al., 2007; Donnelly et al., 2012c) (detailed in Appendix 2.7.3). Muscle forces were estimated for the weight-acceptance (WA) phase of single-leg jump landing using computed muscle control (CMC). CMC is an algorithm that utilizes optimization, forward dynamics and feedback control to estimate individual muscle forces during dynamic movements (Thelen and Anderson, 2006; Thelen et al., 2003) (detailed in Appendix 2.7.4).

Figure 3. Series of images showing one of the seven participants and his subject-specific model performing the single-leg jump landing protocol: 1) jump from preferred leg; 2) attempt contact with a football at approximately 90% of vertical jump height and randomly moved relative to jump path; 3) contact force platform with the same leg used for jump. Three-dimensional, 14-segment, 37 degree-of-freedom and 92 muscle-tendon actuated subject-specific simulations were created in OpenSim 1.9.1 from the experimentally measured kinematic and ground reaction force data to estimate the lower extremity muscle forces during the weight-acceptance phase of the landing.

The WA phase was defined as the time from the initial contact to the end of peak loading in the vertical ground reaction force profile (Fig. 4) (Dempsey et al., 2007). The WA phase was

analyzed as this phase is thought to be when the ACL is at the greatest risk for injury (Dempsey et al., 2007; Donnelly et al., 2012a).
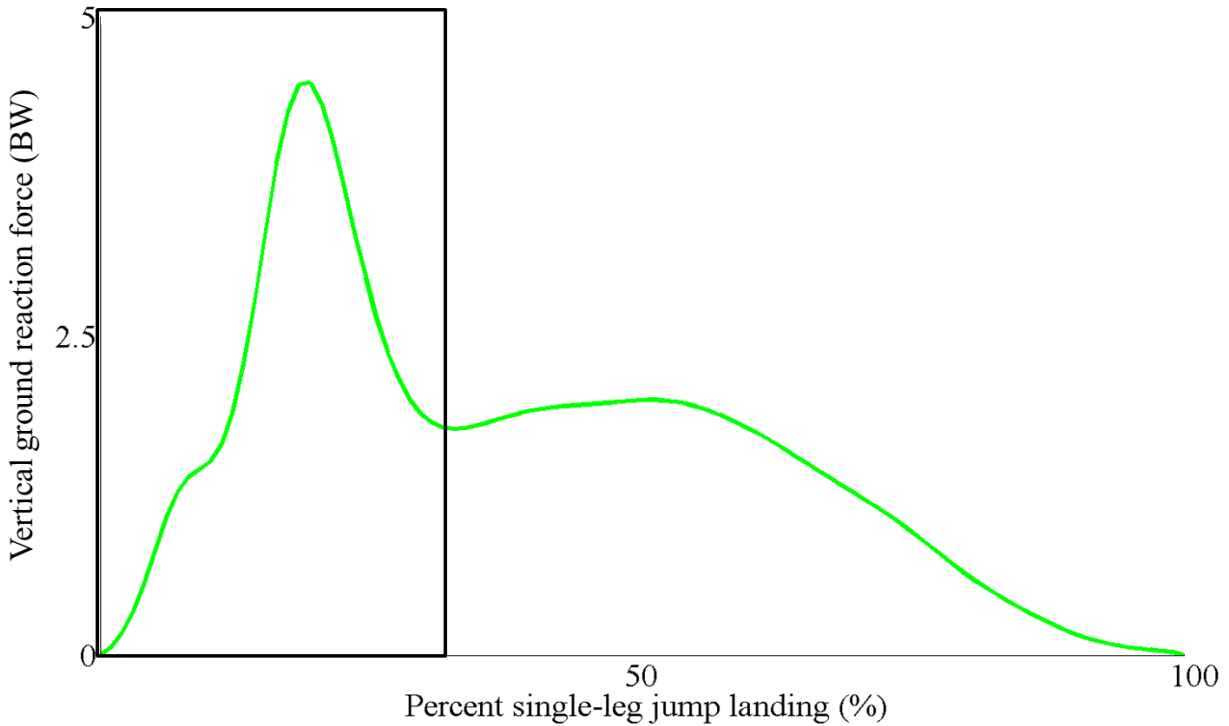
Figure 4. Vertical ground reaction force (vGRF) for an individual for a single-leg jump landing. The black box represents the weight-acceptance phase of the landing.

2.3.3 Muscle Force Estimates during Single-leg Jump Landing

Muscle force estimates for nine muscles crossing the knee and the soleus were analyzed to determine their contribution during the WA phase of single-leg jump landing. The mean normalized maximum muscle forces for the nine muscles (vastus medialis, vastus lateralis, vastus intermedius, rectus femoris, biceps femoris, semitenidnosus, semimbranosus, medial gastrocnemius, lateral gastrocnemius) crossing the knee and the soleus were analyzed individually and in groups of functional relevance (i.e., quadriceps, hamstrings and gastrocnemii) (Fig. 5). The time to reach maximum muscle force for the quadriceps, hamstrings and gastrocnemii muscle groups relative to the time to peak vertical GRF were also calculated. One-way ANOVAs were

27

conducted to compare the mean individual maximum muscle force estimates, the means of each muscle group and the mean time of the maximum force production with respect to the time to peak vertical GRF. A Tukey post-hoc analysis was performed to determine if differences observed in the one-way ANOVA analysis were significant ($\alpha = 0.05$).
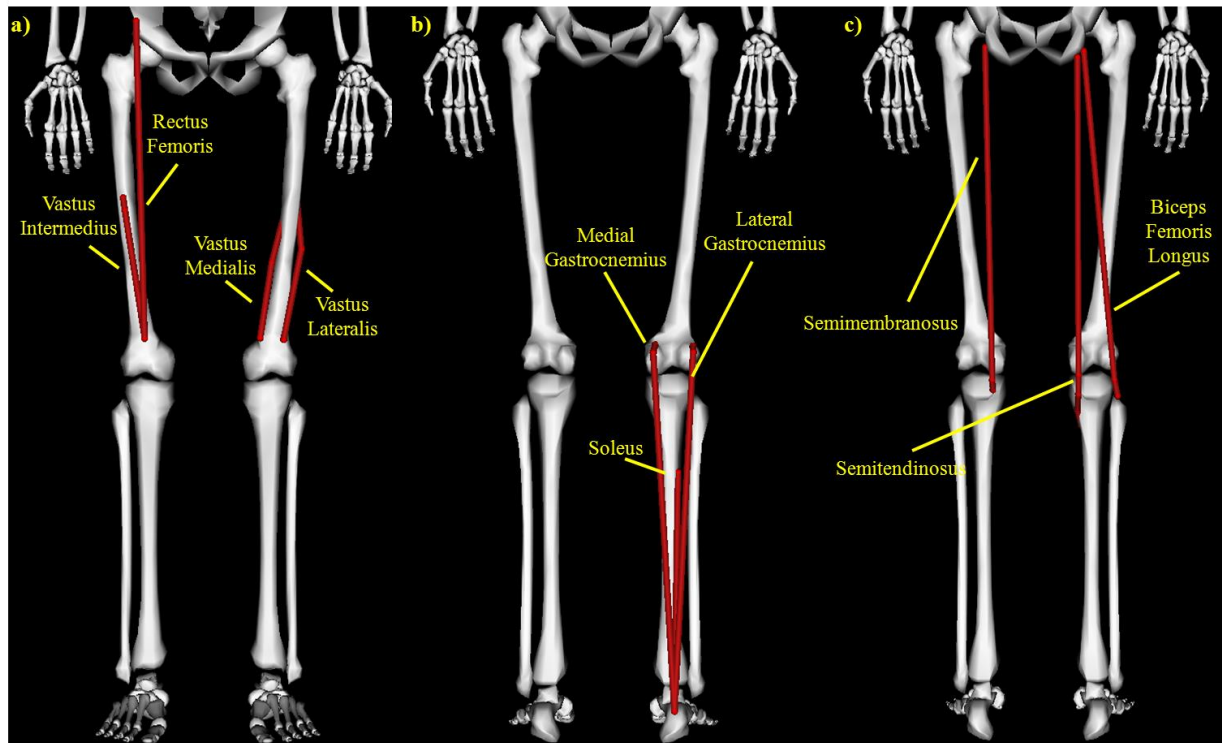
Figure 5. Lower extremity muscles. a) The four quadriceps muscles. b) The hamstring muscles. c) The gastrocnemii muscles.

CMC computed muscle forces were then used to calculate the force in the ACL during single-leg jump landing. The mean forces of the quadriceps, hamstrings and gastrocnemii muscle groups were compared for the trials when the forces in the ACL fell below 2160 ± 157N, a threshold determined by Woo et al. (1991), to trials when the ACL forces exceeded this threshold. A one-way ANOVA was conducted to compare the muscle group means for the aforementioned conditions while a Tukey post-hoc analysis was conducted to determine the significance of the observed differences between the two groups ($\alpha = 0.05$). The time to maximum ACL force and

maximum vGRF were also calculated. A one-way ANOVA was conducted to compare the mean time difference between the time to maximum vGRF to the time to maximum ACL force for when the force fell above and below the Woo et al. (1991) defined injury threshold. A Tukey post-hoc analysis was conducted to determine if the observed temporal differences were significant. The ACL force calculation was explained in Appendix 2.7.5.

2.4 Results

Gastrocnemii and quadriceps forces were, on average, higher than hamstrings forces during the WA phase of single-leg jump landing based on the subject-specific simulations. No differences were observed in individual muscle force production between the subjects and trials by conducting a one-way ANOVA that compared the means of the maximum individual muscle forces based on the swing direction. Thus, all fourteen trials were analyzed together. The individual muscle forces for the nine muscles crossing the knee were normalized by their individual maximum isometric force values used during the simulation and plotted as such to determine their relative force contribution (Fig. 6); however, their non-normalized forces were compared for the one-way ANOVA (Table 1). The largest muscle force estimates during the WA phase of single-leg jump landing in decreasing order were the quadriceps (1,730±271N), gastrocnemii (1,256±512N) and hamstrings (442±234N) (Table 2). The maximum force production between these muscle groups were significantly different ($p < 0.001$) with the post-hoc analysis showing the quadriceps muscles produced significantly greater force than both the gastrocnemii ($p = 0.002$) and hamstrings ($p < 0.001$) muscles and mean maximum gastrocnemii muscle force estimates were significantly greater than the hamstrings ($p < 0.001$).

Differences in the time for each muscle group to reach its maximum force production relative to the time to peak vertical GRF were observed. The quadriceps reached maximum

muscle force first (3.4±14.8ms) followed by the gastrocnemii muscles (15.2±16.6ms) and then finally the hamstring muscles (19.6±23.5ms); however, these temporal differences were not significant (p=0.073) (Table 3). All three muscle groups reached maximum force, on average, after peak vertical GRF was observed.

The quadriceps produced significantly lower muscle forces (1582 ± 234N) when the ACL fell below the loading injurious threshold compared to when the injurious threshold was exceeded (1878 ± 230N). The gastrocnemii and hamstrings produced larger forces when the maximum ACL force was below potential injury threshold than when it was above (Table 4). Overall the maximum vGRF reached maximum force 9.9 ± 8.9ms before maximum ACL force occurred (Fig. 7, Table 5). For the trials when the ACL force exceeded the cadaveric defined potential ACL injury threshold, the maximum ACL force occurred 8.1 ± 4.6ms after maximum vGRF compared to 11.7 ± 12.1 ms for the trials when ACL force did not exceed the threshold. This difference was not significant. Overall in all fourteen trials maximum ACL force was reached 49.8 ± 16.6 ms into the WA phase of single-leg jump landing.

The mean deviation between experimental (IK) and muscle-actuated simulation kinematics was 3.5 ± 1.4° for all lower extremity joint angles during the WA phase of single-leg jump landing for all participants with a maximum of 9.9° abduction at the hip (Fig. 8, Table 6). These deviations in simulated joint kinematics and external moments are needed to improve the dynamic consistency with experimentally recorded GRF. All simulations were shown to be dynamically consistent with low peak residual forces (5N) and moments (8Nm) at the pelvis. The CMC excitations used to drive the simulation were closely aligned with the experimentally measured sEMG activation data (Fig. 9). The consistency between the simulated joint

kinematics, kinetics, and muscle excitations compared with the experimentally recorded data suggests simulations of single-leg jump landing represented the experimental sport task.

Table 1. Mean maximum and minimum muscle force estimates for the individual muscles during the weight-acceptance phase of single-leg jump landing for fourteen trials.

Muscle	Value															
		Participant Muscle Force (N)														
		1a	1b	2a	2b	3a	3b	4a	4b	5a	5b	6a	6b	7a	7b	Mean ± StDev
Vastus Medialis	Max	2,895	3,144	3,273	3,136	2,495	2,511	3,125	1,893	2,670	1,961	1,270	1,388	1,629	3,424	2,488±734[b]
	Min	452	72	101	64	71	73	682	503	184	137	73	72	229	88	200±199
Vastus Lateralis	Max	1,065	683	696	706	1,136	2,251	226	1,995	220	1,188	676	2,645	1,599	254	1,096±770[c,d,e,f]
	Min	101	117	34	59	111	133	97	98	121	281	128	131	317	137	133±76
Vastus Intermedius	Max	1,978	242	1,155	1,375	1,202	1,276	2,347	271	1,359	1,177	1,612	2,494	2,251	2,476	1,515±731[c,d,e]
	Min	78	83	101	75	81	91	80	83	65	39	888	99	69	103	138±216
Rectus Femoris	Max	1,651	2,016	2,231	1,972	2,098	2,499	2,084	2,890	844	1,055	2,470	408	689	2,605	1,822±778[b,c]
	Min	411	964	1098	899	197	1279	92	98	90	18	1489	155	203	867	561±514
Medial Gastrocnemius	Max	1,746	2,344	928	3,174	732	1,332	2,561	2,115	3,076	1,098	378	154	692	1,745	1,577±975[c,d]
	Min	151	125	80	84	283	247	650	482	171	351	176	41	117	314	234±171
Lateral Gastrocnemius	Max	1,360	1,016	1,098	1,558	481	1,223	353	919	312	606	1,356	1,335	374	1,094	935±430[d,e,f]
	Min	509	296	568	671	107	455	39	482	66	182	625	884	103	155	367±267
Biceps Femoris Longus	Max	467	963	29	176	234	137	245	754	18	579	351	189	181	73	314±282[f]
	Min	21	71	1	1	60	77	9	1	1	62	19	5	34	2	26±29
Semimbranosus	Max	983	1,522	1,031	1,273	729	107	1,019	592	446	476	510	91	124	912	701±444[e,f]
	Min	153	316	85	107	6	2	81	92	164	109	211	2	9	2	96±93
Semitendinosus	Max	333	571	399	377	232	284	235	173	291	462	225	96	114	569	312±150[f]
	Min	33	49	105	29	42	25	85	96	78	203	62	13	36	18	62±50
Soleus	Max	4,445	3,012	5,189	5,055	3,562	2,112	2,152	3,323	2,073	2,729	2,861	3,582	4,031	2,390	3,323±1049[a]
	Min	245	186	233	163	181	239	30	70	576	41	293	250	4	9	180±152

ANOVA identified a significant difference for the maximum values of the individual muscles ($p < 0.001$; n = 14).

Symbols a,b,c,d,e,f indicate Tukey's adjusted post-hoc difference ($\alpha = 0.05$) in mean maximum muscle force between the individual muscles. Muscles with the same letters are not significantly different from each other. Conversely, if muscles do not share a letter, the means are significantly different.

Participant 1 jump landing trials are designated by 1a, 1b. Participant 2's trials are 2a,2b etc.
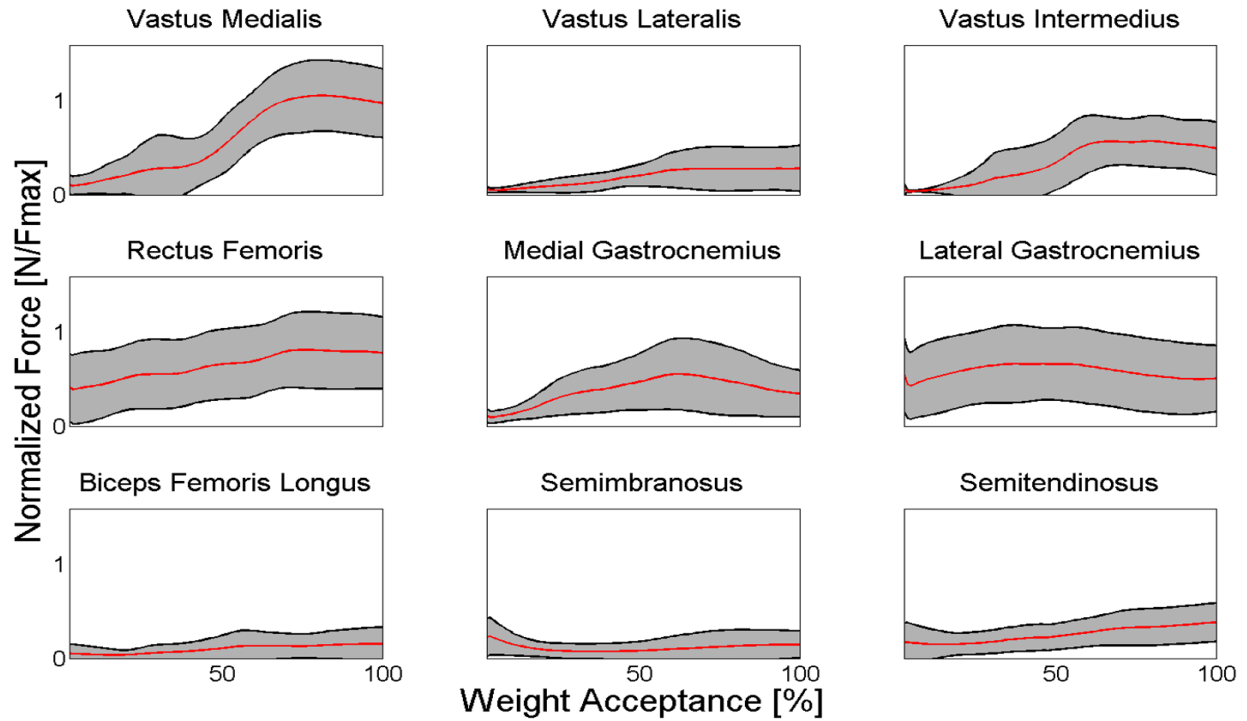
Figure 6. Lower extremity muscle force estimates (normalized by peak isometric force, Fmax) for muscles crossing the knee joint during the weight acceptance phase of single-leg jump landing. Mean forces (solid line) and one standard deviation (gray area) for the fourteen trials by the seven participants. Note, due to the force-velocity relationship of the muscle model, some normalized force estimates are higher than 1 as a result of eccentric contractions taking place.

Table 2. Mean maximum and minimum muscle force estimates for the three muscle groups during the weight-acceptance phase of single-leg jump landing for fourteen trials.

Muscle	Value	1a	1b	2a	2b	3a	3b	4a	4b	5a	5b	6a	6b	7a	7b	Mean ± StDev
Quadriceps	Max	1,897	1,521	1,839	1,797	1,733	2,134	1,946	1,762	1,273	1,345	1,507	1,734	1,542	2,190	1730±271[a] 258±143
	Min	261	309	334	274	115	394	238	196	115	119	645	114	205	299	
Gastrocnemii	Max	1,553	1,680	1,013	2,366	607	1,278	1,457	1,517	1,694	852	867	745	533	1,420	1256±512[b] 301±116
	Min	330	211	324	378	195	351	345	482	119	267	401	463	110	235	
Hamstrings	Max	594	1,019	486	609	398	176	500	506	252	506	362	125	140	518	442±234[c] 61±41
	Min	69	145	64	46	36	35	58	63	81	125	97	7	26	7	

ANOVA identified a significant difference for the maximum values of the muscle groups ($p < 0.001$; n = 3).

Symbols a,b,c indicate Tukey's adjusted post-hoc difference ($\alpha = 0.05$) in mean maximum muscle force between the muscle groups. Muscle groups with the same letters are not significantly different from each other. Conversely, if muscle groups do not share a letter, the means are significantly different.

Participant 1 jump landing trials are designated by 1a, 1b. Participant 2's trials are 2a, 2b etc.

Table 3. Comparison of time differences between peak vertical ground reaction force (GRF) and maximum muscle force estimates for each muscle group during the weight-acceptance phase of single-leg jump landing for fourteen participants. Positive time values indicate that the muscle group reached maximum force after peak GRF was reached.

	Participant Time to Maximum Force (ms)														
Muscle Group	**1a**	**1b**	**2a**	**2b**	**3a**	**3b**	**4a**	**4b**	**5a**	**5b**	**6a**	**6b**	**7a**	**7b**	**Mean ± StDev**
Quadriceps	31.5	-5.9	-1.6	-0.9	-10.9	17.7	-5.4	3.5	19.5	-9.8	23.4	-0.6	-20.5	8.1	3.4± 14.8
Gastrocnemii	36.0	25.5	-22.3	13.5	17.8	26.4	-5.6	24.7	2.2	14.0	40.0	2.4	15.4	22.3	15.2± 16.6
Hamstrings	43.1	6.8	59.2	8.2	-17.9	6.8	32.3	24.7	34.6	48.4	36.0	9.4	-13.1	-3.6	19.6± 23.5

ANOVA identified a significant difference for the time to maximum muscle group force for the muscle groups ($p = 0.073$ and n = 3).

Negative values indicate the muscle group reached maximum force before vertical ground reaction force maximum.

Table 4. Mean maximum ACL and muscle force estimates for the three muscle groups for when the loading falls below and exceeds an ACL threshold cutoff value during the weight-acceptance phase of single-leg jump landing.

	Maximum Force in ACL (N)	
	1661±557	3279±690
	Below ACL Threshold	**Above ACL Threshold**
Muscle Group	**Muscle Force (N)**	**Muscle Force (N)**
Quadriceps	1582±234[a]	1878 ±230[b]
Gastrocnemii	1374±623	1138 ±383
Hamstrings	533±251	350 ±191

ANOVA identified a significant difference for the maximum values of the muscle groups ($p < 0.001$; n = 3).
Symbols a,b,c indicate Tukey's adjusted post-hoc difference ($\alpha = 0.05$) in mean maximum muscle force between the muscle groups. Muscle groups with the same letters are not significantly different from each other. Conversely, if muscle groups do not share a letter, the means are

Table 5. Comparison of time differences between the maximum ACL force estimates during the weight-acceptance phase of single-leg jump landing for the trials above and below potential ACL injury threshold and the maximum vertical ground reaction force (vGRF).

Groups	Time (ms)
Trials Below ACL Threshold	11.7 ± 12.1
Trials Above ACL Threshold	8.1 ± 4.6

ANOVA identified a significant difference for the time to maximum ACL force for trials above and below potential ACL injury threshold ($p = 0.05$ and n = 7).
Symbols a,b indicate Tukey's adjusted post-hoc difference ($\alpha = 0.05$) in mean time between maximum ACL force and vGRF were significant. Groups with the same letters are not significantly different from each other. Conversely, if groups do not share a letter, the means are significantly different.
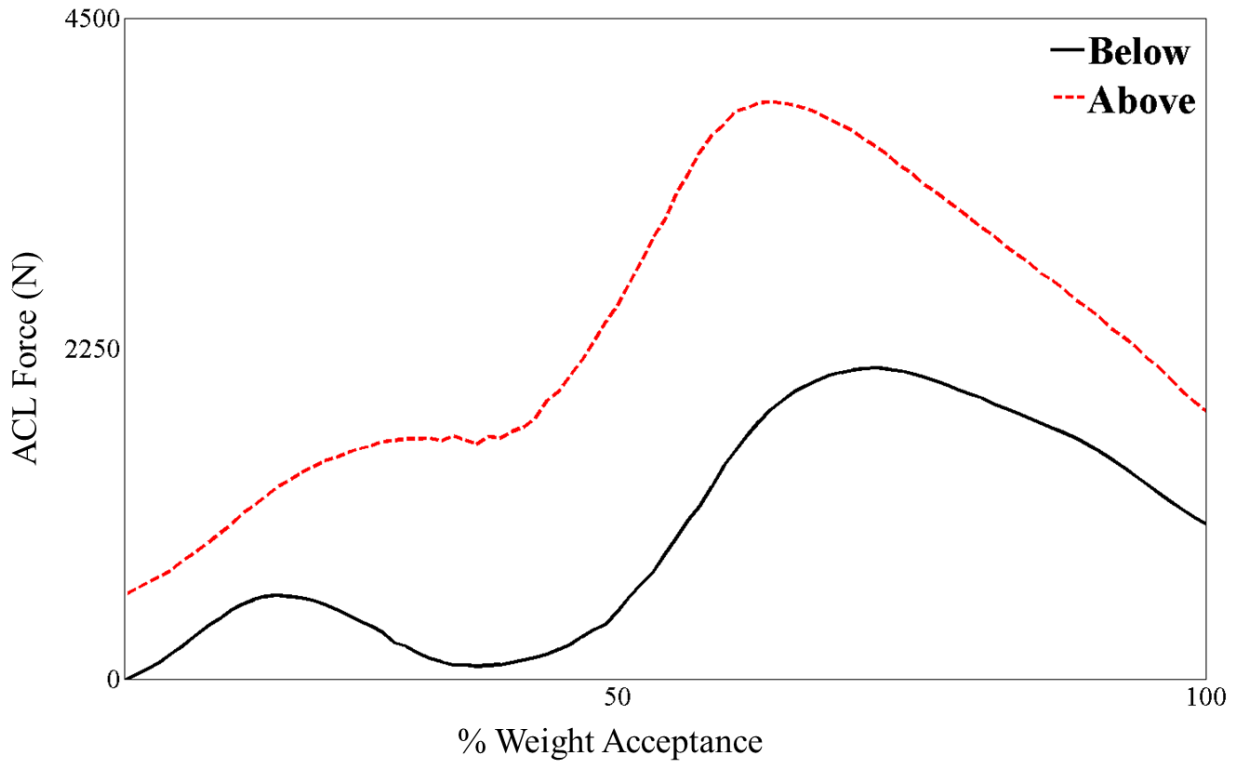
Figure 7. Comparison of the ACL force waveforms for two participants. The black waveform represents the individual whose ACL force falls below the Woo et al. (1991) cadaveric injury threshold and the red represents an individual whose ACL force exceeds the threshold.
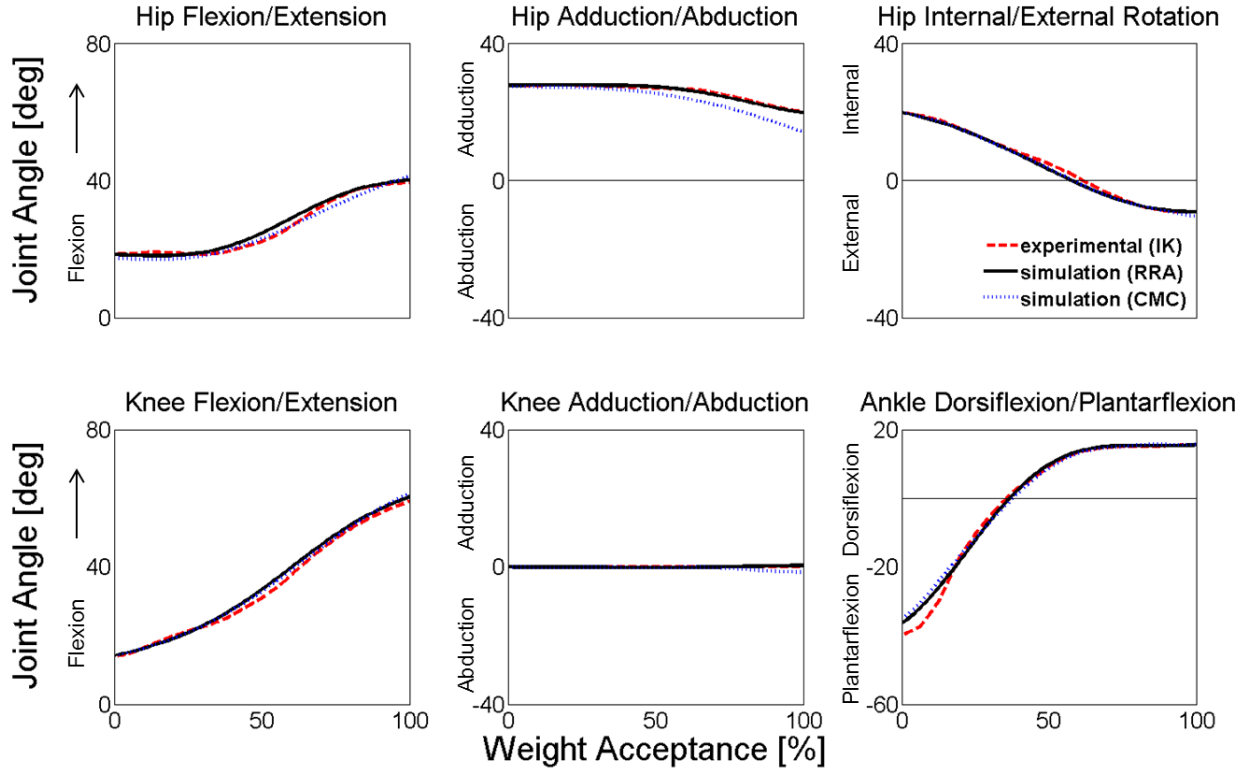
Figure 8. Comparison of lower extremity joint angles at different steps in the process of creating a muscle-actuated dynamic simulation during the weight-acceptance phase of single-leg jump landing for an example participant. The dashed-line represents the joint angles calculated by inverse kinematics (IK), the solid line represents joint angles following residual reduction analysis (RRA) to make the motion dynamically consistent with ground reaction forces, and the dotted line represents joint angles from the muscle-actuated simulation generated with computed muscle control (CMC).

Table 6. Comparison of the mean maximum joint kinematics, kinetics and vertical ground reaction force (GRF) for the fourteen trials during the weight-acceptance phase of single-leg jump landing.

Kinematics (degrees)	
Hip flexion	22.3±15.6
Hip adduction	22.0±8.5
Hip internal rotation	12.9±15.1
Knee flexion	53.4±7.2
Knee adduction	0.5±1.3
Knee internal rotation	8.3±17.3
Ankle dorsiflexion	17.8±7.1
Joint moments (Nm/kg-m)	
Hip extension	2.3±1.3
Hip abduction	0.8±0.8
Hip external rotation	0.6±0.2
Knee extension	3.1±0.6
Knee abduction	1.1±0.4
Knee internal rotation	0.1±0.1
Ankle plantarflexion	2.2±0.6
Ground Reaction Force (BW)	
Vertical ground reaction force	4.3±0.6
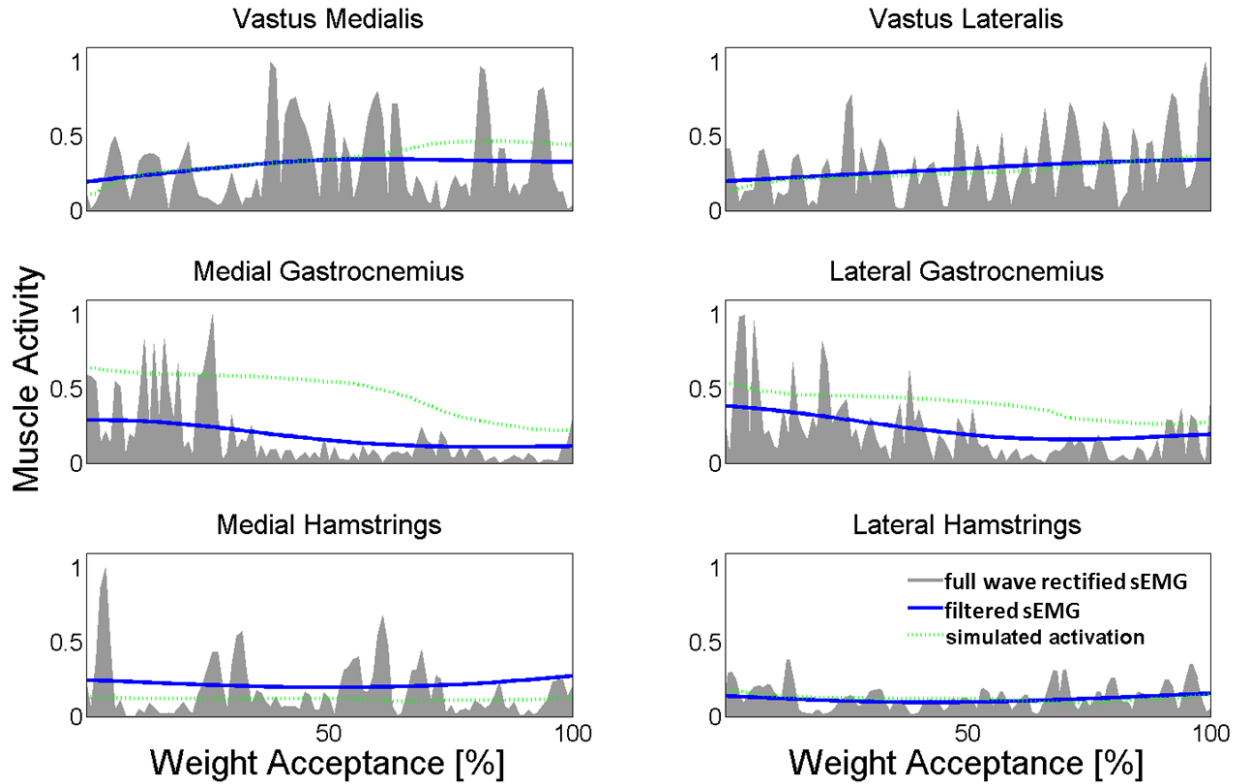
Figure 9. Comparison of experimental surface electromyography (sEMG) and simulated muscle excitations during the weight-acceptance phase of single-leg jump landing for an example participant. Experimental unfiltered full wave rectified (gray area) and filtered (solid line) sEMG and simulated muscle excitations (dashed line) estimated during the weight acceptance phase of single-leg jump landing. The experimental unfiltered full wave rectified (gray area) and filtered (solid line) sEMG data are individually normalized to the maximum recorded signal of each muscle over one of the landing trials. Simulated excitations (dashed line) are defined to be between 0 (no excitation) and 1 (full excitation).

2.5 Discussion

The purpose of this study was to characterize the force production of the muscles supporting the knee during the WA phase of single-leg jump landing. Results showed that the quadriceps generated the greatest force followed by the gastrocnemii and then the hamstrings. This trend was present both when the force measured in the ACL exceeded and fell below the loading at which it is believed to tear (Woo et al., 1991). Additionally, the quadriceps reached

maximum force earlier than the gastrocnemii and hamstrings. Future research for effectively designing preventative training protocols should consider targeting the strength and coordination of these muscle groups, particularly the quadriceps and gastrocnemii, for injury prevention practice among community-level athletic populations.

There are several possible biomechanical explanations for why each muscle group crossing the knee produces force differently to stabilize and support the knee during singe-leg jump landing. The co-contraction of the quadriceps, gastrocnemii and hamstrings is likely utilized to improved joint stability and reduce the strain exerted on the ACL during single-leg landing (Podraza and White, 2010; Riemann and Lephart, 2002). The comparisons of the muscle forces for when ACL force fell above and below the dangerous loading threshold calculated by Woo et al. (1991), found that the gastrocnemii and hamstring muscle forces were higher when the force in the ACL was lower. And while both the force in gastrocnemii and hamstrings increased, the force produced by the hamstrings was not enough to counterbalance the quadriceps force and further support the role of the gastrocnemii to help stabilize the knee. These results also support the notion that the primary motor control task during landing is to produce a support moment capable of maintaining the center of mass (CoM) upright as the quadriceps and gastrocnemii provide knee extension and ankle plantarflexion moments, respectively (Winter, 1980). These results suggest co-contraction between the quadriceps and gastrocnemii, not the quadriceps and hamstrings, are the primary muscle groups used to stabilize and support the knee from external joint loading during landing.

The hamstrings produced less maximum force and peaked later than the gastrocnemii muscles. This finding adds to the clinical understanding of how muscles function to support the knee during single-leg landing. Previous clinical research proposed hamstrings are activated to a

similar extent as gastrocnemii during landing (Cowling and Steele, 2001). Clinical research has also proposed that elevated hamstrings activation in response to quadriceps activation is used to increase co-contraction, stabilize the knee and protect the knee ligaments, including the ACL, from external valgus and/or torsional loading (Alentorn-Geli et al., 2009; Hewett et al., 2006; Li et al., 1999; Wojtys et al., 2002). However, these clinical findings are based on muscle activation estimates (sEMG), rather than muscle force estimates. The current study's results suggest the gastrocnemii, rather than the hamstrings, generate forces to counterbalance elevated quadriceps forces and stabilize the knee joint during the WA phase of single-leg jump landing.

The mean maximum soleus force produced by the participants during the single-leg jump landing task (3,323±1049 N) is consistent with peak isometric *in-vivo* force measurements (3,469 ± 720 N) reported by Rubenson et al. (2012). Previous research suggested this additional force would add to the gastrocnemii-soleus complex force generating capacity, suggesting the role of the gastrocnemii in supporting the knee during single-leg landing may be underestimated (Mokhtarzadeh et al., 2013; Podraza and White, 2010; Rubenson et al., 2012).

The gastrocnemii are biarticular muscles that have multiple functions about the knee and ankle. Gastrocnemii's primary function is to plantarflex the foot during landing, which contributes to the production of a support moment (Winter, 1980). Results presented here suggest its secondary function may be to co-contract with the quadriceps to stabilize the knee and protect the ACL from external joint loading. These results are supported by previous research that has shown elevated gastrocnemii activity compared to the hamstrings during jump landings (Chappell et al., 2007; Colby et al., 2000; Fagenbaum and Darling, 2003; Myer et al., 2009; Nyland et al., 2010; Padua et al., 2005; Viitasalo et al., 1998). The mean gastrocnemii force was greater than the hamstrings, and was consistent across all fourteen simulations in this

41

study irrespective of swing direction. These findings suggest a generalized muscle force strategy may be used to generate a support moment to resist the fall of the center of mass, while also supporting the knee and ACL from external knee loading and injury risk (Boden et al., 2009).

Although not the focus of this research, specific temporal patterns in maximum muscle force generation were observed. Mean maximum force of the gastrocnemii occurred 15.2 ms after peak vertical GRF, which is when peak ACL strain is observed during a similar jump-landing task (Cerulli et al., 2003). Gastrocnemii maximum force was preceded by the quadriceps but shortly followed by the hamstrings. In this study, trials that exhibited lower maximum ACL forces reached peak force later than trials that reported higher maximum ACL forces. However, in both cases the maximum force occurred after peak vGRF and quadriceps force but prior to maximum gastrocnemii and hamstrings force. The fact that lower maximum ACL forces occur closer to maximum gastrocnemii and hamstring forces could indicate that the gastrocnemii and hamstrings force production functions to minimize the loading on the ACL as noted by Blackburn et al. (2013). The timing of maximum muscle force production provides useful information about how muscles help distribute loads at the articular surface among the muscles and ligaments, like the ACL (Iida et al., 2011; Lloyd and Buchanan, 2001). The timing of muscle activation is a critical factor between successful and failed jump landings as late activation of quadriceps with respect to hamstrings led to failed jump landings (Wikstrom et al., 2008). The pattern included early gastrocnemii activation and could show how individuals use a bottom up strategy to stabilize the knee and, in turn, reduce ACL injury risk.

Musculoskeletal modeling for biomechanical analysis is challenging. Often assumptions regarding model parameters have to be made to perform these analyses. The model included a 3 DoF knee, with prescribed kinematics to allow for the knee's rolling motion in the sagittal plane

(Delp et al., 1990); however, the model did not include knee ligaments or an articular surface, which can function to support the knee against external frontal plane knee moments. Using OpenSim joints and actuators without implementation of complex contact model components, there are three possible approaches to address this limitation: 1) lock frontal plane knee motion (which is unrealistic as it assumes the knee only moves in two planes); 2) allow the knee to move freely in the frontal plane similar to the hip (which is unrealistic as it fails to account for the ligaments and articular surface that help support/resist motion in the frontal plane); and 3) allow the knee to move in the frontal plane but use an ideal torque actuator to represent the ligaments and articular surface supporting the knee against external frontal plane knee moments. This third option was employed. Since the simulated muscle excitations were similar to experimentally recorded excitations the inclusion of the ideal torque actuator did not significantly affect muscle force results in this study. The torque actuator worked with and not against the muscles to help stabilize the knee during landing as the model accurately tracked the frontal plane knee kinematics.

The model's maximum isometric muscle forces had to be uniformly increased 60% to better represent the muscle architecture of a young healthy athletic adult male population (Arnold et al., 2010; Lexell et al., 1988), since the baseline force values were derived from elderly cadavers (Delp et al., 1990). While these increases in maximum isometric muscle force were sufficient to facilitate the generation of accurate single-leg jump landing simulations, a more universal method for adjusting muscle forces for varying populations may be necessary and should be addressed in future research.

Despite these assumptions, the simulated kinematics, kinetics and muscle excitations were comparable against experimental kinematic, kinetic and muscle activation estimates and

provided confidence that the results are representative of muscle forces during single-leg jump landing.

This study investigated male muscle force estimates during single-leg jump landing with implications for ACL injury risk despite the fact that females suffer ACL injuries at a disproportionately higher rate than men (Hewett et al., 2006). Female's tend to produce a smaller knee flexor moment than men and this inability to counterbalance the quadriceps and reduce anterior tibial translation may be the potential cause for this higher rate (Hewett et al., 2006; Hewett et al., 1996). The males in this study demonstrated that elevated force production by the gastrocnemius-soleus complex may be the way to address this muscle imbalance and resist anterior tibial translation, a finding observed in the literature (Mokhtarzadeh et al., 2013; Podraza and White, 2010). While female models would have different skeletal geometry and muscle strength, the females (muscles) should have the same goal for muscle force production to generate a moment to support the CoM, stiffen the knee and mitigate the loads on the ACL. Since both males and females should have the same injury mechanism where the ACL ruptures when the load is greater than the tissue tolerance, females may simply have a larger quadriceps to gastrocnemii and hamstrings deficit which could be why they get injured more.

The combination of experimental and computational tools used in this study were capable of producing fourteen independent dynamically consistent simulations of single-leg jump landing, with a muscle force estimates supported by previous clinical (Chappell et al., 2007; Colby et al., 2000; Nyland et al., 2010; Padua et al., 2005; Podraza and White, 2010) and *in-silico* (Shin et al., 2007) research. These results indicate a strategy where quadriceps, gastrocnemii, and hamstrings play different roles in supporting the knee and this information can

serve as the foundation for novel muscle-targeted training intervention programs to reduce ACL

injuries.

2.6 References

Alentorn-Geli, E., Myer, G.D., Silvers, H.J., Samitier, G., Romero, D., Lazaro-Haro, C., Cugat, R., 2009. Prevention of non-contact anterior cruciate ligament injuries in soccer players. Part 1: Mechanisms of injury and underlying risk factors. Knee Surg. Sports Traumatol. Arthrosc. 17, 705-729.

Arnold, A.S., Schwartz, M.H., Thelen, D.G., Delp, S.L., 2007. Contributions of muscles to terminal-swing knee motions vary with walking speed. J. Biomech. 40, 3660-3671.

Arnold, E.M., Ward, S.R., Lieber, R.L., Delp, S.L., 2010. A model of the lower limb for analysis of human movement. Ann. Biomed. Eng. 38, 269-279.

Besier, T.F., Lloyd, D.G., Ackland, T.R., 2003. Muscle activation strategies at the knee during running and cutting maneuvers. Med. Sci. Sports Exerc. 35, 119-127.

Blackburn, J. T., Norcross, M. F., Cannon, L. N., Zinder, S. M., 2013. Hamstrings stiffness and landing biomechanics linked to anterior cruciate ligament loading. J of Ahletic Training., 48(4).

Boden, B.P., Griffin, L.Y., Garrett, W.E., 2000. Etiology and prevention of noncontact ACL injury Physician Sportsmed. 28, 53-60.

Boden, B.P., Torg, J.S., Knowles, S.B., Hewett, T.E., 2009. Video analysis of anterior cruciate ligament injury: abnormalities in hip and ankle kinematics. Am. J. Sports Med. 37, 252-259.

Cerulli, G., Benoit, D.L., Lamontagne, M., Caraffa, A., Liti, A., 2003. In vivo anterior cruciate ligament strain behaviour during a rapid deceleration movement: case report. Knee Surg. Sports Traumatol. Arthrosc. 11, 307-311.

Chappell, J.D., Creighton, R.A., Giuliani, C., Yu, B., Garrett, W.E., 2007. Kinematics and electromyography of landing preparation in vertical stop-jump: risks for noncontact anterior cruciate ligament injury. Am. J. Sports Med. 35, 235-241.

Cochrane, J.L., Lloyd, D.G., Buttfield, A., Seward, H., McGivern, J., 2007. Characteristics of anterior cruciate ligament injuries in Australian football. J. Sci. Med. Sport 10, 96-104.

Colby, S., Francisco, A., Yu, B., Kirkendall, D., Finch, M., Garrett, W., Jr., 2000. Electromyographic and kinematic analysis of cutting maneuvers. Implications for anterior cruciate ligament injury. Am. J. Sports Med. 28, 234-240.

Cowling, E.J., Steele, J.R., 2001. Is lower limb muscle synchrony during landing affected by gender? Implications for variations in ACL injury rates. J. Electromyogr. Kinesiol. 11, 263-268.

Delp, S.L., Anderson, F.C., Arnold, A.S., Loan, P., Habib, A., John, C.T., Guendelman, E., Thelen, D.G., 2007. OpenSim: open-source software to create and analyze dynamic simulations of movement. IEEE Trans. Biomed. Eng. 54, 1940-1950.

Delp, S.L., Loan, J.P., Hoy, M.G., Zajac, F.E., Topp, E.L., Rosen, J.M., 1990. An interactive graphics-based model of the lower extremity to study orthopaedic surgical procedures. IEEE Trans. Biomed. Eng. 37, 757-767.

Dempsey, A.R., Elliott, B.C., Munro, B.J., Steele, J.R., Lloyd, D.G., 2012. Whole body kinematics and knee moments that occur during an overhead catch and landing task in sport. Clin. Biomech. (Bristol, Avon) 27, 466-474.

Dempsey, A.R., Lloyd, D.G., Elliott, B.C., Steele, J.R., Munro, B.J., Russo, K.A., 2007. The effect of technique change on knee loads during sidestep cutting. Med. Sci. Sports Exerc. 39, 1765-1773.

Donnelly, C.J., Elliott, B.C., Ackland, T.R., Doyle, T.L., Beiser, T.F., Finch, C.F., Cochrane, J.L., Dempsey, A.R., Lloyd, D.G., 2012a. An anterior cruciate ligament injury prevention framework: incorporating the recent evidence. Res. Sports Med. 20, 239-262.

Donnelly, C.J., Elliott, B.C., Doyle, T.L.A., Finch, C.F., Dempsey, A.R., Lloyd, D.G., 2012b. Changes in knee joint biomechanics following balance and technique training and a season of Australian football. Br. J. Sports Med. 46, 917-922.

Donnelly, C.J., Lloyd, D.G., Elliott, B.C., Reinbolt, J.A., 2012c. Optimizing whole-body kinematics to minimize valgus knee loading during sidestepping: implications for ACL injury risk. J. Biomech. 45, 1491-1497.

Fagenbaum, R., Darling, W.G., 2003. Jump landing strategies in male and female college athletes and the implications of such strategies for anterior cruciate ligament injury. Am. J. Sports Med. 31, 233-240.

Fleming, B. C., Renstrom, P. A., Ohlen, G., Johnson, R. J., Peura, G. D., Beynnon, B. D., Badger, G. J., 2001. The gastrocnemius muscle is an antagonist of the anterior cruciate ligament. J. Orthop. Res, 19, 1178-1184.

Giffin, J. R., Vogrin, T. M., Zantop, T., Woo, S. L., and Harner, C. D., 2004. Effects of increasing tibial slope on the biomechanics of the knee. The American journal of sports medicine, 32(2), 376-382.

Hagood, S., Solomonow, M., Baratta, R., Zhou, B.H., D'Ambrosia, R., 1990. The effect of joint velocity on the contribution of the antagonist musculature to knee stiffness and laxity. Am. J. Sports Med. 18, 182-187.

Hamner, S.R., Seth, A., Delp, S.L., 2010. Muscle contributions to propulsion and support during running. J. Biomech. 43, 2709-2716.

Herzog, W., and Read, L. J., 1993. Lines of action and moment arms of the major force-carrying structures crossing the human knee joint. Journal of anatomy, 182(Pt 2), 213-230.

Hewett, T.E., Myer, G.D., Ford, K.R., 2006. Anterior cruciate ligament injuries in female athletes: Part 1, mechanisms and risk factors. Am. J. Sports Med. 34, 299-311.

Hewett, T.E., Myer, G.D., Ford, K.R., Heidt, R.S., Jr., Colosimo, A.J., McLean, S.G., van den Bogert, A.J., Paterno, M.V., Succop, P., 2005. Biomechanical measures of neuromuscular control and valgus loading of the knee predict anterior cruciate ligament injury risk in female athletes: a prospective study. Am. J. Sports Med. 33, 492-501.

Hewett, T.E., Stroupe, A.L., Nance, T.A., Noyes, F.R., 1996. Plyometric training in female athletes. Decreased impact forces and increased hamstring torques. Am. J. Sports Med. 24, 765-773.

Hewett, T. E., Shultz, S. J., Griffin, L. Y., 2007. Understanding and preventing non-contact ACL injuries. eds. Human Kinetics, Champaign, IL.

Iida, Y., Kanehisa, H., Inaba, Y., Nakazawa, K., 2011. Activity modulations of trunk and lower limb muscles during impact-absorbing landing. J. Electromyogr. Kinesiol. 21, 602-609.

Kao, J.T., Giangarra, C.E., Singer, G., Martin, S., 1995. A comparison of outpatient and inpatient anterior cruciate ligament reconstruction surgery. Arthroscopy 11, 151-156.

Kernozek, T. W., and Ragan, R. J., 2008. Estimation of anterior cruciate ligament tension from inverse dynamics data and electromyography in females during drop landing. Clinical Biomechanics, 23(10), 1279-1286.

Koga, H., Nakamae, A., Shima, Y., Iwasa, J., Myklebust, G., Engebretsen, L., Bahr, R., Krosshaug, T., 2010. Mechanisms for noncontact anterior cruciate ligament injuries: knee joint kinematics in 10 injury situations from female team handball and basketball. Am. J. Sports Med. 38, 2218-2225.

Krosshaug, T., Nakamae, A., Boden, B.P., Engebretsen, L., Smith, G., Slauterbeck, J.R., Hewett, T.E., Bahr, R., 2007. Mechanisms of anterior cruciate ligament injury in basketball: video analysis of 39 cases. Am. J. Sports Med. 35, 359-367.

Laughlin, W.A., Weinhandl, J.T., Kernozek, T.W., Cobb, S.C., Keenan, K.G., O'Connor, K.M., 2011. The effects of single-leg landing technique on ACL loading. J. Biomech. 44, 1845-1851.

Lexell, J., Taylor, C.C., Sjostrom, M., 1988. What is the cause of the ageing atrophy?: Total number, size and proportion of different fiber types studied in whole vastus lateralis muscle from 15- to 83- year old men. J. Neurol. Sci. 84, 275-294.

Li, G., Rudy, T.W., Sakane, M., Kanamori, A., Ma, C.B., Woo, S.L., 1999. The importance of quadriceps and hamstring muscle loading on knee kinematics and in-situ forces in the ACL. J. Biomech. 32, 395-400.

Lloyd, D.G., Buchanan, T.S., 2001. Strategies of muscular support of varus and valgus isometric loads at the human knee. J. Biomech. 34, 1257-1267.

Markolf, K.L., Burchfield, D.M., Shapiro, M.M., Shepard, M.F., Finerman, G.A., Slauterbeck, J.L., 1995. Combined knee loading states generate high anterior cruciate ligament forces. J. Orth. Res. 13, 930-935.

Markolf, K. L., Gorek, J. F., Kabo, J. M., and Shapiro, M. S., 1990. Direct measurement of resultant forces in the anterior cruciate ligament. An in vitro study performed with a new experimental technique. The Journal of Bone & Joint Surgery, 72(4), 557-567.

Markolf, K.L., Willems, M.J., Jackson, S.R., Finerman, G.A.M., 1998. In Situ Calibration miniature sensors implanted into the Anterior Cruciate Ligament Part I: Strain Measurements. J. Orth. Res. 16, 455-463.

McLean, S.G., Huang, X., Su, A., Van Den Bogert, A.J., 2004. Sagittal plane biomechanics cannot injure the ACL during sidestep cutting. Clin. Biomech. (Bristol, Avon) 19, 828-838.

McLean, S.G., Huang, X., van den Bogert, A.J., 2005. Association between lower extremity posture at contact and peak knee valgus moment during sidestepping: implications for ACL injury. Clin. Biomech. (Bristol, Avon) 20, 863-870.

McLean, S.G., Huang, X., van den Bogert, A.J., 2008. Investigating isolated neuromuscular control contributions to non-contact anterior cruciate ligament injury risk via computer simulation methods. Clin. Biomech. (Bristol, Avon) 23, 926-936.

Mokhtarzadeh, H., Yeow, C.H., Goh, J.C.H., Oetomo, D., Malekipour, F., Lee, P.V.S., 2013. Contributions of the Soleus and Gastrocnemius muscles to the anterior cruciate ligament loading during single-leg landing. J. Biomech. 46, 1913-1920.

Myer, G.D., Ford, K.R., Barber Foss, K.D., Liu, C., Nick, T.G., Hewett, T.E., 2009. The relationship of hamstrings and quadriceps strength to anterior cruciate ligament injury in female athletes. Clin. J. Sport Med. 19, 3-8.

Nyland, J., Klein, S., Caborn, D.N., 2010. Lower extremity compensatory neuromuscular and biomechanical adaptations 2 to 11 years after anterior cruciate ligament reconstruction. Arthroscopy 26, 1212-1225.

Padua, D.A., Carcia, C.R., Arnold, B.L., Granata, K.P., 2005. Gender differences in leg stiffness and stiffness recruitment strategy during two-legged hopping. Journal of motor behavior 37, 111-125.

Pflum, M. A., Shelburne, K. B., Torry, M. R., Decker, M. J., Pandy, M. G., 2004. Model prediction of anterior cruciate ligament force during drop-landings. Med. Sci. Sports Exerc. 36, 1949-1958.

Podraza, J.T., White, S.C., 2010. Effect of knee flexion angle on ground reaction forces, knee moments and muscle co-contraction during an impact-like deceleration landing: implications for the non-contact mechanism of ACL injury. Knee 17, 291-295.

Riemann, B.L., Lephart, S.M., 2002. The Sensorimotor System, Part II: The Role of Proprioception in Motor Control and Functional Joint Stability. Journal of athletic training 37, 80-84.

Rubenson, J., Pires, N.J., Loi, H.O., Pinniger, G.J., Shannon, D.G., 2012. On the ascent: the soleus operating length is conserved to the ascending limb of the force-length curve across gait mechanics in humans. J. Exp. Biol. 215, 3539-3551.

Seedhom, B.B., Longton, E.B., Wright, V., Dowson, D., 1972. Dimensions of the Knee. Radiographic autopsy study sizes require knee prosthesis. Ann. Rheum. Dis. 31, 54-58.

Seth, A., Sherman, M., Reinbolt, J.A., Delp, S.L., 2011. OpenSim: a musculoskeletal modeling and simulation framework for in silico investigations and exchange. Proc Iutam 2, 212-232.

Sherbondy, P. S. Queale, W. S., McFarland, E. G., Mizuno, Y., Cosgarea, A. J., 2003. Soleus and gastrocnemius muscle loading decreases anterior tibial translation in anterior cruciate ligament intact nad deficient knees. J. of Knee Surg. 16, 152.

Shin, C.S., Chaudhari, A.M., Andriacchi, T.P., 2007. The influence of deceleration forces on ACL strain during single-leg landing: a simulation study. J. Biomech. 40, 1145-1152.

Thelen, D.G., Anderson, F.C., 2006. Using computed muscle control to generate forward dynamic simulations of human walking from experimental data. J. Biomech. 39, 1107-1115.

Thelen, D.G., Anderson, F.C., Delp, S.L., 2003. Generating dynamic simulations of movement using computed muscle control. J. Biomech. 36, 321-328.

Utturkar, G. M., Irribarra, L. A., Taylor, K. A., Spritzer, C. E., Taylor, D. C., Garrett, W. E., and DeFrate, L. E., 2013. The effects of a valgus collapse knee position on in vivo ACL elongation. Annals of biomedical engineering, 41(1), 123-130.

Viitasalo, J.T., Salo, A., Lahtinen, J., 1998. Neuromuscular functioning of athletes and non-athletes in the drop jump. Eur. J. Appl. Physiol. 78, 432-440.

Walla, D.J., Albright, J.P., McAuley, E., Martin, R.K., Eldridge, V., El-Khoury, G., 1985. Hamstring control and the unstable anterior cruciate ligament-deficient knee. Am. J. Sports Med. 13, 34-39.

Weinhandl, J.T., Earl-Boehm, J.E., Ebersole, K.T., Huddleston, W.E., Armstrong, B.S., O'Connor, K.M., 2013. Anticipatory effects on anterior cruciate ligament loading during sidestep cutting. Clin. Biomech. (Bristol, Avon) 28, 655-663.

Wikstrom, E.A., Tillman, M.D., Schenker, S., Borsa, P.A., 2008. Failed jump landing trials: deficits in neuromuscular control. Scand. J. Med. Sci. Sports 18, 55-61.

Winter, D.A., 1980. Overall Principle of Lower Limb Support During Stance Phase of Gait. 13, 923-927.

Wojtys, E.M., Ashton-Miller, J.A., Huston, L.J., 2002. A gender-related difference in the contribution of the knee musculature to sagittal-plane shear stiffness in subjects with similar knee laxity. J. Bone Joint Surg. Am. 84-A, 10-16.

Woo, S. L. Y., Hollis, J. M., Adams, D. J., Lyon, R. M., and Takai, S., 1991. Tensile properties of the human femur-anterior cruciate ligament-tibia complex The effects of specimen age and orientation. The American journal of sports medicine, 19(3), 217-225.

Zhao, D., Banks, S.A., D'Lima, D.D., Colwell, C.W., Jr., Fregly, B.J., 2007. In vivo medial and lateral tibial loads during dynamic and high flexion activities. J. Orthop. Res. 25, 593-602.

2.7 Appendix

2.7.1 Scaling

The objective of scaling is to develop a subject-specific model that has the same mass and anthropometric measurements as the subject performing the experiment. This is achieved by first obtaining the experimentally measured subjects mass and redistributing that mass amongst the models' body segments to replicate the subjects body mass (Delp et al., 2007). Then the generic virtual markers on the OpenSim model are repositioned on the model based on the location of the subjects' experimental markers to identify the appropriate joint centers and define the correct segment lengths (Delp et al., 2007). The marker locations from the subjects' experimental static pose is compared to the virtual marker locations in the models static pose to ensure a strong match (i.e. minimal error) between the model and experimental marker sets. The error is the calculated average of the distance between the two marker sets. The result is a model that closely matches the subjects' mass properties and segment dimensions.

2.7.2 Inverse Kinematics (IK)

Inverse kinematics is a process that derives the joint angles that the experimental marker data record during movement. IK works by calculating the ideal location to place the model joint coordinates (angles and position) to match the experimental joint coordinates at regular time points throughout the movement. A weighted least square algorithm (Eq. 2.1) is utilized to reduce these errors between the experimental $\left(X_i^{\exp}\right)$ and model markers $\left(X_i(q)\right)$ and generalized coordinates $\left(q_j^{\exp}, q_j\right)$, where w_i and w_j are the user defined weightings (Delp et al., 2007).

$$\min_q \left[\sum_{i \in markers} w_i \left\| x_i^{\text{exp}} - x_i(q) \right\|^2 + \sum_{j \in unprescribed\ coords} w_j \left(q_j^{\text{exp}} - q_j \right)^2 \right] \quad (2.1)$$

$$q_j = q_j^{\text{exp}} \text{ for all prescribed coordinates } j$$

The weighting coefficients are adjusted to better track markers and coordinates the researchers have the greatest confidence in. The result is model joint angles and positions that accurately track the experimental movement.

2.7.3 Residual Reduction Analysis (RRA)

Residual reduction analysis employs a forward dynamics to create a simulation that recreates the IK motion using torques actuators acting at/on the joints. The result is a dynamically consistent model. A dynamically consistent model is one where the summation of the (derived) model forces matches the experimentally measured GRFs, which are an accurate measurement of the forces exerted on the ground by the individual. However, throughout model development, assumptions are made to determine model marker placement/location, joint angles and joint positions information that are used to derive model accelerations. This can cause errors to accumulate causing the model forces to differ from the GRFs. To make the model forces equal the GRFs, residual forces and torques are added to the model to match GRFs as shown in Equation 2.2 (Delp et al., 2007). Reserve actuators are used to generate the residual forces and torques. There are six reserve actuators and they are represented by a 6 DoF (3 translational, 3 rotational) joint that acts between the pelvis and the ground (Delp et al., 2007). An optimization algorithm is employed to minimize the contribution of the reserve actuators as the reserve forces are phantom forces that are added to ensure model forces equal experimentally measured GRFs (Delp et al., 2007). The optimization function uses the relationship between the weighted $\left(w_{\ddot{q}_i} \right)$ sum of the

model and experimental acceleration difference squared $\left(\ddot{q}_i^{\text{exp}}, \ddot{q}_i^{sim}\right)$, and the normalized residual

forces and torques $\left(\dfrac{R_j\left(x_j^R\right)}{R_j^{\max}}\right)$ along with the normalized joint torques $\left(\dfrac{T_k\left(x_k^T\right)}{T_k^{\max}}\right)$ to calculate the

smallest X shown in Equation (2.3) (Delp et al., 2007, Thelen and Anderson, 2006). The end

result of this process is a dynamically consistent simulation actuated by joint torques and

residuals.

$$\sum F_{\text{mod}el} + \sum F_{residuals} = \text{GRFs} \quad (2.2)$$

$$J(x) = \min_{x^R, x^T}\left[\sum_{i=1}^{n_q} w_{\ddot{q}_i}\left(\ddot{q}_i^{\text{exp}} - \ddot{q}_i^{sim}\right)^2 + \sum_{j=1}^{6}\left(\frac{R_j\left(x_j^R\right)}{R_j^{\max}}\right)^2 + \sum_{k=1}^{n_T}\left(\frac{T_k\left(x_k^T\right)}{T_k^{\max}}\right)^2\right] \quad (2.3)$$

2.7.4 Computed Muscle Control (CMC)

Computed muscle control is an optimization tool developed by Thelen and Anderson

(2006) to identify individual muscle force contribution during movement (Fig. 10). CMC works

by first calculating the desired (joint, generalized) accelerations, $\ddot{q}^*$, from the experimental motion

data $\left(\bar{q}_{\text{exp}}\right)$ that serve as inputs for static optimization (Thelen and Anderson, 2006). Static

optimization calculates the muscle activations that will be translated into the muscle forces that

will actuate the joints to produce the desired motion. Static optimization utilizes a performance

criterion, (J), which is the sum of the actuators (i.e. muscles) squared $\left(x_i^2\right)$, to determine how to

distribute the activations across all of the muscles in the model. The muscle excitations are

derived from the muscle activations generated. Then forward dynamics is applied to determine if

the computed muscle forces produce the desired joint motion. The joint motion is feed back into

the loop to determine how well the model accelerations match the desired accelerations (Eq. 2.4)

(Thelen and Anderson, 2006). A proportional-derivate (PD) controller adjusts its velocity, $\vec{k}_v$, and position, $\vec{k}_p$, error feedback gains to minimize the least-squared error measured between the experimental and model simulated motion (Thelen and Anderson, 2006). The end result is a set of individual muscle forces that produce your desired movement.

$$\ddot{\vec{q}}^{*}(t+T) = \ddot{\vec{q}}_{\mathrm{exp}}(t+T) + \vec{k}_v \cdot \left[\dot{\vec{q}}_{\mathrm{exp}}(t) - \dot{\vec{q}}(t)\right] + \vec{k}_p \cdot \left[\vec{q}_{\mathrm{exp}}(t) - \vec{q}(t)\right] \quad (2.4)$$

$\ddot{\vec{q}}^{*}$ = desired accelerations

$\vec{q}_{\mathrm{exp}}$ = experimental position

$\dot{\vec{q}}_{\mathrm{exp}}$ = experimental velocities

$\ddot{\vec{q}}_{\mathrm{exp}}$ = experimental accelerations

$\vec{q}$ = generalized coordinates

$\dot{\vec{q}}$ = generalized speeds

$\vec{k}_p$ = feedback position gain

$\vec{k}_v$ = feedback velocity gains
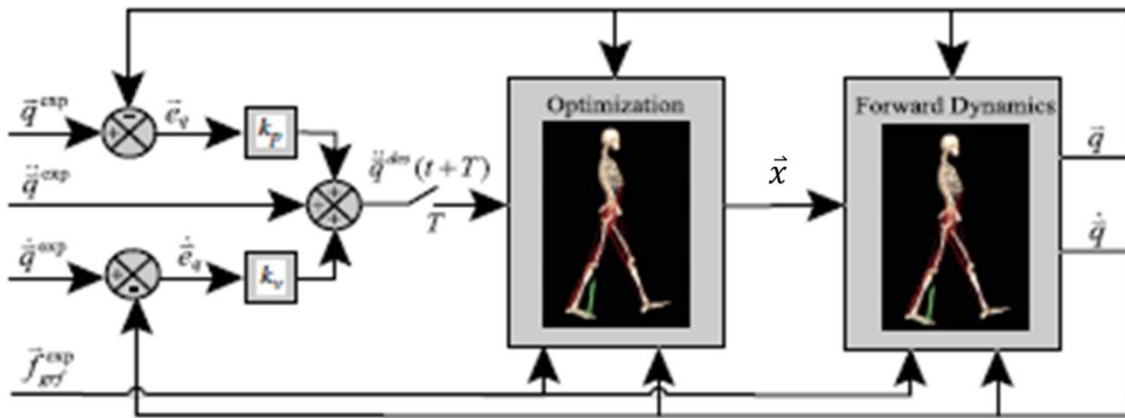
Figure 10. Schematic of Computed Muscle Control Algorithm. The schematic details the proportional-derivative feedback controller that compares the desired and model motion at the beginning of CMC. The optimization block represents the static optimization analysis from which the muscle activations generated there are used to produce the muscle force from which forward dynamics computes the resulting model motion (Thelen et al., 2003, 2006).

2.7.5 ACL Force Calculation

The following steps were used to calculate the force in the ACL (F_{ACL}) in this study. The methodology was developed by Kernozek and Ragan (2008) and recently implemented by Mokhtarzadeh et al., 2013. First Equation 2.5 is used to calculate the anterior-posterior shear force in the ligament ($F_{ligament}$). Here φ_{pat} and φ_{ham} are the quadriceps and hamstrings tendon angles as a function of knee flexion angles, respectively. The equations for quadriceps and hamstrings as a function of knee flexion angles were developed by Herzog and Read (1993). The F_{pat} and F_{ham} represent the quadriceps and hamstring force, respectively. OpenSim's joint reaction analysis was used to compute the tibio-femoral contact force (F_{tf}). The anterior-posterior shear force $\left(F_{\perp} \right)$ was calculated by adding an additional coordinate to the OpenSim model, calculating anterior-posterior translation as a function of knee flexion angle and then performing inverse dynamics to calculate $F_{\perp}$. Research by Giffin et al. (2004) and Kernozek and Ragan (2008) determined that the posterior tibial slope angle $\left(\varphi_{tf} \right)$ to be 8.5°.

$$F_{\perp} = F_{tf} \cdot \sin\varphi_{tf} + F_{pat} \cdot \sin\varphi_{pat} - F_{ham} \cdot \sin\varphi_{ham} + F_{ligament} \qquad (2.5)$$

Once $F_{ligament}$ was calculated in Equation 2.5 it was used to calculate the force in the ACL (F_{ACL}). Here θ_{knee} is the knee flexion angle and F_{100} and F_0 are forces in the ACL when 100N and 0N of anterior tibial force are applied to the ACL (Eq. 2.6). These values can be obtained from Markolf et al. (1990 and 1995).

$$F_{ACL} = \frac{F_{100}(\theta_{knee}) - F_0(\theta_{knee})}{100N} \cdot F_{ligament} + F_0(\theta_{knee}) \qquad (2.6)$$

CHAPTER III

ASSESS HOW INDIVIDUAL MUSCLES RESIST ELEVATED KNEE ABDUCTION MOMENT DURING SINGLE-LEG JUMP LANDING

3.1 Abstract

While the joint kinematics and kinetics associated with ACL injury are well understood, the individual muscle contributions to ACL injury are not. Researchers have implemented ACL injury training inter programs that measured muscle activation during dynamic movements like cutting and jump landing; but, muscle activation does not imply its contribution to joint motion. The purpose of this study was to determine the contribution of the six muscles crossing the knee to frontal, sagittal and transverse plane knee acceleration during single-leg jump landing. We believe that this information will provide better information about the cause-effect relationship between joint motion and muscle function. The three-dimensional, 14-segment, 37 degree-of-freedom, 92 muscle-tendon actuated models of amateur male Australian Rules Football players performing a single-leg landing tasks from Chapter I were used in this analysis. Induced acceleration analysis was performed to compute the individual muscle contribution to frontal, sagittal and transverse knee accelerations during the single-leg landing task. A one-way ANOVA and Tukey post-hoc analysis determined that the mean cumulative summation of the medial gastrocnemius accelerations in the frontal plane were significantly larger than any other muscle ($p < 0.001$). And the medial gastrocnemius along with the vastus medialis muscle provided the largest contribution to accelerating the knee into adduction while the lateral gastrocnemius accelerated the knee into abduction. In the sagittal plane, the medial and lateral vasti were the strongest contributors to knee extension while the gastrocnemii were the strongest contributors to knee flexion. The results determined that the medial gastrocnemii was the greatest contributor to resisting knee abduction and knee extension and should be targeted in any ACL injury training intervention program.

3.2 Introduction

Elevated knee abduction moment is a strong predictor of ACL injury (Hewett et al., 2005). The elevated moment is believed to be a byproduct of poor knee extensor to knee flexor muscle imbalance as stronger knee extensor-flexor muscle balance can help compress and in turn stabilize the joint (Hewett et al, 2006; Markolf et al., 1978; Solomonow et al., 1987). Researchers have focused on increasing hamstring (knee flexor) strength to oppose the dominant quadriceps (knee extensor) activation strength prevalent in individuals at-risk for ACL injury; but, the gastrocnemii muscles can also function as knee flexors and help oppose the quadriceps muscles (Laundry et al., 2007; Laundry et al., 2009; Podraza et al., 2010). The results of the previous study (Chapter II) found that the gastrocnemii muscles produced significantly greater force than the hamstring muscles during the single-leg jump landing task. However, increased force production by the gastrocnemii muscles does not validate their potential role as the primary contributors to opposing the quadriceps and stabilizing and supporting the knee during landing. ACL injury prevention programs are aimed at altering muscle force and activation patterns to circumvent the ACL injury mechanism; however, they are limited by their inability to assess individual muscle contributions to resist excessive knee loading during movement (Chappell et al, 2008; Donnelly et al., 2012b; Hewett et al., 1999; Huston et al., 1996). This inability to compute a muscles contribution to movement has limited the progress of the current ACL injury research and highlights a need for a way to assess muscles contribution movement to address this gap in ACL injury research.

Muscles accelerate joints and determining how they accelerate the knee during landing may be the key to understanding ACL injury prevention. Induced acceleration analysis (IAA) is a technique that determines the accelerations caused or "induced" by individual muscle forces

acting on a model (e.g., contribution of muscle forces to knee accelerations). IAA employs the principle of dynamic coupling, which describes the interconnectedness of the body segments, to deconstruct a muscles ability to actuate joints and body segments throughout the body. IAA has been implemented to compute muscles' contribution to supporting and propelling the center-of-mass (CoM) forward during walking and running and here it will be utilized to evaluate individual muscles contribution to knee motion during single-leg jump landing (Hamner et al., 2010; Lin et al., 2011; Liu et al, 2006; Liu et al., 2008).

A muscles' contribution to movement is dependent on first calculating the force an individual muscle produces and then computing the muscle forces' ability to accelerate (knee) joint motion during landing. After assessing the individual muscle force production during landing via CMC in Chapter II, the next step is to compute individual muscles ability to accelerate the knee during landing. The objective of the present study is to assess muscle contribution to frontal, sagittal and transverse plane knee accelerations and specifically determine which muscles are responsible for resisting certain elevated knee abduction. Knee abduction position observed during ACL injury is characterized as the medial collapse of the knee (Utturkar et al., 2013). We hypothesize that in addition to increased medial and lateral gastrocnemii muscle function, the medial quadriceps, hamstring and gastrocnemius muscles will be the strongest contributors to accelerating the knee into adduction. This research should provide additional insight about the causal relationship (i.e., muscle contributions to movement) between muscle forces and joint biomechanics specifically with regard to ACL injury risk.

3.3 Methodology

3.3.1 Experimental Protocol and Data Collection

Amateur male Western Australian Rules Football players were recruited to perform a single-leg jump landing experimental protocol (Donnelly et al., 2012c). Participants jumped and landed on their preferred leg, which was the right leg for all individuals analyzed in this study. While in flight, the participants were instructed to grab an Australian rules football randomly swung medially, laterally or held central relative to the participants approach direction (Dempsey et al., 2012). The ball height was approximately 90% of each participant's maximal vertical jump height. Participants landed their jump on a force platform. Of the fourteen trials generated by the seven participants (age 20.7 ± 1.8 years; height 1.9 ± 0.1m; mass 87.8 ± 5.1 kg) during the CMC analysis from Chapter II, eight trials were used for IAA as these trials model computed GRF were consistent with the experimentally measured GRF. All experimental procedures were approved by the University of Western Australia Human Research Ethics Committee and all participants provided their informed written consent prior to data collection.

Three-dimensional kinematic marker trajectories, ground reaction forces (GRF) and sEMG data from six muscles crossing the knee were recorded for each participant during the experimental data collection. Fifty-six upper- and lower-body retro-reflective markers were utilized to capture kinematic trajectories (Donnelly et al., 2012b). Marker trajectories were recorded at 250 Hz using a 12-camera Vicon MX motion capture system (VICON Peak, Oxford Metrics Ltd., UK) (Dempsey et al., 2007; Donnelly et al., 2012c). GRF data were synchronously recorded at 2,000 Hz using an AMTI (Advanced Mechanical Technology Inc., Watertown, MA) 1.2 x 1.2m force platform. Both the kinematic and GRF data were low-pass filtered using a zero phase-shift, 4th-order Butterworth filter with a cutoff frequency of 20 Hz in Workstation

(ViconPeak, Oxford Metrics Ltd., UK). The sEMG data were synchronously collected at 2,000 Hz for six muscles: vastus medialis, vastus lateralis, medial and lateral gastrocnemii and medial and lateral hamstrings. Eight surface muscles were measured with sEMG in total; however, this study focused on the six muscles that crossed the knee for analysis. The raw experimental sEMG data were band-pass filtered using a zero phase-shift, 4th-order Butterworth filter with a frequency band between 30 and 500 Hz, full wave rectified and then low-pass filtered using a zero phase-shift, 4th-order Butterworth filter with a cutoff frequency of 6 Hz to create linear envelopes. Following linear enveloping, peak muscle activation from each muscle recorded during the three landing conditions were used to normalize each muscle's sEMG signal to 100% activation. The result is a sEMG waveform from zero to full activation.

3.3.2 Subject-Specific Models and Simulations

Seven three-dimensional, 14-segment, 37 degree-of-freedom (DoF), 92 muscle-tendon actuated subject-specific models were created in OpenSim 1.9.1 to generate simulations of each participant performing the single-leg jump landing task (Fig. 11) . The details of this model have been described previously (Donnelly et al., 2012c). The 92 muscle-tendon units actuated the lower extremity and lower back joint, while the arms were actuated by torque actuators instead of muscle-tendon actuators also described previously (Hamner et al., 2010). The maximum isometric force of each muscle was increased by 60% compared to the model provided in OpenSim (Delp et al., 1990) based on research by Arnold et al. (Arnold et al., 2010). The model included a 3 DoF knee actuated by muscles and ideal torque actuators (±50Nm) which were used to provide the resistance supplied by the knee ligaments and articular surface that help stabilize the knee in the frontal plane. These values are consistent with previous literature (Seedhom et al., 1972; Zhao et al., 2007). Subject-specific joint centers were derived using functional knee and hip joint methods

(Besier et al., 2003), custom biomechanical models in MATLAB (MATLAB 7.8, The MathWorks, Inc., Natick Massachusetts, USA) and Vicon Bodybuilder (Dempsey et al., 2007). The resulting joint centers, marker trajectories and GRF data were then exported to OpenSim 1.9.1. Segment lengths were scaled to each participant's specific joint centers and segment masses to each participant's total body mass. Inverse kinematics (IK) was used to derive simulated joint angles from the experimental marker data recorded during the jump landing. Residual reduction analysis (RRA) was used to create simulations that were dynamically consistent with the experimentally recorded ground reaction forces (Delp et al., 2007; Donnelly et al., 2012c). Muscle forces were estimated for the weight-acceptance (WA) phase of single-leg jump landing using computed muscle control (CMC). CMC is an algorithm that utilizes optimization, forward dynamics and feedback control to estimate individual muscle forces during dynamic movements (Thelen and Anderson, 2006; Thelen et al., 2003).
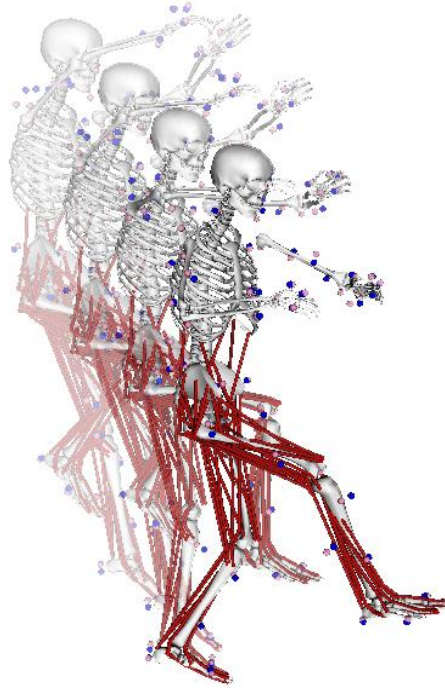
Figure 11. Series of images for a subject-specific simulation during single-leg jump landing using a musculoskeletal model with 37 degrees of freedom and 92 muscle-tendon actuators.

The WA phase was defined as the time from the initial contact to the first trough in the vertical ground reaction force profile (Dempsey et al., 2007). The WA phase was analyzed as this phase is thought to be when the ACL is at the greatest risk for injury (Dempsey et al., 2007; Donnelly et al., 2012a).

3.3.3 Muscle Contribution to Knee Acceleration during Single-leg Jump Landing

In IAA, GRF data is decomposed and the individual muscle forces contribution to joint and body segments accelerations are calculated using the concept of dynamic coupling. The dynamics that describe the relationship between the body segments is modeled via the equations of motion (Eq. 3.1). The two main specifications of IAA involve the selection of the GRF decomposition method and the foot-ground contact model. This study adopted the approach

developed by Dorn et al. (2011) where a Moore-Penrose pseudo-inverse was used for the GRF decomposition analysis and a MULTIPOINT model was employed for the foot-ground contact model. Both of these models are described in detail in Appendix 3.7.

$$M(q)\ddot{q} = C(q,\dot{q}) + G(q) + \begin{bmatrix} 0_{6x1} \\ S(q)F_m \end{bmatrix} + \begin{bmatrix} R_{6x1} \\ r_{n\pi1} \end{bmatrix} + E(q)F_{ext} \qquad (3.1)$$

M = n x n mass matrix
$q, \dot{q}, \ddot{q}$ = n x 1 vectors of generalized displacements, velocities and accelerations
C = n x 1 generalized force vector of velocity terms obtained from the centrifugal and Coriolis force equations
G = n x 1 generalized force vector due to gravity
S = n x k matrix of muscle moment arms
F_m = k x 1 vector of muscle forces
R_{6x1} = the vector of generalized residual forces and torques
$r_{n\pi1}$ = vector of generalized reserve forces and torques
F_{ext} = $3f$ x 1 vector of external reaction forces exerted on the foot by the ground by the f foot contact points that are in contact with the ground
E = n x $3f$ linear generalized Jacobian matrix that defines the relation between the generalized velocity $\dot{q}$ and the linear velocity of the foot-ground contact point

The contributions of the medial and lateral vasti, hamstrings, and gastrocnemii muscles to accelerating the knee in the frontal, sagittal and transverse planes during the WA phase of single-leg jump landing were computed using IAA. The summation of each muscles contribution to knee acceleration in the frontal, sagittal, and transverse planes was analyzed to quantify each muscles contribution to knee acceleration. A one-way ANOVA was conducted to compare the mean individual muscles' knee accelerations in the frontal, sagittal and transverse planes during the WA phase of single-leg jump landing. Tukey post-hoc analysis were conducted to determine if observed differences were significant ($\alpha = 0.05$). The principle of superposition was used to calculate the error between the experimental and model computed GRFs to assess the validity of the results (Dorn et al., 2012; Hamner et al., 2010; Liu et al., 2006). The aforementioned analyses were conducted in OpenSim v2.4.0 and Minitab.

64

3.4 Results

The muscular contributions to knee accelerations varied widely during the WA phase of single-leg jump landing (Fig. 12). In the frontal plane, the muscles that displayed the greatest contribution to knee adduction were the medial gastrocnemius and vastus medialis (Fig. 12a). The lateral gastrocnemius and lateral hamstring produced the largest opposing accelerations as they contributed to knee abduction. In the sagittal plane, the medial and lateral vasti and hamstring muscles all contributed to knee extension while the medial and lateral gastrocnemii functioned to flex the knee (Fig. 12b). The vastus medialis, medial hamstring and lateral gastrocnemius were all shown to contribute to internal rotation at the knee with the lateral vasti and hamstring muscles and medial gastrocnemius opposing internal rotation (Fig. 12c). These trends were consistent across all subjects analyzed.
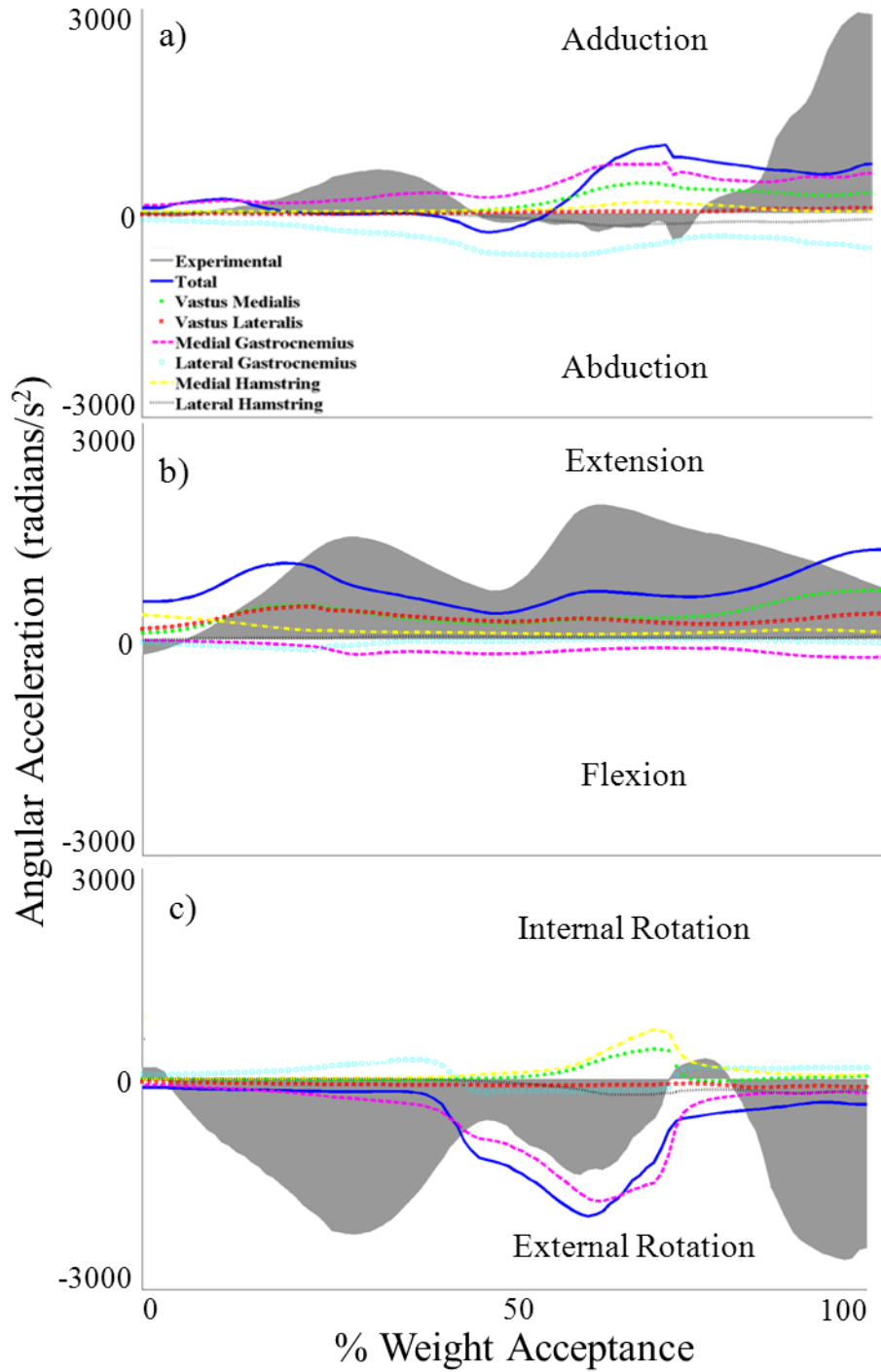
Figure 12. Muscle contributions to experimentally measured knee frontal, sagittal and transverse plane accelerations (shaded regions) for six muscles crossing the knee and the summation of the contributions of the six muscles (solid lines) during the WA phase of single-leg jump landing. Each subplot represents one individual whose waveform represents the data trends.

The cumulative sum of the acceleration over time was the metric used to quantify the trends observed in the aforementioned analysis. Both the medial gastrocnemius and vastus medialis contributed to knee adduction; however, the medial gastrocnemii produced accelerations approximately 2.5 times greater than the vastus medialis (Fig. 13, Table 7). The lateral gastrocnemii generated nearly 7 times the acceleration of the lateral hamstring. The mean cumulative sum of the medial gastrocnemii accelerations were significantly greater than both the vastus medialis and lateral gastrocnemius while the vastus medialis accelerations were significantly larger than the lateral gastrocnemius (Table 7). Comparison of the total adduction to abduction acceleration magnitudes determined that the muscles surrounding the knee generated a greater adduction to abduction acceleration. In the sagittal plane, the cumulative sum of the medial and lateral gastrocnemii accelerations, the main contributors to knee flexion, were half that of the knee extension acceleration (Fig. 14, Table 8). In the transverse plane the knee experienced greater external rotation accelerations compared to internal rotation accelerations (Fig. 15, Tables 9).
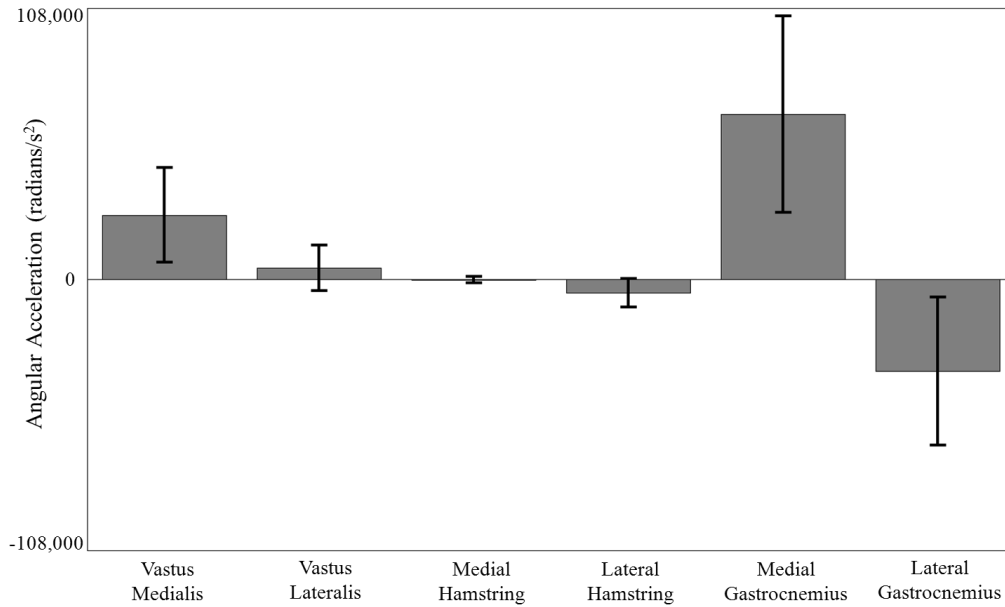
Figure 13. Mean cumulative summations of muscle contributions for the six muscles crossing the knee in the frontal plane for all participants. Each bar plot represents the mean cumulative sum of the muscles contribution throughout the weight-acceptance phase of single-leg landing computed from induced acceleration analysis. The error bars are the black lines, the positive values indicate accelerations into adduction while the negative represent abduction accelerations.
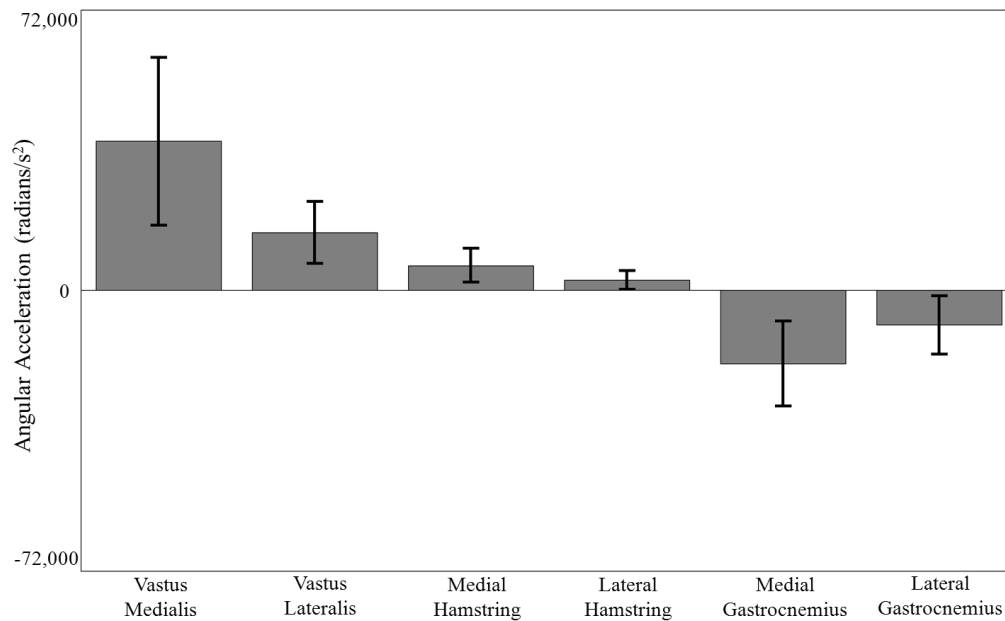
Figure 14. Mean cumulative summations of muscle contributions for the six muscles crossing the knee in the sagittal plane for all participants. Each bar plot represents the mean cumulative sum of the muscles contribution throughout the weight-acceptance phase of single-leg landing computed from induced acceleration analysis. The error bars are the black lines, the positive values indicate accelerations into extension while the negative represent flexion accelerations.
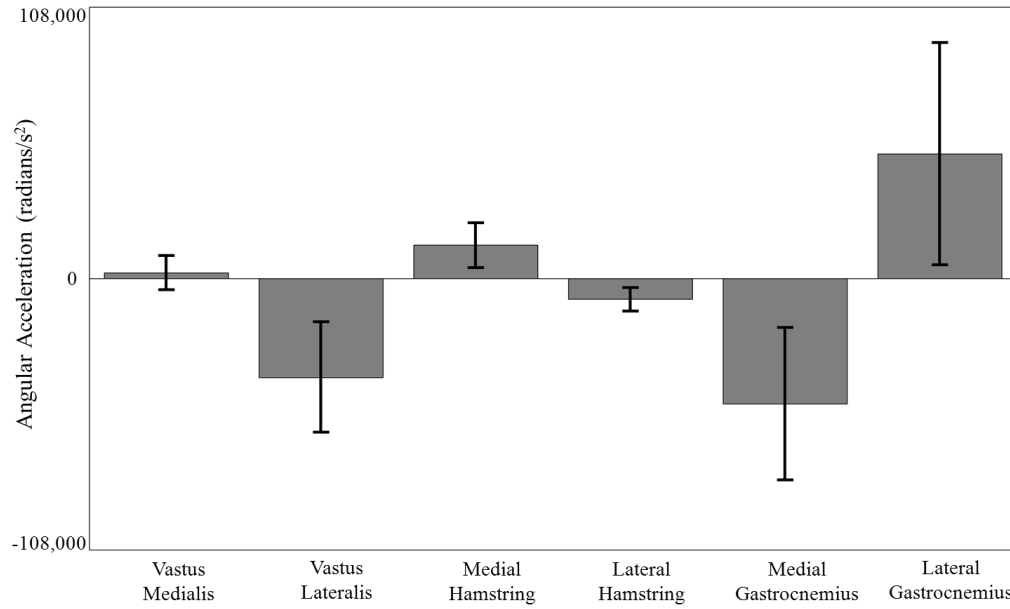
Figure 15. Mean cumulative summations of muscle contributions for the six muscles crossing the knee in the transverse plane for all participants. Each bar plot represents the mean cumulative sum of the muscles contribution throughout the weight-acceptance phase of single-leg landing computed from induced acceleration analysis. The error bars are the black lines, the positive values indicate accelerations into internal rotation while the negative represent external rotation accelerations.

Table 7. Mean cumulative summation of individual muscle and net muscle contribution in the frontal plane during the weight-acceptance phase of single-leg jump landing.

Muscles	Mean ± StDev (rad/s^2)		Mean ± StDev (rad/s^2)
Vastus Medialis	25,205 ± 19,910[b]		
Vastus Lateralis	4,317 ± 9,594[b]	Adduction (+)	94,456 ± 30,794
Medial Hamstrings	-303 ±1,371[b]		
Lateral Hamstrings	-5,429 ± 5,927[,c]		
Medial Gastrocnemius	64,934 ± 41,358[a]	Abduction (-)	-42,053 ± 19,482
Lateral Gastrocnemius	-36,321 ± 31,150[c]		

ANOVA identified a significant difference for the mean cumulative summation of the individual muscles (p < 0.001; n = 6).
Symbols a,b,c, and d indicate Tukey's adjusted post-hoc difference (α = 0.05) in mean cumulative summation between the individual muscles. Muscles with the same letters are not significantly different from each other. Conversely, if muscles do not share a letter, the means are significantly different.

Table 8. Mean cumulative summation of individual muscle and net muscle contribution in the sagittal plane during the weight-acceptance phase of single-leg jump landing.

Muscles	Mean ± StDev (rad/s^2)		Mean ± StDev (rad/s^2)
Vastus Medialis	37,772 ± 22,820[a]		
Vastus Lateralis	14,632 ± 8,393[b]	Extension (+)	61,312 ± 15,789
Medial Hamstrings	6,301 ± 4,601[b]		
Lateral Hamstrings	2,608 ± 2,509[b,c]		
Medial Gastrocnemius	-18,565 ± 11,534[d]	Flexion (-)	-27,403 ± 6,880
Lateral Gastrocnemius	-8,838 ± 7,957[,d]		

ANOVA identified a significant difference for the mean cumulative summation of the individual muscles (p < 0.001; n = 6).
Symbols a,b,c, and d indicate Tukey's adjusted post-hoc difference (α = 0.05) in mean cumulative summation between the individual muscles. Muscles with the same letters are not significantly different from each other. Conversely, if muscles do not share a letter, the means are significantly different.

Table 9. Mean cumulative summation of individual muscle and net muscle contribution in the transverse plane during the weight-acceptance phase of single-leg jump landing.

Muscles	Mean ± StDev (rad/s^2)		Mean ± StDev (rad/s^2)
Vastus Medialis	2,118 ± 7,120[b]		
Vastus Lateralis	-39,009 ± 23,202[,d]	Internal Rotation (+)	63,849 ± 24,448
Medial Hamstrings	12,914 ± 9,363[a,b]		
Lateral Hamstrings	8,375 ± 4,957[b,c]		
Medial Gastrocnemius	-49,529 ± 31,987[d]	External Rotation (-)	-96,912 ± 21,378
Lateral Gastrocnemius	48,817 ± 46,778[a]		

ANOVA identified a significant difference for the mean cumulative summation of the individual muscles (p < 0.001; n = 6).
Symbols a,b,c, and d indicate Tukey's adjusted post-hoc difference (α = 0.05) in mean cumulative summation between the individual muscles. Muscles with the same letters are not significantly different from each other. Conversely, if muscles do not share a letter, the means are significantly different.

A comparison of the experimental and model computed GRFs data showed that while there were slight deviations between the two, the model computed GRFs followed the experimental GRFs reasonable well (Fig. 16).
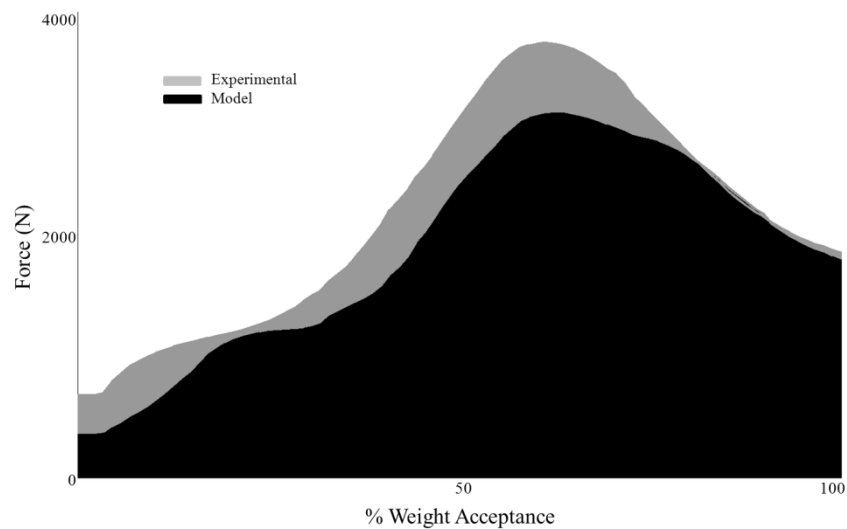
Figure 16. Comparison of the model computed vertical ground reaction forces (black) and the experimentally measured ground reaction forces (gray) for one participant during the weight-acceptance phase of single-leg jump landing.

3.5 Discussion

The objective of this study was to assess the contribution of the muscles surrounding the knee in the frontal, sagittal and transverse planes with particular focus determining the muscles that accelerate the knee into adduction. The results determined that the medial gastrocnemius was the strongest contributor to knee adduction with the vastus medialis also serving to strongly resist knee abduction. Conversely, the lateral gastrocnemius functioned to abduct the knee; however, the total adduction accelerations were greater than the abduction accelerations. The medial and lateral gastrocnemii muscles displayed strong contributions to knee accelerations in all three planes with the medial and lateral quadriceps muscles only exerting strong contributions

to knee extension in the sagittal plane. The large gastrocnemii contributions to knee accelerations, specifically, in comparison to the hamstring muscles, supports the current ACL research that suggests the gastrocnemii should be the muscles targeted for injury prevention programs (Mokhtarzadeh et al., 2013; Podraza et al., 2010; Nyland et al., 2010).

Muscle imbalance is often associated with joint instability (Hewett et al, 2006; Markolf et al., 1978; Solomonow et al., 1987). However, muscle imbalance is not always a negative event. In the sagittal plane, the quadriceps contribution to knee extension is greater than the gastrocnemii muscles contribution to knee flexion. Unfortunately, the ACL is at greater risk for injury when the knee is extended. Alternatively, the frontal plane medial-lateral gastrocnemii imbalance resulted in a net gain in adduction acceleration. And the quadriceps imbalance in the transverse plane produced a net external rotation acceleration. The ACL is not known to be at risk when the knee is adducted and externally rotated (Markolf et al., 1995; Fleming et al., 2001; Shin et al., 2011; Withrow et al., 2006). The quadriceps to gastrocnemii muscle imbalance is the imbalance with the greatest link to potential ACL injury (Boden et al., 2009; Podraza et al. 2010; Mokhtarzadeh et al., 2013). The results from this study suggest that that an increase in gastrocnemii force production has the best chance of contributing to knee flexion acceleration and opposing the quadriceps dominance observed here that is often associated with ACL injury.

The objective of this study was to obtain additional insight into the causal relationship between muscle forces and joint biomechanics specifically with respect to ACL injury risk. Given that elevated knee abduction is often associated with increased ACL injury risk, the results of this study have shown that ACL injury training prevention programs should focus on strengthening the medial gastrocnemius muscle. Researchers have implemented balance, plyometric, resistance and neuromuscular ACL injury training programs; yet, no one type has

stood out as being effective (Hewett et al., 1999; Mandelbaum et al., 2005; Steffen et al., 2008; Wedderkopp et al., 2003). A study by Donnelly et al. (2012b) found that routine Australian Rules Football training was more effective than Australian Rules Football training in conjunction with balance and technique training when comparing peak internal-external rotation and knee valgus moments during running and sidestepping tasks. This indicates that the training the muscles obtain playing the sport is adequate as it does not increasing ACL injury risk. Australian Rules Football is a sport that involves a lot of sidestepping and jumping tasks, which are gastrocnemii dependent movements. Thus ACL injury training prevention programs should focus on putting the athlete's through a series sidestepping, jumping and other gastrocnemii dominant based tasks under unanticipated conditions to improve gastrocnemii strength and muscle activation patterns under game like conditions. While these tasks also involve the lateral gastrocnemius, which was found to abduct the knee, the medial gastrocnemius is larger than the lateral gastrocnemius and produces greater force which resulted in the net adduction acceleration of the knee which is a goal of ACL injury training prevention programs.

Comparison of the GRFs showed that the model GRF did not perfectly match the experimentally recorded GRFs. The reason for this difference can be attributed to limitations in the foot-ground contact model. Foot compression manifests as vertical translational during the impact phase of landing. Neither this translation nor slipping is accounted for in the foot-ground contact model (Dorn et al., 2012). Despite the inability to account for these events in the model, the model GRFs exhibited the same shape of the experimental GRFs and thus we believe that the trends observed in the data are representative of muscle contributions during single-leg jump landing.

Based on these results, the medial gastrocnemius may be the best muscle to target for ACL injury prevention programs since it can generate a large enough acceleration to oppose knee abduction and internal rotation. The lateral gastrocnemius is useful as a knee flexor and in this capacity could potentially resist the anterior translation of the tibia; however, its role in abducting the knee may diminish the significance of the formers contribution to lowering ACL injury risk. Additionally, it was understandable that the hamstrings produced the smallest contributions to knee accelerations in all three planes as they produced significantly smaller maximum forces than the quadriceps and gastrocnemii muscles based on the CMC results from Chapter II. While the hamstrings are knee flexors and should serve to oppose the quadriceps muscles, it appears that increasing the gastrocnemii strength may have a greater effect and should be targeted in future ACL training intervention programs.

3.6 References

Arnold, E.M., Ward, S.R., Lieber, R.L., Delp, S.L., 2010. A model of the lower limb for analysis of human movement. Ann. Biomed. Eng. 38, 269-279.

Besier, T.F., Lloyd, D.G., Ackland, T.R., 2003. Muscle activation strategies at the knee during running and cutting maneuvers. Med. Sci. Sports Exerc. 35, 119-127.

Boden, B. P., Torg, J. S., Knowles, S. B., Hewett, T.E., 2009. Video analysis of anterior Cruciate ligament injury abnormalities in hip and ankle kinematics. Am. J. Sports Med., 37(2), 252-259.

Chappell, J. D., Limpisvasti, O., 2008. Effect of a neuromuscular training program on the kinetics and kinematics of jumping tasks. The American journal of sports medicine, 6(6), 1081-1086.

Delp, S.L., Loan, J.P., Hoy, M.G., Zajac, F.E., Topp, E.L., Rosen, J.M., 1990. An interactive graphics-based model of the lower extremity to study orthopaedic surgical procedures. IEEE Trans. Biomed. Eng. 37, 757-767.

Delp, S.L., Anderson, F.C., Arnold, A.S., Loan, P., Habib, A., John, C.T., Guendelman, E., Thelen, D.G., 2007. OpenSim: open-source software to create and analyze dynamic simulations of movement. IEEE Trans. Biomed. Eng. 54, 1940-1950.

Dempsey, A.R., Lloyd, D.G., Elliott, B.C., Steele, J.R., Munro, B.J., Russo, K.A., 2007. The effect of technique change on knee loads during sidestep cutting. Medicine & Science in Sports & Exercise 39(10), 1765-73.

Dempsey, A.R., Elliott, B.C., Munro, B.J. Steele, J.R. and Lloyd, D.G., 2012. Whole body kinematics and knee moments that occur during an overhead catch and landing task in sport. Clinical Biomechanics 27, 466-74.

Donnelly, C.J., Elliott, B.C., Ackland, T.R., Doyle, T.L., Beiser, T.F., Finch, C.F., Cochrane, J.L., Dempsey, A.R., Lloyd, D.G., 2012a. An anterior cruciate ligament injury prevention framework: incorporating the recent evidence. Res. Sports Med. 20, 239-262.

Donnelly, C.J., Elliott, B.C., Doyle, T.L.A., Finch, C.F., Dempsey, A.R., Lloyd, D.G., 2012b. Changes in knee joint biomechanics following balance and technique training and a season of Australian football. Br. J. Sports Med. 46, 917-922.

Donnelly, C.J., Lloyd, D.G., Elliott, B.C., Reinbolt, J.A., 2012c. Optimizing whole-body kinematics to minimize valgus knee loading during sidestepping: implications for ACL injury risk. J. Biomech. 45, 1491-1497.

Dorn, T. W., Lin, Y. C., Pandy, M. G., 2012. Estimates of muscle function in human gait depend on how foot-ground contact is modelled. Computer methods in biomechanics and biomedical engineering, 15(6), 657-668.

Fleming, B. C., Renstrom, P. A., Beynnon, B. D., Engstrom, B., Peura, G. D., Badger, G. J., Johnson, R. J., 2001. The effect of weightbearing and external loading on anterior cruciate ligament strain. J. Biomech, 34(2), 163-170.

Hamner, S.R., Seth, A., Delp, S.L., 2010. Muscle contributions to propulsion and support during running. J. Biomech. 43, 2709-2716.

Hewett, T. E., Myer, G. D., Ford, K. R., 2006. Anterior cruciate ligament injuries in female athletes part 1, mechanisms and risk factors. The American journal of sports medicine, 34(2), 299-311.

Hewett, T. E., Lindenfeld, T. N., Riccobene, J. V., Noyes, F. R., 1999. The Effect of Neuromuscular Training on the Incidence of Knee Injury in Female Athletes A Prospective Study. The American Journal of Sports Medicine, 27(6), 699-706.

Huston, L. J., Wojtys, E. M., 1996. Neuromuscular performance characteristics in elite female athletes. The American journal of sports medicine, 24(4), 427-436.

Landry, S. C., McKean, K. A., Hubley-Kozey, C. L., Stanish, W. D., Deluzio, K. J., 2009. Gender differences exist in neuromuscular control patterns during the pre-contact and early stance phase of an unanticipated side-cut and cross-cut maneuver in 15–18 years old adolescent soccer players. Journal of Electromyography and Kinesiology, 19(5), e370-e379.

Landry, S. C., McKean, K. A., Hubley-Kozey, C. L., Stanish, W. D., Deluzio, K. J., 2007. Neuromuscular and lower limb biomechanical differences exist between male and female elite adolescent soccer players during an unanticipated side-cut maneuver. The American journal of sports medicine, 35(11), 1888-1900.

Lin, Y. C., Kim, H. J., Pandy, M. G., 2011. A computationally efficient method for assessing muscle function during human locomotion. International Journal for Numerical Methods in Biomedical Engineering, 27(3), 436-449.

Liu, M. Q., Anderson, F. C., Schwartz, M. H., Delp, S. L., 2008. Muscle contributions to support and progression over a range of walking speeds. J. Biomech. 41(15), 3243-3252.

Liu, M. Q., Anderson, F. C., Pandy, M. G., Delp, S. L.,2006. Muscles that support the body also modulate forward progression during walking. J. Biomech., 39(14), 2623-2630.

Mandelbaum, B. R., Silvers, H. J., Watanabe, D. S., Knarr, J. F., Thomas, S. D., Griffin, L. Y., Kirkendall, D. T., Garrett, W., 2005. Effectiveness of a neuromuscular and proprioceptive training program in preventing anterior cruciate ligament injuries in female athletes 2-year follow-up. The american journal of sports medicine, 33(7), 1003-1010.

Markolf, K.L., Burchfield, D.M., Shapiro, M.M., Shepard, M.F., Finerman, G.A., Slauterbeck, J.L., 1995. Combined knee loading states generate high anterior cruciate ligament forces. J. Orth. Res. 13, 930-935.

Markolf, K. L., Graff-Redford A, Amstutz H.C., 1978. In vivo knee stability: aquantitative assessment using an instrumented clinical testing apparatus.J Bone Joint Surg Am. 60, 664-674.

Mokhtarzadeh, H., Yeow, C.H., Goh, J.C.H., Oetomo, D., Malekipour, F., Lee, P.V.S., 2013. Contributions of the Soleus and Gastrocnemius muscles to the anterior cruciate ligament loading during single-leg landing. J. Biomech. 46, 1913-1920.

Nyland, J., Klein, S., Caborn, D.N., 2010. Lower extremity compensatory neuromuscular and biomechanical adaptations 2 to 11 years after anterior cruciate ligament reconstruction. Arthroscopy 26, 1212-1225.

Podraza, J.T., White, S.C., 2010. Effect of knee flexion angle on ground reaction forces, knee moments and muscle co-contraction during an impact-like deceleration landing: implications for the non-contact mechanism of ACL injury. Knee 17, 291-295.

Seedhom, B.B., Longton, E.B., Wright, V., Dowson, D., 1972. Dimensions of the Knee. Radiographic autopsy study sizes require knee prosthesis. Ann. Rheum. Dis. 31, 54-58.

Shin, C. S., Chaudhari, A. M., Andriacchi, T. P., 2011. Valgus plus internal rotation moments increase anterior cruciate ligament strain more than either alone. Med. Sci. Sports Exerc, 43(8), 1484-1491.

Solomonow, M., Baratta, R., Zhou, B. H., Shoji, H., Bose, W., Beck, C., D'ambrosia, R.,1987. The synergistic action of the anterior cruciate ligament and thigh muscles in maintaining joint stability. The American journal of sports medicine, 15(3), 207-213.

Steffen, K., Myklebust, G., Olsen, O. E., Holme, I., Bahr, R., 2008. Preventing injuries in female youth football – a cluster-randomized controlled trial. Scandinavian journal of medicine & science in sports, 18(5), 605-614.

Thelen, D.G., Anderson, F.C., Delp, S.L., 2003. Generating dynamic simulations of movement using computed muscle control. J. Biomech. 36, 321-328.

Thelen, D.G., Anderson, F.C., 2006. Using computed muscle control to generate forward dynamic simulations of human walking from experimental data. J. Biomech. 39, 1107-1115.

Utturkar, G. M., Irribarra, L. A., Taylor, K. A., Spritzer, C. E., Taylor, D. C., Garrett, W. E., DeFrate, L. E., 2013. The effects of a valgus collapse knee position on in vivo ACL elongation. Annals of biomedical engineering, 41(1), 123-130.

Wedderkopp, N., Kaltoft, M., Holm, R., Froberg, K., 2003. Comparison of two intervention programmes in young female players in European handball – with and without ankle disc. Scandinavian journal of medicine & science in sports. 13(6), 371-375.

Withrow, T. J., Huston, L. J., Wojtys, E. M., Ashton-Miller, J. A., 2006. The effect of an impulsive knee valgus moment on in vitro relative ACL strain during a simulated jump landing. Clin. Biomech., 21(9), 977-983.

Zhao, D., Banks, S.A., D'Lima, D.D., Colwell, C.W., Jr., Fregly, B.J., 2007. In vivo medial and lateral tibial loads during dynamic and high flexion activities. J. Orthop. Res. 25, 593-602.

3.7 Appendix

3.7.1 Ground Reaction Force Decomposition

The Moore-Penrose pseudo-inverse method was employed to decompose the GRF. The Moore-Penrose pseudo-inverse method is used in cases where there are multiple solutions to a problem which can arise in an overdetermined system (Lin et al., 2011). This technique uses a weighted least-squares optimization algorithm to compute the individual muscle contribution during the desired task (Lin et al., 2011; Dorn et al., 2012). Equations 3.2-3.4 are involved with the construction of the system matrices and calculating the inverse of these matrices which yield the computed generalized joint accelerations $\left(\ddot{q}^{\alpha}\right)$.

$$\begin{bmatrix} M & -E \\ W \cdot E^T & 0^{3fx3f} \\ 0_{3fxn} & W^{-1} \end{bmatrix} \left\{ \begin{matrix} \ddot{q}^{\alpha} \\ F_{ext}^{\alpha} \end{matrix} \right\} = \left\{ \begin{matrix} F^{\alpha} \\ W \cdot K^{\alpha} \\ 0_{3fx1} \end{matrix} \right\} \quad (3.2)$$

$$A \left\{ \begin{matrix} \ddot{q}^{\alpha} \\ F_{ext}^{\alpha} \end{matrix} \right\} = b \quad (3.3)$$

$$\left\{ \begin{matrix} \ddot{q}^{\alpha} \\ F_{ext}^{\alpha} \end{matrix} \right\} = A^+ b \quad (3.4)$$

M = mass matrix
E = jacobian matrix that maps the external foot contact point forces
F_{ext}^{α} = external foot contact point forces
$\ddot{q}^{\alpha}$ = generalized joint accelerations
W = foot contact point weighting matrix
K = foot point constraints

3.7.2 Foot-Ground Contact Model

Lin et al. (2011) and Dorn et al. (2012) modeled the foot-ground interaction using a five contact point foot-ground model- two contact points were at the medial and lateral sides of the

mid calcaneus (heel), two at the first and fifth metatarsals junctions and one at the toe (Fig. 17). Each contact point was modeled as a rigid contact (i.e. weld joint) leaving the foot unable to accelerate in any direction. To eliminate these discontinuities that would occur when the foot is not in contact with the ground Dorn et al. (2011) utilized a diagonal weight matrix that applied a linear (foot) acceleration constraint to each contact point. These weightings varied from 0 (unconstrained) to 1 (fully constrained, rigidly constrained) based on the contact points location to the center of pressure (CoP) (Dorn et al., 2012).
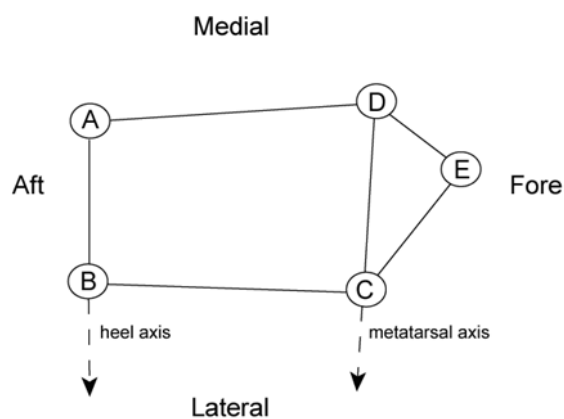
Figure 17. Five ground contact points (per foot) are defined by markers in OpenSim (Lin et al., 2011).

The four phases encountered in this foot-ground contact model were model as a function of CoP location. Phase 1 begins when the CoP lied behind the heel of the foot (i.e. behind A B heel axis). During this phase the AB axis was modeled as a hinge joint and those points were fully constrained. Phase 2 starts when the CoP lies closer to the heel axis within the posterior half of the ABCD section of the foot. During this period, the AB points were again fully constrained while the φ weighting function (Eq. 3.5) was applied to the CD points to model that transition from Phase 1 to Phase 2. When Phase 3 commences, the CoP lies anteriorly in the ABCD section closer to the fore-foot. Here $2(1-\varphi)$ was used to model the transition to Phase 3 on the AB points

while points C and D were fully constrained. The final phase initiates when the CoP lies within

the forefoot (toe) region of the foot model within points CDE. During this period the weighting

function was applied at point E, while 1- γ described the interaction at points C and D. Figure 18

provides a visual representation of the aforementioned phases. Details about the weighting

functions are further described below (Eq. 3.5-3.6).
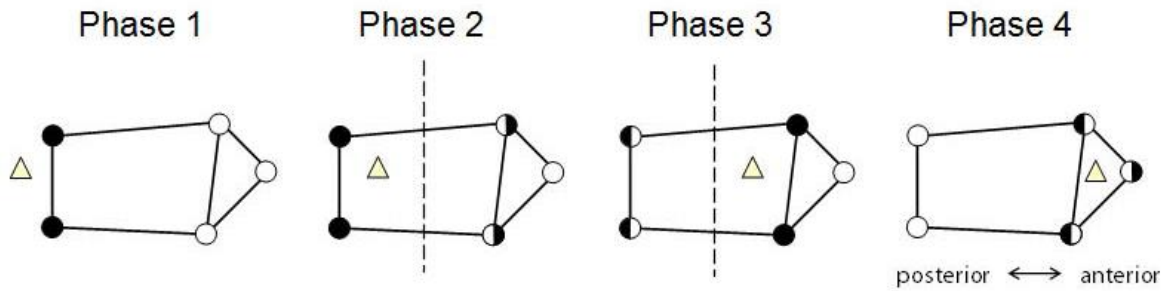
Figure 18. Representation of the four phases of the foot-ground contact model. Here the circles represent the five foot-ground contact points and the triangle is the center of pressure (Dorn et al., 2012).

$$\varphi(d_h, d_m) = \frac{d_h}{d_h + d_m} \quad (3.5)$$

$$\gamma(d_m, d_E) = \frac{d_m}{d_E} \quad (3.6)$$

d_h = shortest distances from the CoP to the heal axis (AB)
d_m = shortest distances from the CoP to the metatarsal axis (CD)
d_E = shortest distance from point E to the metatarsal axis (CD)

CHAPTER IV

DYNAMIC KNEE STABILITY AND PRINCIPAL COMPONENT ANALYSIS: METHODOLOGY FOR ASSESSING ANTERIOR CRUCIATE LIGAMENT INJURY RISK

4.1 Abstract

Anterior cruciate ligament (ACL) injuries are common sports injuries, costing the US economy roughly $1.5 billion per year. To reduce this burden, researchers generally analyze an athlete's joint motion and muscle activation during movements where non-contact ACL injuries have been shown to occur to better understand the underlying mechanisms of ACL injury. To assess an individual's dynamic joint stability during the weight-acceptance phase of single-leg jump landing, Nyquist and Bode stability criteria were applied to quantify frontal plane knee stability. Principal component analysis (PCA), a statistical tool that analyzes multiple waveforms to determine the source of variability between them, was used to analyze an athlete's joint motions and muscle activation waveform patterns to determine if individuals with stable, marginally stable and unstable joint biomechanics adopted different motor recruitment strategies. The unstable group's maximum knee abduction moments were significantly greater than the marginally stable and stable maximum knee abduction moments ($p < 0.001$). Additionally, a frequency analysis quantified joint oscillations that were found to be associated with joint instability. The PCA found that the unstable group muscle activations reported larger medial-lateral and knee flexor-extensor muscle activation imbalances than the stable group. These findings provided added insight into how muscles are used to support the knee during single-leg landing and helped endorse the use of the Nyquist and Bode stability criteria and PCA as a unique methodology for both screening individuals for ACL injury and designing muscle targeted ACL injury prevention protocols to mitigate ACL injury risk.

4.2 Introduction

Anterior cruciate ligament (ACL) injuries are a common sports injury occurring in one in every 3,000 individuals (Boden et al, 2000). An ACL injury results in a loss of (translational and rotational) joint stability that is critical to the successful execution of dynamic movements like single-leg jump landing; however, appropriate muscle activation has the capacity to reduce the loads exerted on the ACL while supporting and stabilizing the knee (Donnelly et al, 2012; Lam et al., 2009; Veltri et al., 1995). Researchers have implemented injury prevention protocols that focused on altering muscle function; yet ACL injury rates continue to rise (Donnelly et al. 2012). Therefore a better understanding of the relationship between joint stability and muscle function is needed.

Dynamic knee stability assessments are used to determine an athlete's return to sport post ACL injury but dynamic stability assessments may be equally effective pre injury as the majority of ACL injuries occur during dynamic movement (Lam et al., 2009). Since dynamic knee stability is used as a metric to assess an individual's ability to return to sport, it is possible that researchers could develop a new metric to quantify dynamic knee stability to help screen individuals for potential ACL injury risk. In the field of controls, stability is a quantifiable measurement of the performance of dynamic systems where a stable system has a bounded input and produces a bounded output (Dorf and Bishop, 2008). Nyquist and Bode stability criteria are techniques that provide graphical and quantitative measures of dynamic stability (Dorf and Bishop, 2008). These techniques have proven effective in assessing postural and aircraft stability and were used to assess knee stability and potential ACL injury risk (Dorf and Bishop, 2008; Haggerty et al., 2012; Hur et al. 2010; Sun et al., 2008). The interaction between the musculoskeletal and neuromuscular systems can be modeled as a feedback control loop (Park et

al., 2004). Here the joint motion serves as the system input where the central nervous system detects disturbances that elicit a response from muscles to stabilize the system. Once stability groups are defined, we can address the systems response to joint instability by identifying how muscle activation strategies vary amongst at-risk individuals.

Principal component analysis (PCA) is a valuable statistical analysis tool used to detect the source of variability within a dataset (Daffertshofer et al, 2004). This method has been successfully applied in clinical settings to 1) identifying differences in lifting kinematics and kinetics between healthy individuals and lower back pain populations; 2) distinguishing between frontal plane kinetics of male and female subjects during unanticipated cutting maneuvers; and 3) assessing the success of two total hip arthroplasty surgical approaches in restoring the normal gait patterns post-surgery (Mantovani et al., 2012; O'Connor et al., 2009; Wrigley et al., 2006). The success of PCA in these clinical applications provides a rationale for its use in identifying specific muscle recruitment strategies specific to populations with stable, marginally stable and unstable joint biomechanics.

This study employs classical control stability techniques along with PCA to quantify dynamic joint stability and associated muscle function in individuals. This study has two objectives. The first is to use Nyyquist and Bode stability criteria to identify individuals at varying risk of ACL injury based on their dynamic knee stability. The second is determine muscle activation strategies distinct to individuals with stable, marginally stable and unstable joint biomechanics during the WA phase of single-leg jump landing. It is hypothesized that unstable individuals will adopt a balanced co-contraction between the medial and lateral vasti, hamstring and gastrocnemii muscles compared to the marginally stable and unstable groups. The

84

goal is to use this methodology to design more effective ACL screening and injury prevention training protocols.

4.3 Methodology

4.3.1 Experimental Protocol and Data Collection

Amateur male Western Australian Rules Football players were recruited to complete a single-leg jump landing protocol (Donnelly et al, 2012b). Five athletes (age 20 ± 1 years; height 1.90 ± 0.1m; mass 87.1 ± 5.4kg) were randomly selected from the aforementioned cohort. Six trials were analyzed per each participant; two per each ball swing direction for a total of 30 trials for the subsequent analysis (Donnelly et al., 2012c). For the single-leg jump landing protocol, subjects were instructed to jump from their preferred leg and while in flight, grab an Australian football that was randomly swung medially, laterally or held central to the subjects approach direction before landing on the force platform with their takeoff leg, which was the right leg for all participants (Dempsey et al., 2012). The height of the ball was approximately 90% of each subject's maximal vertical jump height. All of the experimental procedures were approved by the University of Western Australia Human Research Ethics Committee and all subjects provided their informed written consent prior to data collection.

Experimental kinematic marker trajectories, GRF, and surface electromyography (sEMG) data were collected from each subject during the single-leg jump landing task. Three-dimensional, full-body kinematics were recorded using a12-camera, 250 Hz VICON MX motion capture system (VICON Peak, Oxford Metrics Ltd., UK) (Donnelly et al., 2012c, Dempsey et al. 2007). The GRF data were synchronously recorded at 2,000 Hz using an AMTI (Advanced Mechanical Technology Inc., Watertown, MA) 1.2 x 1.2m force platform. Both the kinematic and GRF data were low-pass filtered at 20 Hz using a zero phase-shift 4th-order Butterworth digital

filter in Workstation (ViconPeak, Oxford Metrics Ltd., UK). sEMG data were collected at 2,000 Hz for six muscles: vastus medialis, vastus lateralis, medial and lateral gastrocnemii and medial and lateral hamstrings. The medial and lateral vasti muscles were measured to represent the quadriceps muscle group. The raw experimental sEMG data were filtered with a zero phase-shift 4th-order Butterworth filter between 30 and 500 Hz, full wave rectified and then low-pass filtered using a zero phase-shift 4th-order Butterworth digital filter at 6 Hz to create linear envelopes. Following linear enveloping, peak muscle activation from each muscle (n=6) recorded during any of the nine landing conditions was used to normalize each muscle's sEMG signal to 100% activation. The result is a sEMG waveform from zero to full activation.

4.3.2 Subject-Specific Models and Simulations

Five three-dimensional 14-segment, 37 degree-of-freedom (DoF) subject-specific models were created in OpenSim 1.9.1 to generate simulations of the participants performing single-leg jump landings (Fig. 19) (Delp et al. 2007). The knee rotated in all three planes and sagittal and transverse plane translations were modeled as a function of knee angle (Donnelly et al., 2012b; Delp et al., 1990). The model's segment lengths and mass were scaled to each subject. And the joint kinematics were calculated from experimental kinematic marker data using inverse kinematics (IK). Residual reduction analysis (RRA) was used to create dynamically consistent simulations with the experimentally recorded ground reaction forces (Donnelly et al., 2012c). These dynamically consistent simulations were analyzed during the weight-acceptance (WA) phase of single-leg jump landing. The WA phase of landing was analyzed since this is the period when knee valgus and internal rotation moments acting on the knee are the highest and thought to be when the ligament is at the greatest risk of injury (Donnelly et al., 2012c; Dempsey et al., 2007).
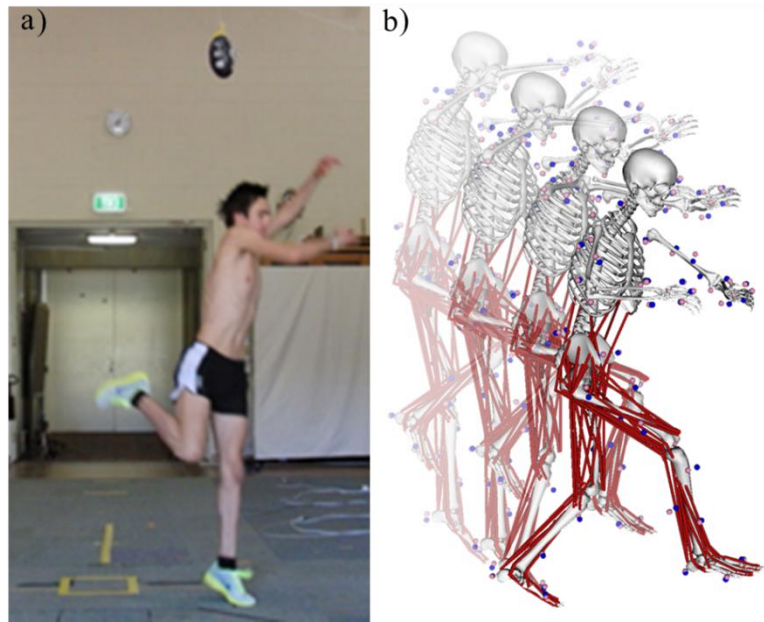
Figure 19. (a) Subject performing the experimental single-leg jump landing protocol in the laboratory. (b) Simulation of single-leg jump landing task using a three-dimensional, 14-segment 37 degrees-of-freedom (DoF) model.

4.3.3 Stability Analysis and Classification

Participant trials were classified as having stable, marginally stable and unstable joint biomechanics using Nyquist and Bode Stability Criteria. A transfer function was needed to perform the Nyquist and Bode stability criteria analyses. A transfer function is the ratio of the systems output to the systems input. To create the transfer function, first a regression analysis of the kinematic and the kinetic sagittal, frontal and transverse knee waveform data was performed to generate a time dependent mathematical model of the waveforms. This time dependent model output was then converted using Laplace transform to develop an open loop transfer function. For the open loop transfer function, the output function was the kinematic and kinetic waveforms while a unit impulse function served as the input function to represent the rapid, jump take-off.

The final analytical step involved evaluating the stability of the open loop model using the aforementioned stability methods.

The Nyquist Stability Criterion employs Cauchy's theorem that maps the transfer function into the complex plane (Dorf and Bishop, 2008). This theorem determines systems stability based on the poles lying in the right half of the complex plane and the number of encirclements of the point (-1, 0) (Dorf and Bishop, 2008). For those cases where no poles are present in the right half plane, a system is stable if it does not encircle (-1, 0); otherwise it is unstable (Dorf and Bishop, 2008). The Bode stability criterion was used to further delineate a marginally stable group. This approach calculates the gain and phase margins that measure the displacement from unstable behavior and estimates critical frequencies in the data, respectively. Positive gain and phase margins indicate stable systems, while negative gain and phase margins indicate an unstable system (Kuo and Golnaraghi 2003). Marginally stable systems were those where one of the gain and phase margins was positive while the other was negative. Participant trials were classified as stable, marginally stable or unstable based on frontal plane kinetic stability analysis as frontal plane biomechanics are predictors of ACL injury risk (Hewett et al. 2005). The means of the sagittal, frontal and transverse plane kinetics and sEMG data were plotted to observe differences between the stability groups. All moments in the study are external moments. The mean number of critical frequencies and the mean frequencies were calculated to assess differences across joint stability groups. The three-parameter lognormal probability plot was generated to display the distributional properties of the frequencies for the stability groups.

4.3.4 Principal Component Analysis and Muscle Activation Assessment

PCA was used to identify waveform variability within frontal plane knee kinetics and sEMG data. To perform the analysis matrices were created to determine the variability between

the stability groups amongst the aforementioned variables. In these matrices the rows were time normalized to 101 points and the columns were of the kinetic and sEMG variables for the stable, marginally stable, and unstable groups.

First the mean was subtracted from each observation for each variable. Next, the covariance matrix was calculated from which the eigenvalue-eigenvector pairs were derived. These eigenvalue-eigenvector pairs represent the PC loadings and principal components (PCs); respectively. The PCs were placed in order from highest to lowest based on their associated loadings. PC 1 represented the PC with the largest associated loading that accounted for the greatest percentage of variance in the data. The first three PCs for each variable were assessed to ensure that a minimum of 90% of the variance was explained with those PCs while also ensuring a consistent comparison across groups (Jolliffe 2002). The PCs generated represent the data in the new rotated space (Jolliffe 2002). These PCs are then used to observe the variations in the data (Lee et al., 2010). Principal components for stable, marginally stable and unstable frontal plane knee kinetics and sEMG data were plotted against each other to assess differences in amplitude, phase shift and oscillatory behavior between the biomechanical waveforms. The stability and PCA analyses were performed using Matlab (MATLAB R2012a, The MathWorks, Inc., Natick Massachusetts, USA).

A one-way ANOVA was performed to compare mean joint and sEMG data maximums and end of WA values across all three stability groups. A Fisher post-hoc analysis was conducted to determine if observed differences were significant ($\alpha = 0.05$). The aforementioned analyses were performed in Minitab.

4.4 Results

Three participant trials were deemed to have stable frontal plane joint kinetics while seventeen and ten were found to have marginally stable and unstable kinetics, respectively. In the frontal plane, the unstable groups' maximum abduction moment (1.74±0.82Nm/kg) was significantly greater than the stable (0.48±0.35Nm/kg) and marginally stable groups (1.20±0.53Nm/kg) (Fig. 20, Table 10). The stable group exhibited a consistently larger flexion angle than the unstable group throughout the WA phase. In the transverse plane knee kinematic deviations were largest at the beginning of WA but dropped to 5.9° at the end of WA.
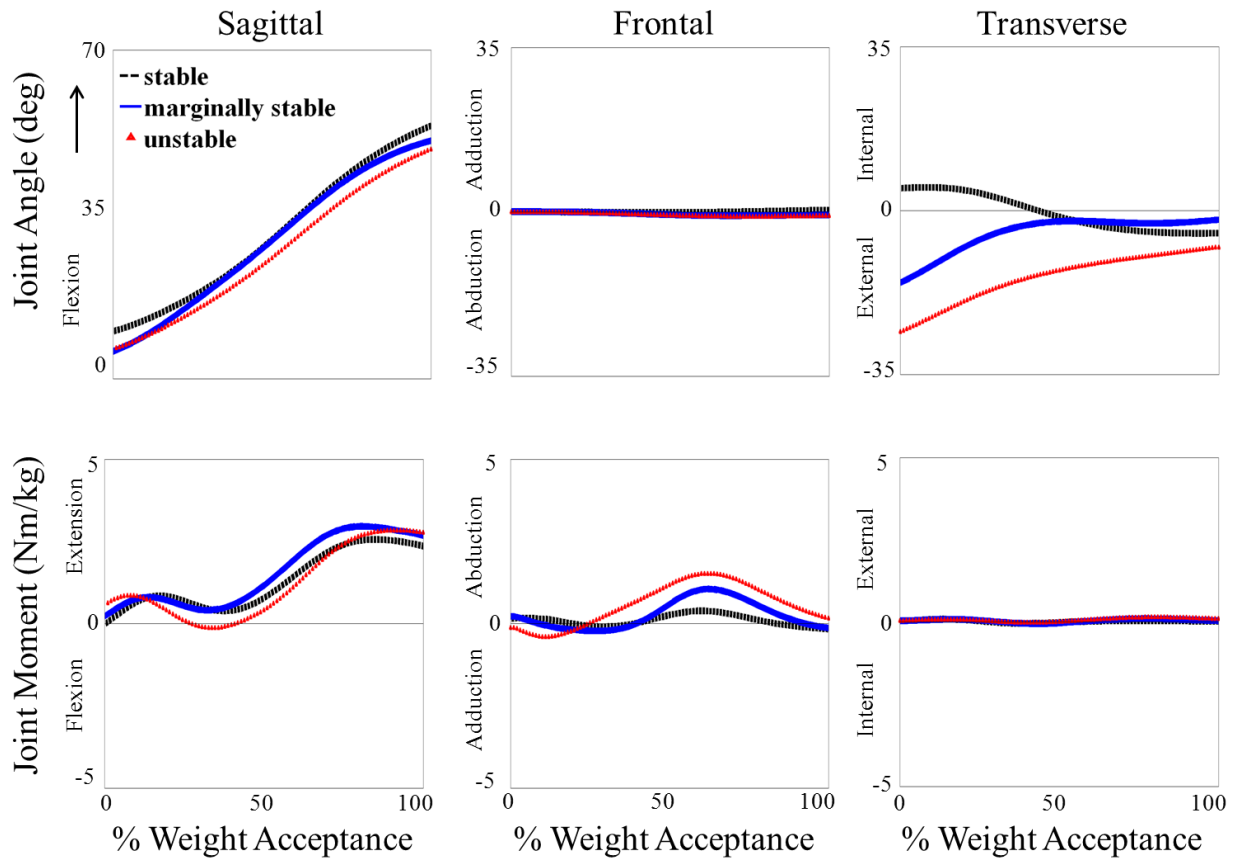
Figure 20. Mean sagittal, frontal and transverse plane knee kinematics (top row) and kinetics (bottom row) of the stable (black dashed line), marginally stable (blue solid line) and unstable (red triangle) groups based on frontal plane knee kinetics during the weight-acceptance phase of single-leg jump landing.

Table 10. Comparison of sagittal, frontal and transverse plane kinetics for the stable, marginally stable and unstable participant groups.

	Stable	Marginally Stable	Unstable
Knee extension/flexion (Nm/kg)			
Maximum extension (+)	2.71±0.36	3.09±0.60	2.93±0.52
Maximum flexion (-)	-0.09±0.35	-0.16±0.54	-0.40±0.58
End WA of phase	2.36±0.68	2.68±0.65	2.78±0.51
Knee abduction/adduction (Nm/kg)			
Maximum abduction (+)	0.48±0.35[a]	1.20±0.53[a]	1.74±0.82[b]
Maximum adduction (-)	-0.34±0.07	-0.52±0.40	-050±0.40
End WA of phase	-0.16±0.18	-0.12±0.37	0.17±0.52
Knee internal/external rotation (Nm/kg)			
Maximum external rotation (+)	0.11±0.04	0.15±0.10	0.20±0.10
Maximum internal rotation (-)	-0.07±0.09	-0.08±0.09	-0.04±0.06
End WA of phase	0.19±0.05	0.04±0.13	0.10±0.10

ANOVA identified a significant difference for the maximum and end of WA phase values of the individual knee kinetics ($p < 0.001$).
Symbols a,b indicate Fisher's adjusted post-hoc difference ($\alpha = 0.05$) in mean kinetics estimates between the stability groups. Estimates with the same letters are not significantly different from each other. Conversely, if estimates do not share a letter, the means are significantly different.

PC 1 detected the same amplitude differences in frontal plane kinetics that were also observed when comparing the mean maximum abduction moments (Table 10) as the unstable group reported a maximum abduction moment almost 5 times larger than the stable group (Fig. 21). PC 1 also exposed timing differences between the stability groups as the marginally stable and unstable groups reached maximum adduction moment earlier than the stable group but generated a delayed maximum abduction moment compared to the stable group. For PC 2 the stable group exhibited minimal oscillatory behavior compared to the two other stability groups having an overall decreasing slope (Fig. 21). The marginally stable and unstable groups both displayed strong oscillatory behavior of seemingly similar amplitudes; however, their respective waveforms were phase shifted 180°. PC 3 revealed oscillatory behavior in all three stability groups with delayed peak moments for the stable group (Fig. 21).
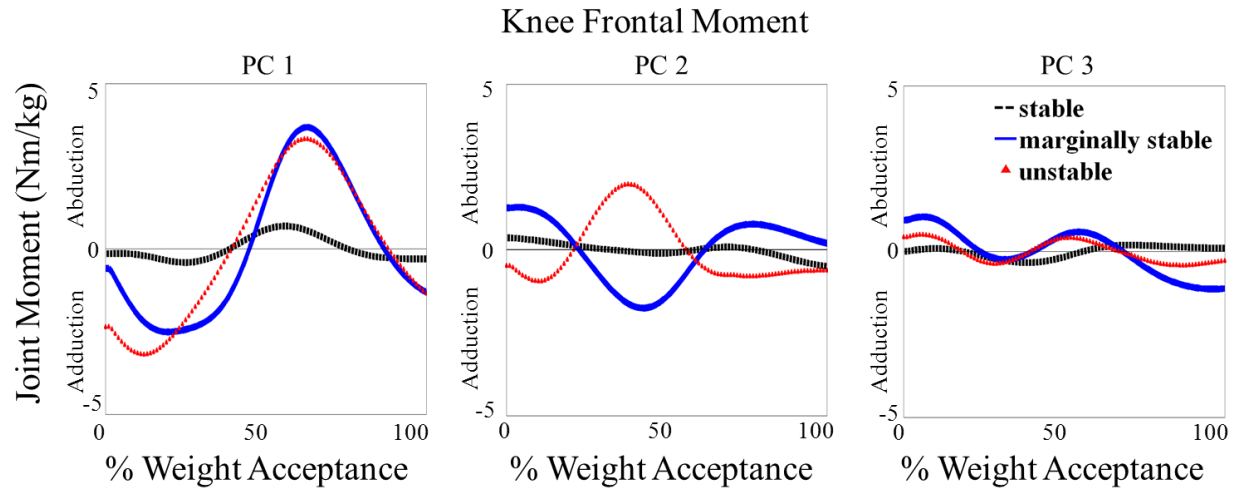
Figure 21. Comparison the first three principal components (PCs) for the stable (black dashed line), marginally stable (blue solid line) and unstable (red triangles) groups during the weight-acceptance phase of single-leg jump landing.

The mean number of frequencies for the stable, marginally stable and unstable groups was 9.7 ± 1.5 rad/s, 10.3 ± 1.3 rad/s and 10.8 ± 1.5 rad/s, respectively (Table 11). And the mean frequency range for the stable group was 50.9 ± 27.5 rad/s, for the marginally stable group was 65.8 ± 40.0 rad/s and the unstable group was 58.9 ± 12.4 rad/s. The aforementioned differences were not significant. The frequencies for the three stability groups follow a three-parameter lognormal distribution with a scale parameter of approximately 1.2 (Table 12). The lower and upper tail values for the marginally stable and unstable groups deviated from the fitted distribution line and fall outside of the 95% confidence bounds (Fig. 22, Table 12).

Table 11. Comparison of the number of frequencies and frequency range for the stable, marginally stable and unstable participant groups computed from the stability frequency analysis.

Frequency	Stable	Marginally Stable	Unstable
Number of Frequencies	9.7 ± 1.5	10.3 ± 1.3	10.8 ± 1.5
Range	50.9 ± 27.5	65.8 ± 40.0	58.9 ± 12.4

93
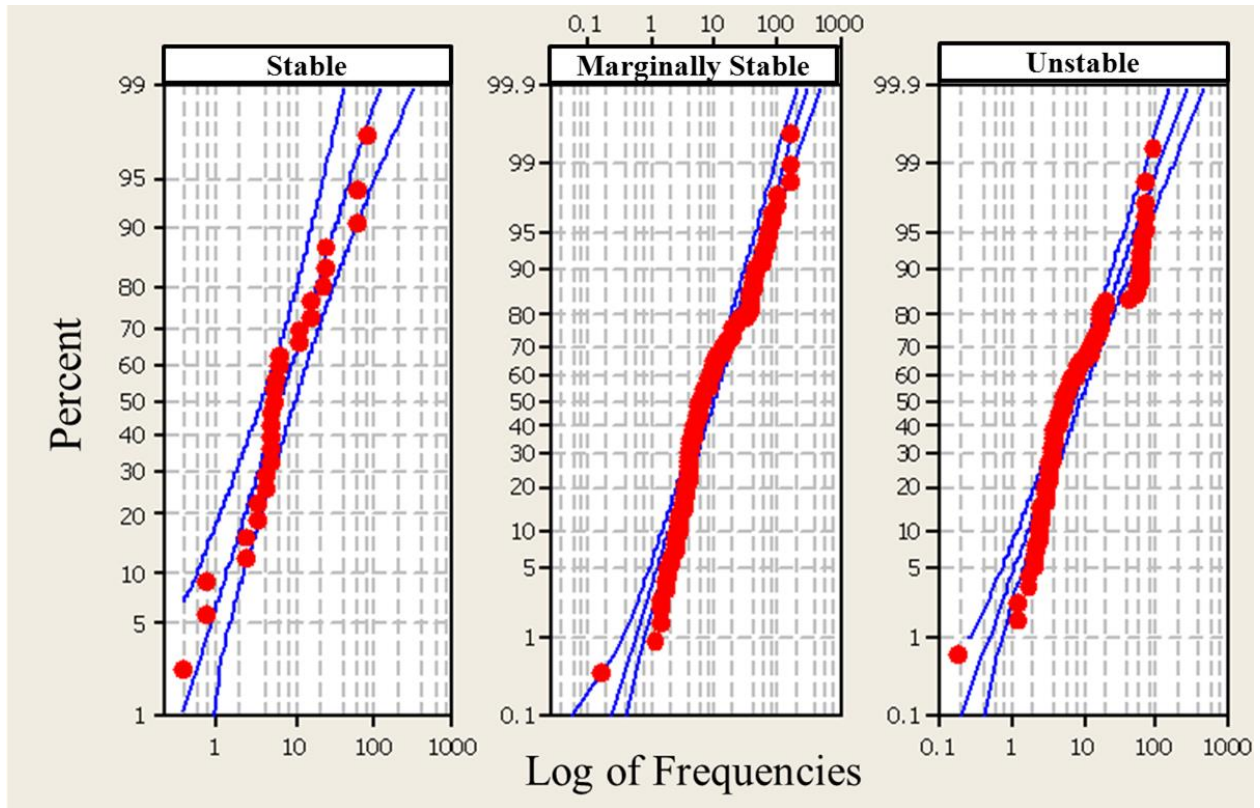
Figure 22. Three-parameter lognormal distribution plot of the stable, marginally stable and unstable group frequencies and 95% confidence bounds for each fitted distribution line. Although plotted on a logarithmic scale the data is the natural log of the frequency minus the threshold and follows a normal distribution with mean (location) and standard deviation (scale).

Table 12. Comparison of location, scale and threshold parameters from the 3-parameter lognormal distribution plot for the stable, marginally stable and unstable groups.

Stability Groups	3 Parameters for Log-Normal Distribution		
	Shape	**Scale**	**Threshold**
Stable	1.866	1.241	6.189
Marginally Stable	2.148	1.175	6.808
Unstable	1.969	1.171	7.935

Mean normalized muscle activation of medial and lateral vasti, hamstring and gastrocnemii muscles showed similar activation patterns across all stability groups (Fig. 23). The medial and lateral gastrocnemii produced the strongest activation at initial contact while the medial and lateral vasti had the greatest activation at the end of WA (Table 13). The medial and lateral hamstrings produced slightly lower activations compared to the vasti and gastrocnemii muscles. The most observable difference in muscle activation among stability groups was that the vastus lateralis produced stronger activations than vastus medialis in the stable group while the reverse was true for the marginally stable and unstable groups.
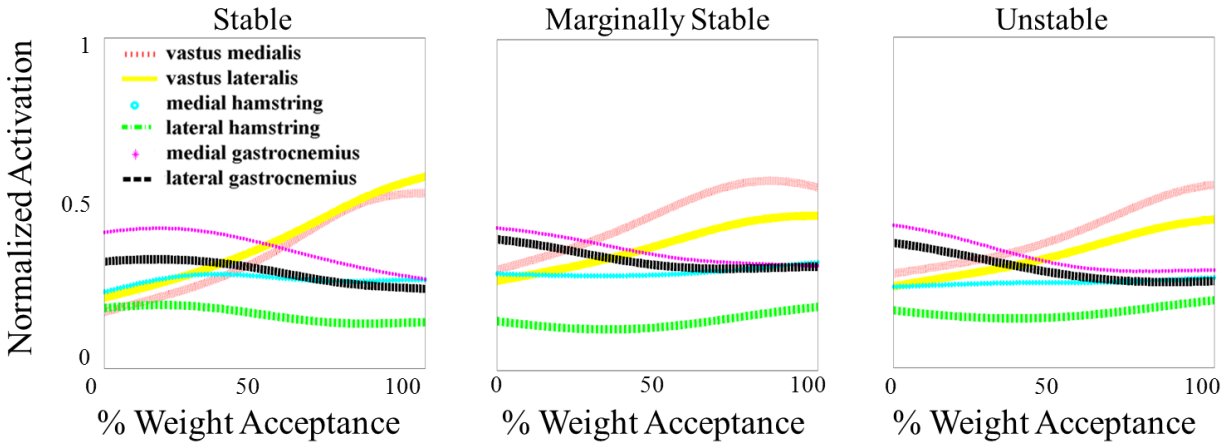
Figure 23. Comparison of the mean experimental surface electromyography (sEMG) data across the stable, marginally stable and unstable groups for the six muscles crossing the knee during the weight-acceptance phase of single-leg jump landing. Stability was based on frontal plane knee kinetics. Experimental filtered sEMG data for the vastus medialis, vastus lateralis, medial hamstring, lateral hamstrings, medial gastrocnemius and lateral gastrocnemius are individually normalized to the maximum recorded signal of each muscle over one of the landing trials.

Table 13. Comparison of surface electromyography data between the stable, marginally stable and unstable groups.

Initial Contact			
Muscle	**Stable**	**Marginally Stable**	**Unstable**
Vastus Medialis	0.17 ± 0.06	0.30 ± 0.17	0.28 ± 0.15
Vastus Lateralis	0.21 ± 0.06	0.27 ± 0.12	0.25 ± 0.10
Medial Hamstring	0.23 ± 0.10	0.29 ± 0.24	0.24 ± 0.25
Lateral Hamstring	0.18 ± 0.09	0.15 ± 0.09	0.17 ± 0.09
Medial Gastrocnemius	0.41 ± 0.07	0.43 ± 0.18	0.43 ± 0.20
Lateral Gastrocnemius	0.32 ± 0.07	0.40 ± 0.18	0.38 ± 0.20
End of Weight Acceptance Phase			
Muscle	**Stable**	**Marginally Stable**	**Unstable**
Vastus Medialis	0.53 ± 0.17	0.55 ± 0.18	0.55 ± 0.17
Vastus Lateralis	0.37 ± 0.11	0.47 ± 0.11	0.45 ± 0.10
Medial Hamstring	0.27 ± 0.12	0.33 ± 0.24	0.27 ± 0.26
Lateral Hamstring	0.14 ± 0.09	0.19 ± 0.08	0.20 ± 0.09
Medial Gastrocnemius	0.27 ± 0.10	0.32 ± 0.16	0.30 ± 0.13
Lateral Gastrocnemius	0.24 ± 0.10	0.31 ± 0.19	0.26 ± 0.18
Maximum			
Muscle	**Stable**	**Marginally Stable**	**Unstable**
Vastus Medialis	0.54 ± 0.20	0.60 ± 0.19	0.56 ± 0.17
Vastus Lateralis	0.58 ± 0.10	0.48 ± 0.12	0.46 ± 0.10
Medial Hamstring	0.34 ± 0.01	0.37 ± 0.26	0.30 ± 0.26
Lateral Hamstring	0.22 ± 0.08	0.23 ± 0.08	0.24 ± 0.07
Medial Gastrocnemius	0.43 ± 0.06	0.45 ± 0.18	0.46 ± 0.18
Lateral Gastrocnemius	0.34 ± 0.05	0.41 ± 0.18	0.38 ± 0.20
Minimum			
Muscle	**Stable**	**Marginally Stable**	**Unstable**
Vastus Medialis	0.17 ± 0.06	0.30 ± 0.16	0.28 ± 0.15
Vastus Lateralis	0.21 ± 0.06	0.27 ± 0.12	0.25 ± 0.10
Medial Hamstring	0.17 ± 0.07	0.25 ± 0.22	0.22 ± 0.24
Lateral Hamstring	0.10 ± 0.03	0.10 ± 0.04	0.13 ± 0.06
Medial Gastrocnemius	0.27 ± 0.09	0.29 ± 0.14	0.25 ± 0.12
Lateral Gastrocnemius	0.23 ± 0.08	0.27 ± 0.17	0.24 ± 0.19

Amplitude differences observed as deviations from zero were strongest in the marginally stable and unstable groups compared to the stable group for all three PCs (Fig. 24). PC 1 detected the opposing function of the knee flexor (hamstrings and gastrocnemii) and extensor (vasti) muscles. The hamstrings muscles varied most in PC 1 as they opposed the gastrocnemii

activation in the marginally stable group while the medial hamstring opposed the lateral hamstring in the unstable group. The vastus medialis and medial hamstring opposed their lateral counterparts in PC 2 (Fig. 24). PC 2 also exposed a 180° phase shift between the muscles observed across all three stability groups. The notable trend for PC 3 was the oscillatory behavior of the muscle activations amongst the stability groups (Fig. 24). Although the oscillations increased across all stability groups the amplitudes decreased thus masking major differences in muscle activation patterns between the muscles.
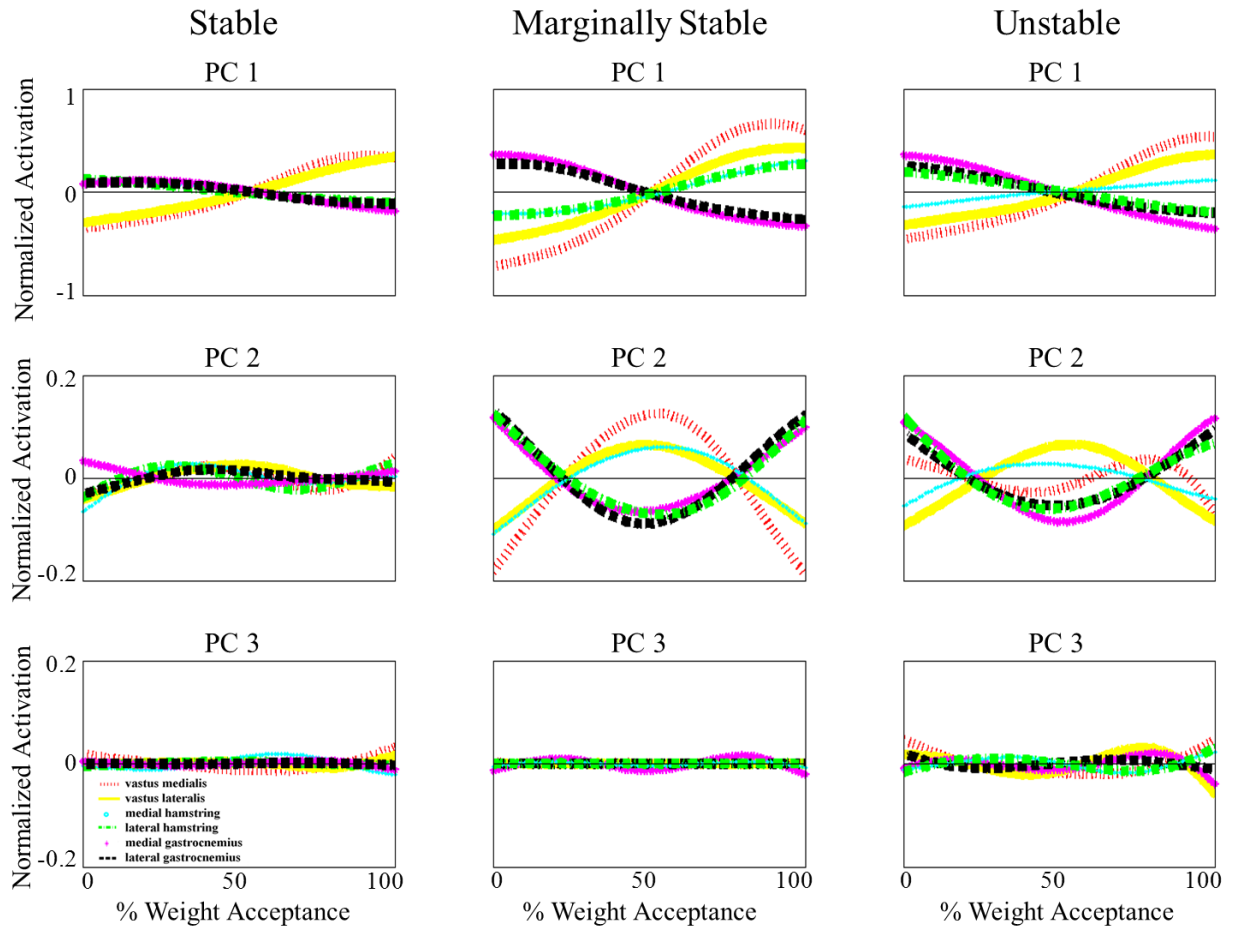
Figure 24. Comparison of the first three principal components (PCs) for the experimental surface electromyography (sEMG) data for six muscles crossing the knee during the weight-acceptance phase of single-leg jump landing for the stable, marginally stable and unstable groups based on frontal plane knee kinetics.

4.5 Discussion

Both the stability and PCA analyses found the large maximum knee abduction moment exhibited by the unstable group to be a significant factor associated with joint instability. The mean maximum knee abduction moments generated by the unstable and marginally stable were greater than abduction moments generated by individuals who have suffered an ACL injury thus these individuals exhibited landing biomechanics that placed them at elevated risk for ACL injury (Hewett et al., 2005). A secondary feature associated with joint instability was the identification of potentially dangerous frontal plane frequencies. These frequencies represent the oscillations or rapid transition between frontal plane adduction and abduction orientation during landing. The probability plots showed that the upper and lower tail frequencies fell outside the confidence bounds thus indicating that those frequencies may lead to greater frontal plane instability. This oscillatory frontal plane behavior has been observed in at-risk biomechanics but had not been quantified as in this study (Ford et al., 2006, Hewett et al., 2005, McLean et al., 2004). ACL injuries are characterized by small knee flexion angles and increased knee abduction (valgus) moment which were traits of the unstable group in this study (Cochrane et al., 2007, Koga et al, 2010, Krosshau et al., 2007). These findings help support the use of these stability techniques as a dynamic joint stability classification methodology.

Mean sEMG analysis found that greater vastus lateralis activation and a delayed interaction between the vasti and gastrocnemii muscles as the strongest differences in muscle activation between the stability groups. PC 2 detected both a medial-lateral vasti and hamstring imbalance. Medial-lateral vasti and hamstring imbalance was found to contribute to elevated abduction moments as shown by the elevated maximum abduction moments of the marginally stable and unstable groups where the imbalance was the strongest. The knee flexor-extensor

imbalance observed in PC 1 corresponded to the differences in sagittal plane biomechanics kinetics among the stability groups with the unstable group reporting smaller knee flexion angles than the stable group. Research has shown that smaller knee flexion angles limit the medial vasti and hamstring muscles ability to resist an external abduction moment (Lloyd and Buchanan et al., 2001). The aforementioned muscle activation imbalances and their corresponding joint biomechanics support that research. Moreover the alternating hamstring activation in the marginally stable and unstable groups may reflect the role hamstrings play in joint stability during landing, a common belief in ACL injury literature (Blackburn et al., 2013; Donnelly et al., 2012; Lloyd & Buchanan 2001; Riemann and Lephart, 2002; Withrow et al., 2008). The oscillatory behavior of all of the muscles in PC 3 matched the joint oscillations and frequencies observed and quantified in the joint stability and PCA analyses (Figs. 18 and 21). During landing muscles function as shock absorbers and PCA may have shown how muscles function to dissipate the underlying joint oscillations (Yeow 2013; Zhang et al., 2000). The sEMG PCA detected differences in amplitude, phase shift and oscillatory behavior in the muscles that were attributed to differences in muscle activation strength, function and energy dissipation capacity. These findings support a relationship between the musculoskeletal and neuromuscular systems that were not obtained by analyzing mean sEMG data alone. Based on these results the muscle-targeted training programs should focus on coordinating the activation between the knee flexor-extensors and medial-lateral muscles with emphasis on the medial hamstring muscle.

The muscle activation patterns exhibited by the marginally stable and unstable groups may be in response to altered landing kinematics and kinetics at initial contact. Although the differences in sagittal, frontal and transverse plane joint kinematics and kinetics decreased between the stability groups by the end of WA phase they were not equal. Thus the marginally

stable and unstable activation patterns were still not ideal. While greater muscle activation may be needed to overcome initial unstable joint biomechanics it is possible that the muscle activation prior to landing should be analyzed. Studies have analyzed jump landing motor strategies and recognized that to execute a successful jump landing is dependent upon the muscle coordination during all phases: take-off, flight and landing (Mrdakovic et al., 2008; Viitasalo et al., 1998; Wikstrom et al., 2007). This information indicates that future work should investigate muscle activation at take-off and flight as well.

Here the stability criteria determined that 33% of the trials performed showed unstable motion; however, while current ACL injury rates are increasing they are not that high. In this study, joint instability does not imply ACL injury but rather the potential for injury. Individuals who consistently exhibit unstable joint biomechanics may be at elevated risk for ACL injury and should be selected for muscle-targeted training protocols. Based on the present results, training protocols should focus on coordinating both the strength and timing of the muscle activation with emphasis on the hamstrings and vastus medialis muscles to be most effective.

PCA was used as an exploratory method to identify muscles important to stabilizing the knee during landing. PCA is typically used on large datasets to identify key PCs that explain the variability in the data. Although the sample size of 30 trials is relatively large for a computational modeling study it is on the small side for PCA based studies. Furthermore, using the stability techniques to divide the trials into groups produced a group of three trials. Small groups are not desirable; yet, due to how the stability criteria are used it is impossible to predict the distribution of trials into the stability groups regardless of how large the initial pool is. Despite the small sample size, our test was successful in identifying differences in sagittal and frontal plane kinetics at initial contact and differences in maximum knee abduction moment

between the unstable and stable groups considered to be at high and low risk for ACL injury (Ford et al, 2010; Hewett et al, 2005).Thus we are confident the small group size had a minimal influence on the results.

Our research fills the gap by quantifying dynamic knee stability with the coordinated muscle function analysis. The stability groups classified using Nyquist and Bode stability criteria displayed the same trends in frontal plane kinetics as the literature while quantifying oscillatory behavior only previously described visually. PCA found that the unstable individuals have less balanced co-contraction of their medial and lateral vasti, hamstring and gastrocnemii muscles. Stable individuals have this balance and displayed how the hamstring and gastrocnemii muscles both function to oppose the vasti muscles during the WA phase of landing. The ACL is a dynamic knee stabilizer and these criteria provide a robust metric for assessing joint stability during dynamic movement. Together with PCA this unique methodology provides additional insight into the cause and effect relationship between the musculoskeletal and neuromuscular systems that should be applied to developing ACL screening and muscle-targeted training protocols for at-risk individuals.

4.6 References

Blackburn, J. T., Norcross, M. F., Cannon, L. N., Zinder, S. M., 2013. Hamstrings stiffness and landing biomechanics linked to anterior cruciate ligament loading. Journal of Athletic Training, 48(6).

Boden, B.P., Dean, G.S., Feagin, J.A. Jr., Garrett, W.E. Jr., 2000. Mechanisms of anterior cruciate ligament injury. Orthopedics 23(6), 573-78.

Cochrane, J. L., Lloyd, D. G., Buttfield, A., Seward, H., & McGivern, J., 2007. Characteristics of anterior cruciate ligament injuries in Australian football. Journal of Science and Medicine in Sport, 10(2), 96-104.

Daffertshofer, A., Lamoth, C.J.C., Meijer, O.G., Beek, P.J., 2004. PCA in studying coordination and variability: a tutorial. Clinical Biomechanics 19, 415-28.

Delp, S.L., Anderson, F.C., Arnold, A.S., Loan, P., Habib, A., John, C.T., Guendelman, E., Thelen, D.G., 2007. OpenSim: open-source software to create and analyze dynamic simulations of movement. IEEE Transactions on Biomedical Engineering 54, 1940-50.

Dempsey, A.R., Lloyd, D.G., Elliott, B.C., Steele, J.R., Munro, B.J., Russo, K.A., 2007. The effect of technique change on knee loads during sidestep cutting. Medicine & Science in Sports & Exercise 39(10), 1765-73.

Dempsey, A.R., Elliott, B.C., Munro, B.J. Steele, J.R. and Lloyd, D.G., 2012. Whole body kinematics and knee moments that occur during an overhead catch and landing task in sport. Clinical Biomechanics 27, 466-74.

Donnelly, C. J., Elliott, B.C., Ackland, T.R., Doyle, T.L.A., Besier, T.F., Finch, C.F., Cochrane, J.L., Dempsey, A.R., Lloyd, D.G., 2012. An anterior cruciate ligament injury prevention framework: incorporating the recent evidence. Research in Sports Medicine: An International Journal, 20:3-4, 239-62.

Donnelly, C.J., Elliott, B.C., Doyle, T.L.A., Finch, C.F., Dempsey, A.R., Lloyd, D.G., 2012c. Changes in knee joint biomechanics following balance and technique training and a season of Australian football. British Journal of Sports Medicine 46, 917-22.

Donnelly, C.J., Lloyd, D.G., Elliott, B.C., Reinbolt, J.A., 2012b. Optimizing whole-body kinematics to minimize valgus knee loading during sidestepping: implications for ACL injury risk. Journal of Biomechanics 45, 1491-97.

Dorf, R.C. and Bishop, R.H., 2008. Modern Control Systems. Upper Saddle River, NJ: Pearson Prentice Hall.

Ford, K. R., Myer, G. D., Smith, R. L., Vianello, R. M., Seiwert, S. L., Hewett, T. E., 2006. A comparison of dynamic coronal plane excursion between matched male and female athletes when performing single leg landings. Clinical Biomechanics, 21(1), 33-40.

Ford, K. R., Shapiro, R., Myer, G. D., Van Den Bogert, A. J., Hewett, T. E., 2010. Longitudinal sex differences during landing in knee abduction in young athletes. Medicine and Science in Sports and Exercise, 42(10), 1923-31.

Haggerty, S., Jiang, L. T., Galecki, A., Sienko, K. H., 2012. Effects of biofeedback on secondary-task response time and postural stability in older adults. Gait & Posture, 35(4), 523-528.

Hewett, T. E., Myer, G. D., Ford, K. R., Heidt, R. S., Colosimo, A. J., McLean, S. G., van den Bogert, A. J., Paterno, M.V., Succop, P., 2005. Biomechanical measures of neuromuscular control and valgus loading of the knee predict anterior cruciate ligament injury risk in female athletes A prospective study. The American Journal of Sports Medicine, 33(4), 492-501.

Hur, P., Duiser, B. A., Salapaka, S. M., Hsiao-Wecksler, E. T., 2010. Measuring robustness of the postural control system to a mild impulsive perturbation. Neural Systems and Rehabilitation Engineering, IEEE Transactions on, 18(4), 461-467.

Jolliffe, I.T., 2002. Principal Component Analysis, 2nd Ed Springer, New York.

Koga, H., Nakamae, A., Shima, Y., Iwasa, J., Myklebust, G., Engebretsen, L., Bahr, R., Krosshaug, T., 2010. Mechanisms for noncontact anterior cruciate ligament injuries: knee joint kinematics in 10 injury situations from female team handball and basketball. The American Journal of Sports Medicine, 38, 2218-2225.

Krosshaug, T., Nakamae, A., Boden, B.P., Engebretsen, L., Smith, G., Slauterbeck, J.R., Hewett, T.E., Bahr, R., 2007. Mechanisms of anterior cruciate ligament injury in basketball: video analysis of 39 cases. The American Journal of Sports Medicine, 35, 359-367.

Kuo, B. C., and Golnaraghi, M. F.,2003. Automatic control systems (Vol. 4). New York: John Wiley & Sons.

Lam, M., Daniel, T. F., Yung, P. S., Ho, E. P., Chan, W., Chan K., 2009. Knee stability assessment on anterior cruciate ligament injury: Clinical and biomechanical approaches. BMC Sports Medicine, Arthroscopy and Rehabilitation 1(1), 20-29.

Lee S., Zou, F. Wright, F.A. 2010. Convergence and prediction of principal component scores in high-dimensional settings. The Annals of Statistics 38, 3605-29.

Lloyd, D. G., Buchanan, T. S., 2001. Strategies of muscular support of varus and valgus isometric loads at the human knee. Journal of Biomechanics, 34(10), 1257-1267.

Mantovani, G., Lamontagne, M., Varin, D., Cerulli, G.G. Beaulé, P.E., 2012. Comparison of total hip arthroplasty surgical approaches by principal component analysis. Journal of Biomechanics 45, 2109-15.

McLean, S. G., Lipfert, S. W., van den Bogert, A. J., 2004. Effect of gender and defensive opponent on the biomechanics of sidestep cutting. Medicine and Science in Sports and Exercise, 36(6), 1008-1016.

Mrdakovic, V., Ilic, D. B., Jankovic, N., Rajkovic, Z., Stefanovic, D., 2008. Pre-activity modulation of lower extremity muscles within different types and heights of deep jump. Journal of Sports Science & Medicine, 7(2), 269-78.

O'Connor, K.M and Bottum, M.C., 2009. Differences in cutting knee mechanics based on principal component analysis. Medicine & Science in Sports & Exercise 41(4), 867-78.

Park, S., Horak, F. B., Kuo, A. D., 2004. Postural feedback responses scale with biomechanical constraints in human standing. Experimental Brain Research, 154(4), 417-427.

Riemann, B. L., and Lephart, S. M., 2002. The sensorimotor system, part II: the role of proprioception in motor control and functional joint stability. Journal of Athletic Training, 37(1), 80-84.

Sun, J., Chen, M., and Karimi, K. J., 2008. Aircraft power system harmonics involving single-phase PFC converters. Aerospace and Electronic Systems, IEEE Transactions on, 44(1), 217-226.

Veltri, D.M., Deng, X.H., Torzilli, P.A., Warren, R.F., Maynard, M.J., 1995. The role of the cruciate and posterolateral ligaments in stability of the knee: A biomechanical study. American Journal of Sports Medicine 23(4), 436-43.

Viitasalo, J. T., Salo, A., Lahtinen, J., 1998. Neuromuscular functioning of athletes and non-athletes in the drop jump. European Journal of Applied Physiology and Occupational Physiology, 78(5), 432-440.

Wikstrom, E. A., Tillman, M. D., Schenker, S., Borsa, P. A., 2008. Failed jump landing trials: deficits in neuromuscular control. Scandinavian Journal of Medicine & Science in Sports, 18(1), 55-61.

Withrow, T. J., Huston, L. J., Wojtys, E. M., Ashton-Miller, J. A., 2008. Effect of varying hamstring tension on anterior cruciate ligament strain during in vitro impulsive knee flexion and compression loading. The Journal of Bone & Joint Surgery, 90(4), 815-823.

Wrigley, A.T., Wayne, J.A., Deluzio, K.J., Stevenson, J.M., 2006. Principal component analysis of lifting waveforms. Clinical Biomechanics 21, 567-78.

Yeow, C. H., 2013. Hamstrings and quadriceps muscle contributions to energy generation and dissipation at the knee joint during stance, swing and flight phases of level running. The Knee, 20(2), 100-105.

Zhang, S. N., Bates, B. T., Dufek, J. S., 2000. Contributions of lower extremity joints to energy dissipation during landings. Medicine and Science in Sports and Exercise, 32(4), 812-819.

4.7 Appendix

4.7.1 Nyquist and Bode Stability Analysis

To evaluate knee stability in the sagittal, frontal and transverse planes, a regression analysis utilizing Matlab polyfit and polyval commands were used to develop the time dependent mathematical model to represent the joint kinematics and kinetic waveforms as a function of time. Next the Laplace transform of the time dependent mathematical model was calculated. The Laplace transform is a linear operator that converts the waveform from the time to frequency domain. The open loop transfer function was derived using the kinematic and kinetic waveforms as the output function and an impulse function as the input function. The transfer function served as the inputs for the Nyquist and Bode Stability analyses. Figure 25 provides descriptive plots of stable and unstable systems based on the Nyquist and Bode stability criteria. All of these analyses were performed in Matlab (MATLAB R2012a, The MathWorks, Inc., Natick Massachusetts, USA).
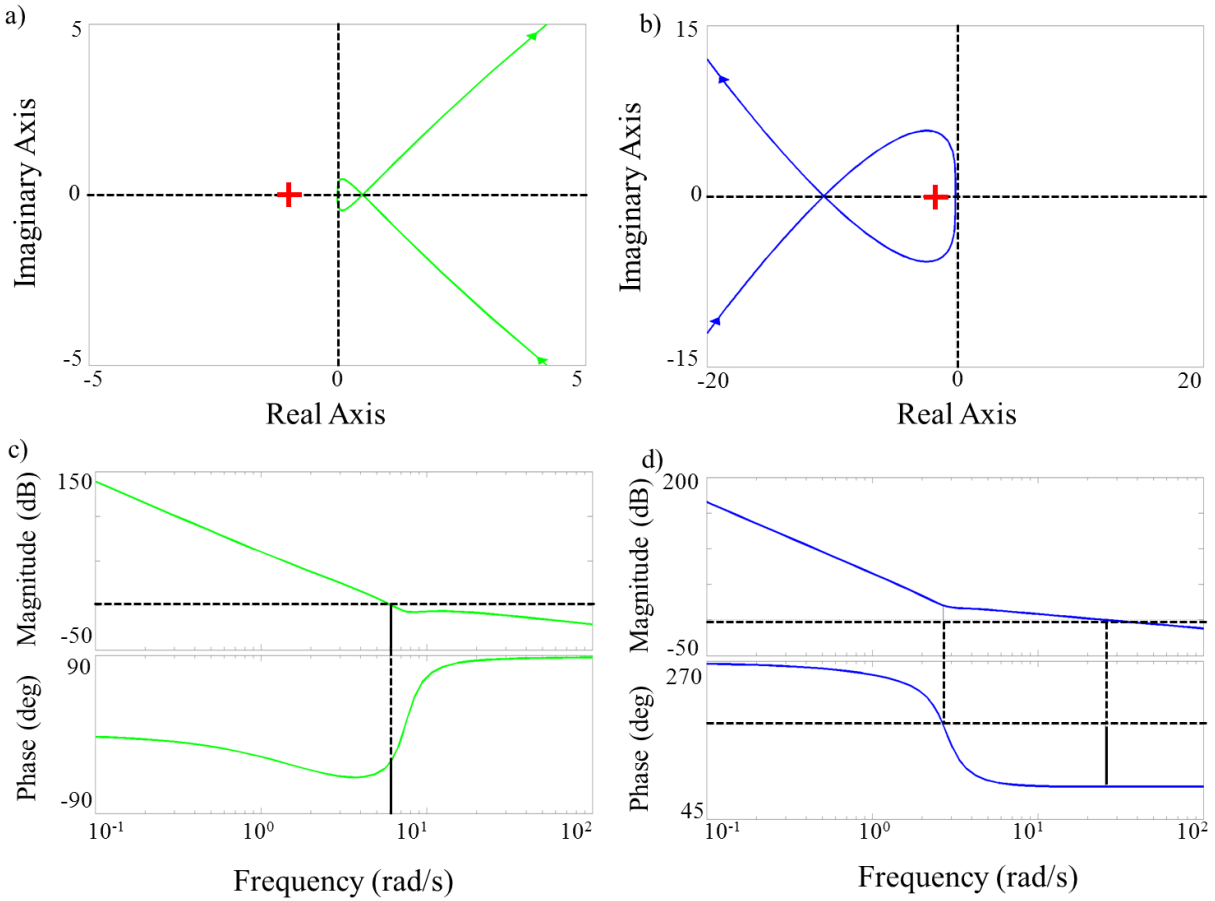
Figure 25. Nyquist and Bode stability plots for stable and unstable joint biomechanics. a) Nyquist stability plot for stable joint biomechanics. b) Nyquist stability plot for unstable joint biomechanics. c) Bode gain and phase margin plots for a stable system. The phase margin was +infinity and the gain margin was 149° at 6.14 rad/s. d) Bode gain and phase margins plots for an unstable system. The phase margin was -20dB at 2.68rad/s and gain margin was -90.2° at 25.6 rad/s.

CHAPTER V

UTILIZING STABILITY AND WAVELET ANALYSES TO DETECT MUSCLE ACTIVATION PATTERNS ASSOCIATED WITH ACL INJURY RISK

5.1 Abstract

An anterior cruciate ligament (ACL) tear is a common knee injury in sports and, despite current prevention research, injury rates are sharply increasing. To better understand the relationship between joint motion and muscle function this study will employ Nyquist and Bode Stability criteria along with wavelet analysis to assess knee joint stability and detect muscle activation strategies unique to individuals at varying risk of ACL injury. Frontal plane knee kinetic data collected from male Australian Football players performing a single-leg jump landing task was used to classify individuals as stable, marginally stable and unstable. The surface EMG data collected during the landing task was analyzed using the Daubechies wavelet analysis to identify muscle activation patterns. Patterns were detected using Hurst exponents and Order Recurrence Plots. The maximum knee abduction moment produced by the unstable group was significantly greater than the maximum knee abduction moments for the marginally stable and unstable groups ($p < 0.001$). Furthermore, the medial and lateral gastrocnemii muscles for the stable group exhibited different muscle activation patterns than the marginally stable and unstable groups. These findings support the use of the Nyquist and Bode stability criteria as an effective tool of assessing knee stability and that wavelet analysis as a valuable means of assessing muscle function.

5.2 Introduction

Recent reports now state that approximately 400,000 anterior cruciate ligament (ACL) injuries occur every year in the United States up from 250,000 seven years ago (Utturkar et al., 2013, Griffin et al., 2006). The last decade has seen the implementation of balance, plyometric and neuromuscular training yet these studies have yielded mixed results as indicated by the increasing ACL injury rates (Chappell et al., 2008; Donnelly et al., 2012a; Myer et al., 2008; Mykleburst et al., 2003). The dramatic increase in ACL injuries rates presents the opportunity for unique approaches to be explored. This study will use techniques from engineering and mathematics to develop a prescreening ACL injury tool and detect muscle activation patterns distinct to individuals with varying risk of ACL injury.

Hausdorff et al. (2007) showed how heart rate outputs reflect the autonomic nervous system regulation (stability) and demonstrated how stride interval could be used to reflect neuromuscular control system stability. This is a simple but powerful way to show how a waveform can be used to describe the performance of an entire system. In this study, frontal plane knee moment waveforms were used to assess the performance of the knee (i.e. knee stability) during single-leg jump landings. This study investigated the neuromuscular control system by analyzing the relationship between knee stability and muscle activation patterns. Deconstructing this relationship could be the key to determining the association between knee joint motion and muscle function with respect to ACL injury.

Hewett et al. (2005) identified knee abduction moment as the strongest predictor of ACL injury as dynamic valgus motion was greater in the ACL injured cohort thus relating dynamic valgus to joint stability. While researchers agree that increasing dynamic valgus motion is linked to joint instability, researchers have not agreed upon a value for which the knee joint instability

(i.e. peak knee abduction moment) puts individuals at risk for ACL injury (Hewett et al., 200; Hewett et al., 2006; Ford et al., 2005; Ford et al., 2010). Control theory is a field that analyzes system dynamics and stability. There stability is a quantifiable measurement of the performance of dynamic systems (Dorf and Bishop, 2008). Nyquist and Bode stability criteria are used to assess the system stability with applications ranging from aircraft to postural stability (Dorf and Bishop, 2008; Hur et al., 2010; Haggerty et al., 2012; Sun et al., 2008). Here these criteria will be used to assess dynamic frontal plane knee stability to classify the time varying frontal plane knee moment waveforms as stable, marginally stable and unstable. The goal is to use the stability criteria as a prescreening ACL injury tool where stable, marginally stable and unstable frontal plane knee waveforms will identify individuals at low, moderate and high- risk for ACL injury. The significance of using these criteria is that the individual's stability is not based on one discrete measurement but the entire frontal plane waveform. Furthermore, an individual's stability is not reliant on how their peak abduction moment (a discrete measurement) compares to the peak abduction moments of individuals in a larger cohort performing the same task. Thus an individual's stability is not a relative measurement based on others' performance.

In the neuromuscular system, the muscles function as dynamic stabilizers providing dynamic restraint of a joint (Riemann and Lephart 2002). Thus it may be possible to deduce a relationship between dynamic knee valgus (i.e. joint motion) and the dynamic knee stabilizers (i.e. muscles). The idea is that once the knee joint motion is classified as stable, marginally stable and unstable, we can analyze muscle activation data to determine if there are activation patterns unique to individuals in these three stability groups. Patterns are prevalent in every aspect of everyday life whether it is financial data or heart rhythms and wavelet analysis is an effective method for identifying said patterns (Ramsey 1999; Chau 2001; Thomasson et al. 2001; Magdy

110

et al., 2013). Wavelet analysis is a preferred method of time series analysis over alternative techniques; such as, Fourier analysis and autoregressive integrated moving average (ARIMA) models, because wavelets preserve both the spatial and temporal components of the original signal, whereas in the case of the Fourier analysis only the frequency component is retained (Dillard 2010). Daubechies wavelet analysis was employed for its event detection and signal discrimination capabilities (Chau 2001; Tamura et al., 1997; Wachowiak et al., 2000). Both the wavelet approximation and detail waveforms will be investigated to detect patterns minimized when EMG data is filtered both within and between the muscles. The Hurst exponent was used to quantify patterns observed in the wavelet results. The Hurst exponent falls under the branch of fractal analysis which analyzes the self-similarity property of time series data to determine if the patterns observed in the data are regressing towards or deviating from a mean (Chau 2001; Hausdorff et al., 1997; Hausdorff et al., 2007; Mitra et al., 2012). This technique has been used in biomechanics and will be useful in detecting underlying trends in EMG data.

While the temporal plots of the wavelet analysis data will be examined to identify abnormalities, an additional technique, Order Recurrence Plots (ORPs), will be used as a method for visually observing the anomalies in the data captured by the Daubechies wavelet analysis. ORPs are used to analyze dynamic systems where the focus is to distinguish between ordered patterns or chaos in the data or determine the point of transition between ordered and chaotic behavior (Marwan et al., 2007). Utilizing ORPs in combination with Daubechies wavelets will allow us to further determine if there are any patterns in the Daubechies approximation and detail data that can be associated with injury risk. In this study, Daubechies wavelet analysis and ORPs were used to explore EMG data for muscle activity abnormalities in the six muscles surrounding the knee.

This study has two objectives. The first is to utilize Nyquist and Bode stability criteria to determine frontal plane knee stability to classify individuals as stable, marginally stable and unstable. The second is to determine muscle activation patterns associated with frontal plane knee joint instability. The results of the three previous Chapters (II-IV) suggest that medial-lateral gastrocnemii imbalance could be related to frontal plane knee instability. Based on those findings it is hypothesized that the Hurst exponent and ORP analysis of the Daubechies wavelet will detect differences in medial-lateral muscle activation in the gastrocnemii muscles in the unstable and marginally stable groups compared to the stable group. The overall goal of this study is to use this information to develop an ACL injury prescreening tool.

5.3 Methodology

5.3.1 Experimental Protocol and Data Collection

Amateur male Western Australian Rules Football players were recruited to complete a single-leg jump landing protocol (Donnelly et al, 2012b). Five athletes (age 20 ± 1 years; height 1.90 ± 0.1m; mass 87.1 ± 5.4kg) were randomly selected from the aforementioned cohort. Six trials were analyzed per each participant; two per each ball swing direction for a total of 30 trials for the subsequent analysis (Donnelly et al., 2012c). For the single-leg jump landing protocol, subjects were instructed to jump from their preferred leg and while in flight, grab an Australian football that was randomly swung medially, laterally or held central to the subjects approach direction before landing on the force platform with their takeoff leg, which was the right leg for all participants (Dempsey et al., 2012). The height of the ball was approximately 90% of each subject's maximal vertical jump height. All of the experimental procedures were approved by the University of Western Australia Human Research Ethics Committee and all subjects provided their informed written consent prior to data collection.

112

Experimental kinematic marker trajectories, GRF, and surface electromyography (sEMG) data were collected from each subject during the single-leg jump landing task. Three-dimensional, full-body kinematics were recorded using a12-camera, 250 Hz VICON MX motion capture system (VICON Peak, Oxford Metrics Ltd., UK) (Donnelly et al., 2012c; Dempsey et al. 2007). The GRF data were synchronously recorded at 2,000 Hz using an AMTI (Advanced Mechanical Technology Inc., Watertown, MA) 1.2 x 1.2m force platform. Both the kinematic and GRF data were low-pass filtered at 20 Hz using a zero phase-shift 4th-order Butterworth digital filter in Workstation (ViconPeak, Oxford Metrics Ltd., UK). sEMG data were collected at 2,000 Hz for six muscles: vastus medialis, vastus lateralis, medial and lateral gastrocnemii and medial and lateral hamstrings. The medial and lateral vasti muscles were measured to represent the quadriceps muscle group. Wavelet analysis was performed on the raw experimental sEMG data.

5.3.2 Subject-Specific Models and Simulations

Five three-dimensional 14-segment, 37 degree-of-freedom (DoF) subject-specific models were created in OpenSim 1.9.1 to generate simulations of the participants performing single-leg jump landings (Fig. 26) (Delp et al. 2007). The knee rotated in all three planes and sagittal and transverse plane translations were modeled as a function of knee angle (Donnelly et al., 2012b, Delp et al., 1990). The model's segment lengths and mass were scaled to each subject. The joint kinematics were calculated from experimental kinematic marker data using inverse kinematics (IK). Residual reduction analysis (RRA) was used to create dynamically consistent simulations with the experimentally recorded ground reaction forces (Donnelly et al., 2012c). These dynamically consistent simulations were analyzed during the weight-acceptance (WA) phase of single-leg jump landing. The WA phase of landing was analyzed since this is the period when

knee valgus and internal rotation moments acting on the knee are the highest and thought to be when the ligament is at the greatest risk of injury (Donnelly et al., 2012a; Dempsey et al., 2007).
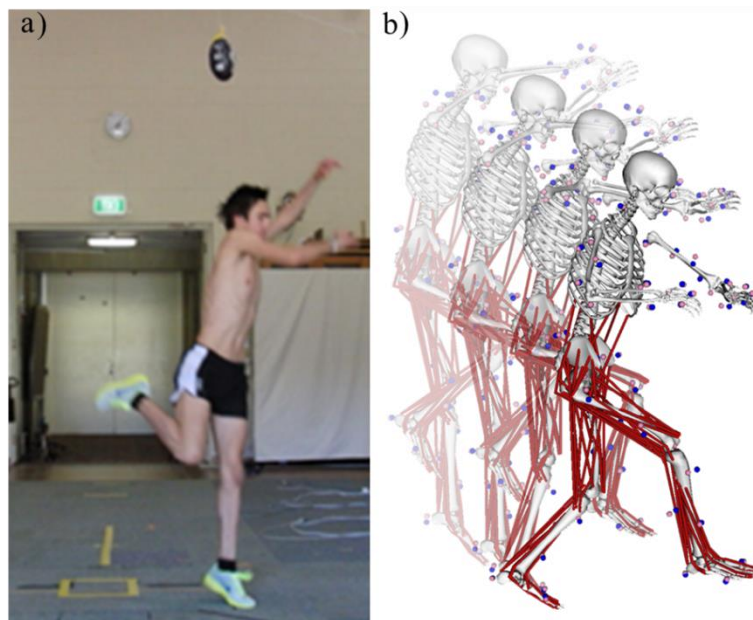
Figure 26. (a) Subject performing the experimental single-leg jump landing protocol in the laboratory. (b) Simulation of single-leg jump landing task using a three-dimensional, 14-segment 37 degrees-of-freedom (DoF) model.

5.3.3 Stability Analysis and Classification

Participant trials were classified as having stable, marginally stable and unstable joint biomechanics using Nyquist and Bode Stability Criteria. A transfer function was needed to perform the Nyquist and Bode stability criteria analyses. A transfer function is the ratio of the systems output to the systems input. To create the transfer function, first a regression analysis of the kinematic and the kinetic sagittal, frontal and transverse knee waveform data was performed to generate a time dependent mathematical model of the waveforms. This time dependent model output was then converted using Laplace transform to develop an open loop transfer function. For the open loop transfer function, the output function was the kinematic and kinetic waveforms while a unit impulse function served as the input function to represent the rapid, jump take-off.

The final analytical step involved evaluating the stability of the open loop model using the aforementioned stability methods.

The Nyquist Stability Criterion employs Cauchy's theorem that maps the output transfer function into the complex plane (Dorf and Bishop, 2008). This theorem determines systems stability based on the poles lying in the right half of the complex plane and the number of encirclements of the point (-1, 0) (Dorf and Bishop, 2008). For those cases where no poles are present in the right half plane, a system is stable if it does not encircle (-1, 0); otherwise it is unstable (Dorf and Bishop, 2008). The Bode stability criterion was used to further delineate a marginally stable group. This approach calculates gain and phase margins that measure the displacement from unstable behavior and estimates critical frequencies in the data, respectively. Positive gain and phase margins indicate stable systems, while negative gain and phase margins indicate an unstable system (Kuo and Golnaraghi 2003). Marginally stable systems were those where one of the gain and phase margins was positive while the other was negative. Participant trials were classified as stable, marginally stable or unstable based on frontal plane kinetic stability analysis as frontal plane biomechanics are predictors of ACL injury risk (Hewett et al. 2005). The means of the sagittal, frontal and transverse plane kinetics were plotted to observe differences between the stability groups. All moments in the study are external moments.

5.3.4 Daubechies 4 Wavelet Transform Analysis

Twenty-eight sEMG data trials collected for the five athletes previously identified and placed into the low-, moderate- and high-risk groups based on the stability analysis. Two trials were lost due to malfunctioning equipment. sEMG waveforms for six of the muscles that cross the knee; which are the vastus medialis, vastus lateralis, medial and lateral hamstrings and medial and lateral gastrocnemii, was analyzed during the WA phase of single-leg jump landing. Daubechies 4

wavelet transform analysis was performed on each waveform to calculate the approximations and details. This process was performed using Matlab (MATLAB R2012a, The MathWorks, Inc., Natick Massachusetts, USA) and is explained in further detail in Appendix 5.7.

5.3.5 Muscle Activation Assessment

The Hurst exponent (H) was computed for the first three wavelet levels for each of the six muscles for all the 28 trials. The Hurst exponent is a value that ranges from 0 to 1. A Hurst exponent between $0 < H < 0.5$ indicates that there is a 'mean reverting' pattern to the data (Mitra 2012). This means that the data will oscillate about a mean. A Hurst exponent closer to zero will indicate that the waveform has strong mean reverting behavior (Mitra 2012). A waveform that exhibits either an increasing or decreasing trend has an H value that lies between 0.5 and 1 ($0.5 < H < 1$). Values closer to 1 indicate a stronger increasing or decreasing behavior. When H equals 0.5 there is no pattern in the data. The mean and range of Hurst exponent for the individual muscles were compared for both the approximation and detail data. A one-way ANOVA and Tukey post-hoc analysis were conducted to compare mean Hurst exponent (H) values for the medial and lateral vasti, hamstrings and gastrocnemii muscles within and across stability groups to detect potential trends in the data ($\alpha = 0.05$). ORPs were generated to visually observe trends in muscle activation patterns between the medial and lateral vasti, hamstring and gastrocnemii muscles. This process was also performed using Matlab (MATLAB R2012a, The MathWorks, Inc., Natick Massachusetts, USA). Details about the Hurst exponent calculation and Order Recurrence Plot generation are explained in Appendix 5.7.

5.4 Results

Three participant trials were classified as exhibiting stable frontal plane joint kinetics while seventeen and ten were found to have marginally stable and unstable kinetics, respectively.

116

Comparisons of the maximum knee abduction moment revealed that the unstable group produced a maximum knee abduction moment of 1.74 ± 0.82 which was significantly greater than the marginally stable (1.20 ± 0.53 Nm/kg) and unstable (0.48 ± 0.35Nm/kg) groups (Fig. 27, Table 14). The marginally stable group displayed a larger knee extension moment than the unstable and stable groups. Differences in knee extension moment were compared at various time points throughout the WA phase of landing; however, none of the differences were significant.
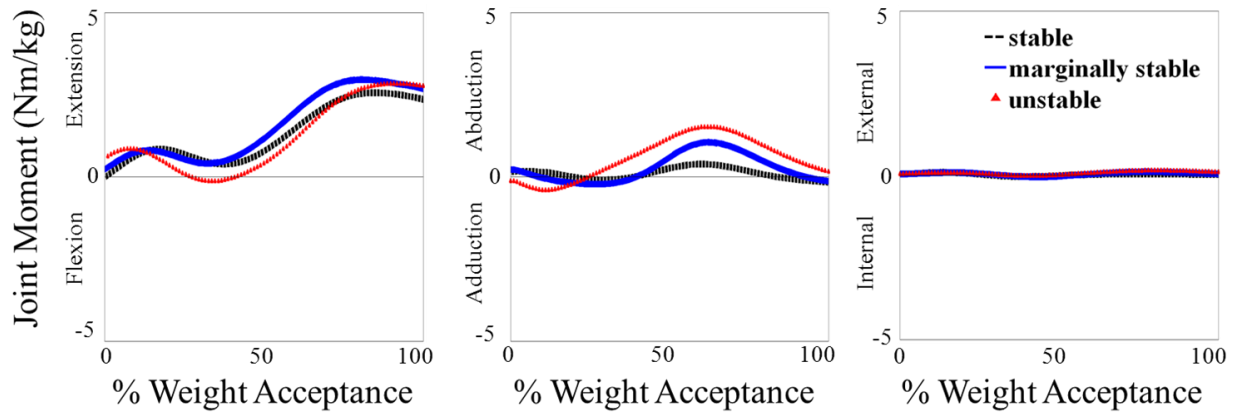
Figure 27. Mean sagittal, frontal and transverse plane knee kinetics (bottom row) of the stable (black dashed line), marginally stable (blue solid line) and unstable (red triangle) groups based on frontal plane knee kinetics during the weight-acceptance phase of single-leg jump landing.

Table 14. Comparison of sagittal, frontal and transverse plane kinetics for the stable, marginally stable and unstable participant groups.

	Stable	Marginally Stable	Unstable
Knee extension/flexion (Nm/kg)			
Maximum extension (+)	2.71±0.36	3.09±0.60	2.93±0.52
Maximum flexion (-)	-0.09±0.35	-0.16±0.54	-0.40±0.58
End WA of phase	2.36±0.68	2.68±0.65	2.78±0.51
Knee abduction/adduction (Nm/kg)			
Maximum abduction (+)	0.48±0.35[a]	1.20±0.53[a]	1.74±0.82[b]
Maximum adduction (-)	-0.34±0.07	-0.52±0.40	-050±0.40
End WA of phase	-0.16±0.18	-0.12±0.37	0.17±0.52
Knee internal/external rotation (Nm/kg)			
Maximum external rotation (+)	0.11±0.04	0.15±0.10	0.20±0.10
Maximum internal rotation (-)	-0.07±0.09	-0.08±0.09	-0.04±0.06
End WA of phase	0.19±0.05	0.04±0.13	0.10±0.10

ANOVA identified a significant difference for the maximums and end of WA phase values of the individual knee kinetics ($p < 0.001$).
Symbols a,b indicate Fisher's adjusted post-hoc difference ($\alpha = 0.05$) in mean kinetics estimates between the stability groups. Estimates with the same letters are not significantly different from each other. Conversely, if estimates do not share a letter, the means are significantly different.

The average Hurst exponent (H) was calculated was calculated for the first three levels for both the approximation and detail wavelets (Fig. 28). The H value for all of the detail wavelets were less than 0.5, which meant they exhibited mean reverting behavior making it difficult to detect muscle activation trends. Thus we focused on the approximation waveforms for the subsequent analysis. The first three approximation wavelet levels revealed that the trends became more pronounced from level 1 to level 3 of the lateral muscles for the stable group compared to the unstable group (Tables 15-17). For the level 3 approximation, the stable group reported lower medial vasti, hamstring and gastrocnemii H values than their lateral counterparts with the largest difference of 0.28 occurring between the vasti muscles. Both the marginally stable and unstable groups reported larger H values for the vastus lateralis compared to the vastus medialis; however, the opposite trend was reported for the hamstrings and gastrocnemii muscles. Comparison of the H values between the six muscles for each approximation level for

all three stability groups found that only significant differences reported were in the stable level

3 approximation data (Table 17).
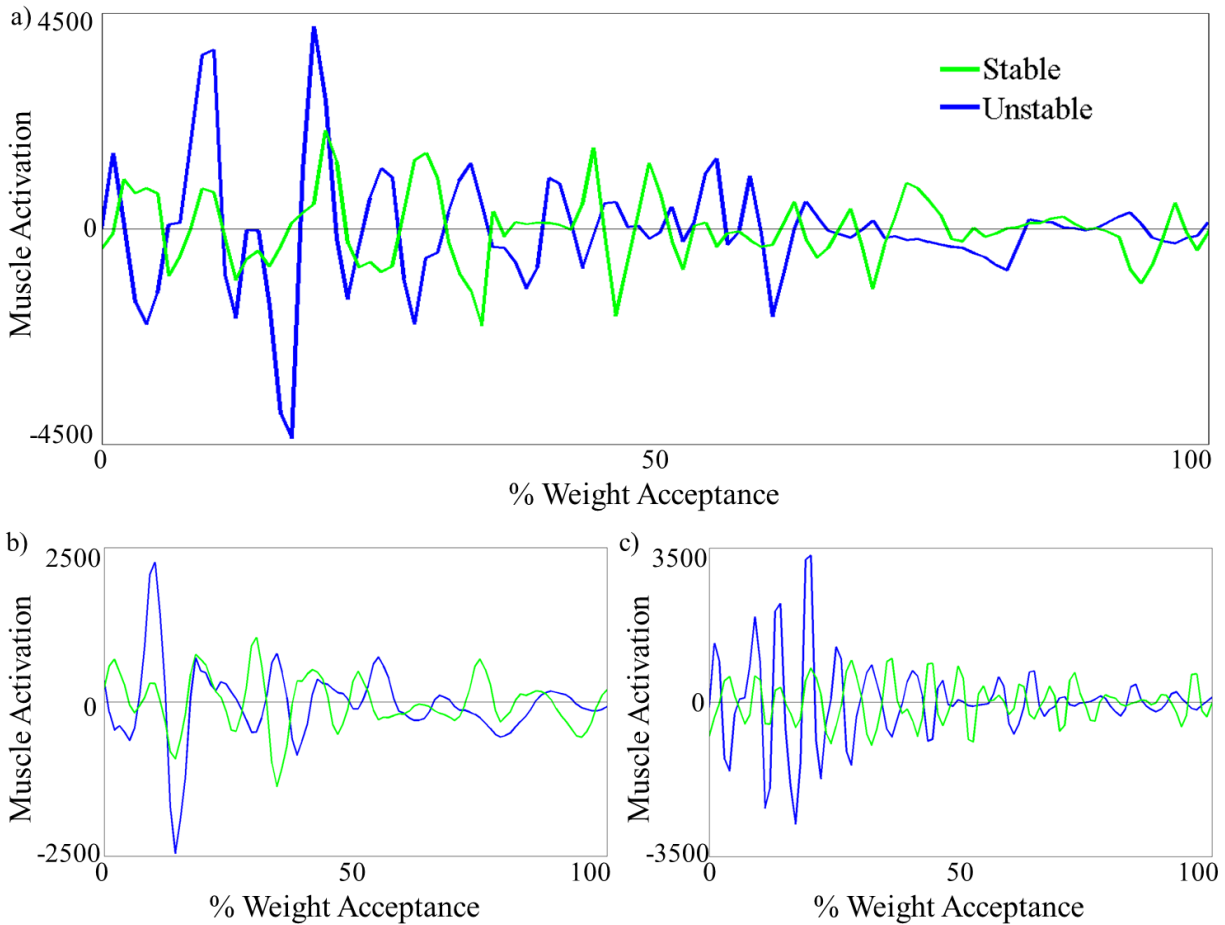
Figure 28. Comparison of a stable and unstable medial gastrocnemius muscle activation waveforms for the weight-acceptance phase of single-leg jump landing. a) Compares the raw muscle activation waveforms. b) Compares the Daubechies 4 approximation level 2 waveforms. c) Compares the Daubechies 4 detail level 2 waveforms. Stable waveforms plotted in green and the unstable in blue.

Table 15. Mean Hurst exponent (H) calculated from the approximation 1 wavelets for the six muscles surrounding the knee.

Stability Groups	Individual Muscles					
	Vastus Medialis	**Vastus Lateralis**	**Medial Hamstring**	**Lateral Hamstring**	**Medial Gastrocnemius**	**Lateral Gastrocnemius**
Stable	0.56 ± **---**	0.78 ± 0.19	0.69 ± 0.08	0.83 ± 0.13	0.53 ± **---**	0.52 ± 0.01
Marginally Stable	0.67 ± 0.11	0.72 ± 0.12	0.74 ± 0.15	0.81 ± 0.19	0.69 ± 0.14	0.80 ± 0.15
Unstable	0.70 ± 0.12	0.72 ± 0.06	0.76 ± 0.15	0.67 ± 0.24	0.72 ± 0.15	0.76 ± 0.24

ANOVA identified a significant difference for the maximum values of the individual muscles ($p < 0.001$; n = 6).
Symbols a,b,c,d,e,f indicate Tukey's adjusted post-hoc difference ($\alpha = 0.05$) in mean maximum muscle force between the individual muscles. Muscles with the same letters are not significantly different from each other. Conversely, if muscles do not share a letter, the means are significantly different.

Table 16. Mean Hurst exponent (H) calculated from the approximation 2 wavelets for the six muscles surrounding the knee.

Stability Groups	Individual Muscles					
	Vastus Medialis	**Vastus Lateralis**	**Medial Hamstring**	**Lateral Hamstring**	**Medial Gastrocnemius**	**Lateral Gastrocnemius**
Stable	0.61 ± **---**	0.79 ± 0.19	0.71 ± 0.04	0.84 ± 0.12	0.61 ± **---**	0.57 ± 0.06
Marginally Stable	0.70 ± 0.06	0.73 ± 0.12	0.73 ± 0.14	0.78 ± 0.19	0.65 ± 0.13	0.77 ± 0.14
Unstable	0.70 ± 0.13	0.69 ± 0.05	0.73 ± 0.16	0.79 ± 0.16	0.72 ± 0.18	0.77 ± 0.22

ANOVA identified a significant difference for the maximum values of the individual muscles ($p < 0.001$; n = 6).
Symbols a,b,c,d,e,f indicate Tukey's adjusted post-hoc difference ($\alpha = 0.05$) in mean maximum muscle force between the individual muscles. Muscles with the same letters are not significantly different from each other. Conversely, if muscles do not share a letter, the means are significantly different.

Table 17. Mean Hurst exponent (H) calculated from the approximation 3 wavelets for the six muscles surrounding the knee.

Stability Groups	Individual Muscles					
	Vastus Medialis	**Vastus Lateralis**	**Medial Hamstring**	**Lateral Hamstring**	**Medial Gastrocnemius**	**Lateral Gastrocnemius**
Stable	0.55 ± 0.03[b]	0.83 ± 0.15[a,b]	0.72 ± 0.12[a,b]	0.90 ± 0.08[a]	0.60 ± 0.08[b]	0.67 ± 0.04[a,b]
Marginally Stable	0.75 ± 0.01	0.72 ± 0.17	0.72 ± 0.17	0.79 ± 0.15	0.69 ± 0.14	0.85 ± 0.10
Unstable	0.70 ± 0.11	0.66 ± 0.10	0.74 ± 0.14	0.77 ± 0.19	0.69 ± 0.17	0.73 ± 0.19

ANOVA identified a significant difference for the maximum values of the individual muscles ($p < 0.001$; n = 6).
Symbols a,b,c,d,e,f indicate Tukey's adjusted post-hoc difference ($\alpha = 0.05$) in mean H values between the individual muscles. Muscles with the same letters are not significantly different from each other. Conversely, if muscles do not share a letter, the means are significantly different.

ORPs for the medial and lateral gastrocnemii muscles for the three stability groups showed that the stable group displayed a larger, ordered, repeating checkerboard block pattern compared to the marginally stable and unstable groups (Fig. 29). The unstable group displayed small patterns accompanied with bowing or wavy behavior at multiple points throughout the image.
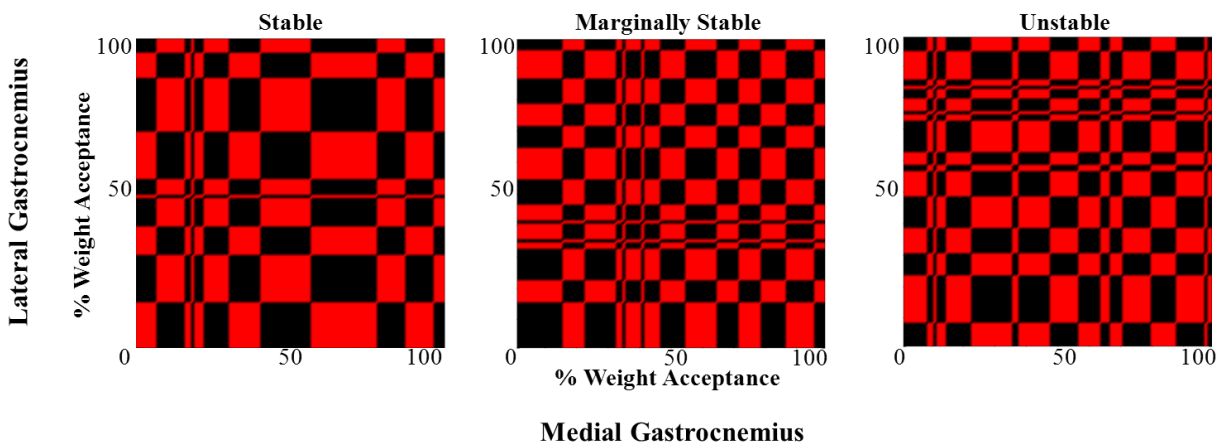
Figure 29. Order recurrence plots (ORPs) comparing the level 3 medial and lateral gastrocnemii approximation wavelets of individuals in the stable, marginally stable and unstable groups.

5.5 Discussion

The comparison of the maximum knee abduction moments between the stability groups found the unstable group reported a significantly greater moment than the stable groups (Fig. 27, Table 14). This finding is consistent with the literature as ACL injured populations produce greater maximum knee abduction moments than uninjured populations (Hewett et al., 2005). This agreement with the literature helps support the implementation of the Nyquist and Bode stability criteria as a means for assessing knee stability.

The Hurst exponent analysis of the Daubechies 4 approximation and detail wavelets identified differences in trend strength between the medial and lateral vasti, hamstring and

121

gastrocnemii muscles for all three stability groups across all three levels. The level 3 results show that the stable group exhibits the largest differences in medial-lateral muscle imbalance for all three muscle groups compared the two other stability groups. Furthermore, the marginally stable and unstable groups display smaller differences in H values between the medial and lateral vasti and hamstring muscles compared to the gastrocnemii muscles. This observation reflects that the medial-lateral gastrocnemii imbalance may be more detrimental to frontal plane stability than the medial-lateral vasti and hamstring imbalance as shown in Chapter III. These findings also support the notion that greater emphasis should be placed on analyzing the role of the gastrocnemii with regards to ACL injury (Mokhtarzadeh et al., 2013; Podraza et al., 2010; Nyland et al., 2010). While the difference in mean H values was larger between the gastrocnemii muscles in the stable compared to the unstable group, if one adds the standard deviation of each value, the range of stable H values is much smaller than the unstable group. Thus it is reasonable to assume that the differences in H values between the medial and lateral gastrocnemii for the participants in the stable group may not be as dramatic as the differences for participants in the unstable group.

The mean H-values were all greater than 0.5 indicates that the muscles were exhibiting either an increasing or decreasing trend. ORPs were used to determine if the trends between the medial and lateral muscles were in the same or opposing directions. The medial-lateral gastrocnemii muscles displayed greater similarity than the in the marginally stable and unstable groups. The larger checkerboard the ORP pattern produced is associated with more ordered data while smaller grain like patterns are associated with more chaotic systems (Thomasson et al., 2001). The bowing in ORPs indicates a change in the systems dynamics. The changing system dynamics may relate to how amplitude and phase shift differences between the medial and lateral

gastrocnemii muscles approximation wavelets increases throughout the WA phase of landing for individuals with unstable joint biomechanics. Since this bowing is present in the later stages of the WA phase for the lateral gastrocnemius approximation wavelet for the unstable trial, it shows how ORPs can detect time dependent changes in muscle activation wavelets that are associated with increased ACL injury risk (Thomasson et al., 2001).

The Hurst exponent is an effective tool in detecting trends or patterns within waveforms but it does not provide information about patterns or similarities between datasets. Future work could investigate using tools like the kendall tau rank correlation coefficient as well to draw relationships between datasets (Bolboaca and Jantschi 2006). However, using the Hurst exponent in conjunction with ORPs enabled us to visually observe similarities amongst the muscles.

The study revealed that the medial and lateral gastrocnemii muscles in stable trials exhibit similar and more ordered muscle activation patterns. These findings in conjunction with the Nyquist and Bode stability criteria serve as a basis for the development of an ACL injury prescreening tool that provides a robust metric for quantifying knee joint stability that is not compared to and/or linked to the performance of another individual. Via these arrays of approaches we have been able to quantify frontal plane knee stability, investigate muscle activation and address strategies specific to each stability group. Future work should focus on additional data mining methods.

5.6 References

Bolboaca, S. D., and Jantschi, L., 2006. Pearson versus Spearman, Kendall's tau correlation analysis on structure-activity relationships of biologic active compounds. Leonardo Journal of Sciences, 5(9), 179-200.

Chappell, J. D., and Limpisvasti, O., 2008. Effect of a neuromuscular training program on the kinetics and kinematics of jumping tasks. The American Journal of Sports Medicine, 36(6), 1081–1086.

Chau, T., 2001. A review of analytical techniques for gait data. Part 2: neural network and wavelet methods. Gait & Posture, 13(2), 102-120.

Daubechies, I., 1990. The wavelet transform, time-frequency localization and signal analysis. Information Theory, IEEE Transactions on, 36(5), 961-1005.

Delp, S.L., Loan, J.P., Hoy, M.G., Zajac, F.E., Topp, E.L., Rosen, J.M., 1990. An interactive graphics-based model of the lower extremity to study orthopaedic surgical procedures. IEEE Trans. Biomed. Eng. 37, 757-767.

Delp, S.L., Anderson, F.C., Arnold, A.S., Loan, P., Habib, A., John, C.T., Guendelman, E., Thelen, D.G., 2007. OpenSim: open-source software to create and analyze dynamic simulations of movement. IEEE Trans. Biomed. Eng. 54, 1940-1950.

Dempsey, A.R., Lloyd, D.G., Elliott, B.C., Steele, J.R., Munro, B.J., Russo, K.A., 2007. The effect of technique change on knee loads during sidestep cutting. Medicine & Science in Sports & Exercise 39(10), 1765-73.

Dempsey, A.R., Elliott, B.C., Munro, B.J. Steele, J.R. and Lloyd, D.G., 2012. Whole body kinematics and knee moments that occur during an overhead catch and landing task in sport. Clinical Biomechanics 27, 466-74.

Dillard, B., 2010. Hey, who turned off the lights?, Chance, Springer. p. 28-37.

Donnelly, C.J., Elliott, B.C., Doyle, T.L.A., Finch, C.F., Dempsey, A.R., Lloyd, D.G., 2012a. Changes in knee joint biomechanics following balance and technique training and a season of Australian football. British Journal of Sports Medicine 46, 917-22.

Donnelly, C.J., Lloyd, D.G., Elliott, B.C., Reinbolt, J.A., 2012b. Optimizing whole-body kinematics to minimize valgus knee loading during sidestepping: implications for ACL injury risk. Journal of Biomechanics 45, 1491-97.

Dorf, R.C. and Bishop, R.H., 2008. Modern Control Systems. Upper Saddle River, NJ: Pearson Prentice Hall.

Ford, K. R., Myer, G. D., Toms, H. E., and Hewett, T. E., 2005. Gender differences in the kinematics of unanticipated cutting in young athletes. Med Sci Sports Exerc, 37(1), 124-129.

Ford, K. R., Shapiro, R., Myer, G. D., Van Den Bogert, A. J., Hewett, T. E., 2010. Longitudinal sex differences during landing in knee abduction in young athletes. Medicine and Science in Sports and Exercise, 42(10), 1923-31.

Griffin, L. Y., Albohm, M. J., Arendt, E. A., Bahr, R., Beynnon, B. D., DeMaio, M., Dick, R.W., Engebretsen, L., Garrett, W. E., Hannafin, J. A., Hewett et al., Huston, L. J., Ireland, M. L., Johnson, R. J., Lephart, S., Mandelbaum, B. R., Mann, B. J., Marks, P. H., Marshall, S. W., Myklebust, G., Noyes, F.R., Powers, C., Shields Jr., C., Shultz, S.J., Silvers, H., Slauterbeck, J., Taylor, D. C., Teitz, C. C., Wojtys, E. M., Yu, B., 2006. Understanding and Preventing Noncontact Anterior Cruciate Ligament Injuries A Review of the Hunt Valley II Meeting, January 2005. Am. J. Sports Med. 34(9), 1512-1532.

Haggerty, S., Jiang, L. T., Galecki, A., Sienko, K. H., 2012. Effects of biofeedback on secondary-task response time and postural stability in older adults. Gait & Posture, 35(4), 523-528.

Hausdorff, J. M., Mitchell, S. L., Firtion, R., Peng, C. K., Cudkowicz, M. E., Wei, J. Y., and Goldberger, A. L., 1997. Altered fractal dynamics of gait: reduced stride-interval correlations with aging and Huntington's disease. Journal of Applied Physiology, 82(1), 262-269.

Hausdorff, J. M., 2007. Gait dynamics, fractals and falls: finding meaning in the stride-to-stride fluctuations of human walking. Human movement science, 26(4), 555-589.

Hewett, T. E., Myer, G. D., Ford, K. R., Heidt, R. S., Colosimo, A. J., McLean, S. G., van den Bogert, A. J., Paterno, M.V., Succop, P., 2005. Biomechanical measures of neuromuscular control and valgus loading of the knee predict anterior cruciate ligament injury risk in female athletes A prospective study. The American Journal of Sports Medicine, 33(4), 492-501.

Hewett, T.E., Myer, G.D., Ford, K.R., 2006. Anterior cruciate ligament injuries in female athletes: Part 1, mechanisms and risk factors. Am. J. Sports Med. 34, 299-311.

Hur, P., Duiser, B. A., Salapaka, S. M., Hsiao-Wecksler, E. T., 2010. Measuring robustness of the postural control system to a mild impulsive perturbation. Neural Systems and Rehabilitation Engineering, IEEE Transactions on, 18(4), 461-467.

Kuo, B. C., and Golnaraghi, M. F.,2003. Automatic control systems (Vol. 4). New York: John Wiley & Sons.

Magdy, A., Saeb, M., Mohamed, A. B., and Khadragi, A.,2013. The Haar Wavelet Transform of the DNA Signal Representation. World Academy of Science, Engineering and Technology,73 667-673.

Marwan, N., Carmen Romano, M., Thiel, M., and Kurths, J., 2007. Recurrence plots for the analysis of complex systems. Physics Reports, 438(5), 237-329.

Mitra, S. K., 2012. Is Hurst Exponent Value Useful in Forecasting Financial Time Series?. Asian Social Science, 8(8).

Mokhtarzadeh, H., Yeow, C.H., Goh, J.C.H., Oetomo, D., Malekipour, F., Lee, P.V.S., 2013. Contributions of the Soleus and Gastrocnemius muscles to the anterior cruciate ligament loading during single-leg landing. J. Biomech. 46, 1913-1920.

Myer, G. D., Chu, D. A., Brent, J. L., and Hewett, T. E., 2008. Trunk and hip control neuromuscular training for the prevention of knee joint injury. Clinics in Sports Medicine, 27(3), 425-448.

Myklebust, G., Engebretsen, L., Braekken, I. H., Skjolberg, A., Olsen, O. E., and Bahr, R., 2003. Prevention of anterior cruciate ligament injuries in female team handball players: A prospective intervention study over three seasons. Clinical Journal of Sports Medicine, 13(2), 71–78.

Nyland, J., Klein, S., Caborn, D.N., 2010. Lower extremity compensatory neuromuscular and biomechanical adaptations 2 to 11 years after anterior cruciate ligament reconstruction. Arthroscopy 26, 1212-1225.

Todd Ogden.,1997. Essential wavelets for statistical applications and data analysis. Springer.

Podraza, J.T., White, S.C., 2010. Effect of knee flexion angle on ground reaction forces, knee moments and muscle co-contraction during an impact-like deceleration landing: implications for the non-contact mechanism of ACL injury. Knee 17, 291-295.

Ramsey, J. B., 1999. The contribution of wavelets to the analysis of economic and financial data. Philosophical Transactions of the Royal Society of London. Series A: Mathematical, Physical and Engineering Sciences, 357(1760), 2593-2606.

Riemann, B.L., Lephart, S.M., 2002. The Sensorimotor System, Part II: The Role of Proprioception in Motor Control and Functional Joint Stability. Journal of athletic training 37, 80-84.

Sun, J., Chen, M., and Karimi, K. J., 2008. Aircraft power system harmonics involving single-phase PFC converters. Aerospace and Electronic Systems, IEEE Transactions on, 44(1), 217-226.

Tamura T, Sekine M, Ogawa M, Togawa T, and Fukui Y., 1997.Classification of acceleration waveforms during walking by wavelet transform. Methods of Information in Medicine, 36, 356–359.

Thomasson, N., Hoeppner, T. J., Webber Jr, C. L., and Zbilut, J. P., 2001. Recurrence quantification in epileptic EEGs. Physics Letters A, 279(1), 94-101.

Utturkar, G. M., Irribarra, L. A., Taylor, K. A., Spritzer, C. E., Taylor, D. C., Garrett, W. E., and DeFrate, L. E., 2013. The effects of a valgus collapse knee position on in vivo ACL elongation. Annals of biomedical engineering, 41(1), 123-130.

Wachowiak MP, Rash GS, Quesada PM, and Desoky AH., 2000. Wavelet based noise removal for biomechanical signals: a comparative study. IEEE Transactions on Biomedical Engineering 2000;47(3):360–8.

Walker, J.S., A primer on wavelets and their scientific applications. 2008: CRC Press.

5.7 Appendix

5.7. 1 Daubechies 4 Wavelet Transform Generation

Daubechies wavelet was developed by Ingrid Daubechies (1990). Daubechies 4 approximation (*a*) and detail (*d*) waveforms are generated by computing the scalar product of the original waveform (*f*) with the scaling $\left(V_m^1\right)$ and mother wavelet functions $\left(W_m^1\right)$, respectively (Eqs. 5.1-5.2). The scaling and wavelet functions are expressed in terms of their Fourier transforms (Eqs. 5.3.-5.4).

$$a^1 = f \cdot V_{N/2}^1 = \left(fV_1^1, fV_2^1, fV_3^1, ..., fV_{N/2}^1\right) \quad (5.1)$$

$$d^1 = f \cdot W_{N/2}^1 = \left(fW_1^1, fW_2^1, fW_3^1, ..., fW_{N/2}^1\right) \quad (5.2)$$

$$\varphi(\omega) = -e^{-\frac{i\omega}{2}} m_o\left(\frac{\omega}{2} + \pi\right) \hat{\phi}\left(\frac{\omega}{2}\right) \quad (5.3)$$

$$\hat{\phi}(\omega) = \frac{1}{\sqrt{2\pi}} \prod_{j=1}^{\infty} m_o\left(2^{-j}\omega\right) \quad (5.4)$$

5.7.2 Hurst Exponent (H) Calculation

The Hurst exponent (H) calculation is a multistep process. First the time series mean and standard are calculated and the former is subtracted from the waveform to create a mean adjusted series. Next the cumulative deviate of this mean adjusted series is calculated and the series range determined. A rescaled range is calculated using the series range and standard deviation results. The log of the ratio of the rescaled range to standard deviation metric is plotted against the log of the time series length. The slope of the resulting linear plot is the Hurst exponent (H) (Mitra 2012).

5.7. 3 Order Recurrence Plots (ORPs) Analysis

ORPs are used to analyze dynamic systems to distinguish between ordered patterns or chaos in the data and can determine the point of transition between ordered and chaotic behavior (Marwan et al., 2007). ORPs were created for the Daubechies 4 approximations of the medial and lateral vasti, hamstring and gastrocnemii muscles data. These ORPs were calculated using Equations (5.5) and (5.6) (Marwan et al., 2007) and results in a displayed of containing black and red boxes.

$$R_{i,j}(\varepsilon) = \Theta\left(\varepsilon - \left\|\vec{x}_i - \vec{x}_j\right\|\right), \quad i, j = 1,...,N, \quad (5.5)$$

N = number of measured points of $\vec{x}_i$

Θ = heaviside function

ε = threshold or cut off distance

$\left\|\cdot\right\|$ = norm

$$R_{i,j}(\varepsilon) = \begin{cases} 1 : \left\|\vec{x}_i - \vec{x}_i\right\| \le \varepsilon \\ 0 : otherwise \end{cases} \quad \vec{x}_i \in R^d, i, j = 1,...,N, \quad (5.6)$$

128

CHAPTER VI

CONCLUSION

6.1 Significance of Research

Effective non-contact ACL injury intervention programs have the enormous potential to drastically reduce the incidence of ACL injuries in active populations. However, improving the effectiveness of training programs is challenging because the cause-effect relationship between muscle function and joint biomechanics with respect to ACL injury is not well understood. Dynamic simulations provide the capability to determine the functional roles of individual muscles, which is essential to elucidating this relationship. Utilizing dynamic simulations helps to determine the biomechanical factors that influence knee motion to discern the cause of ACL injury. We anticipate that the insights gained from this work will provide new guidelines for designing ACL injury prevention programs resulting in a significant drop in ACL injuries.

Models and computational tools developed will find broad applications. Numerous studies have been performed to record neuromuscular excitation patterns, understand muscle contraction dynamics, characterize musculoskeletal geometry, and quantify multijoint movement kinematics. However, linking the detailed knowledge of these elements of the neuromusculoskeletal system to create an integrated understanding of normal and disordered movement remains a major challenge in the application of biomechanics to a wide range of biomechanics problems and basic science research.

This work developed methodologies for interpreting the dynamic functions of muscles during movement, generated novel data mining approaches to undercover the ACL injury mechanism, and provided a general computational framework for pursuing further research. The

simulations were developed in freely available musculoskeletal modeling and simulation software, which enables these results to be shared with other research groups. Over the past two years, there have been over 60,000 downloads of models, simulations, and software from the project's website (see simtk.org/home/opensim) with over 9,000 active users of these freely available biomechanics tools. This project adds to this development and will further highlight the need for additional studies of the neuromuscular biomechanics of persons at high risk for ACL injury.

6.2 Research Innovation

The principles that govern the relationships between muscles contributions and purposeful movement in individuals during single-leg jump landings have not been uncovered. For decades, experimental approaches have advanced our understanding of biomechanics. However, the inability to experimentally measure muscle forces and identify the cause-effect relationships (i.e. muscle contributions to movement) between muscle forces and joint biomechanics has limited research progress. The difficulty in determining an individual muscles' contribution to movement stems from the fact that muscles accelerate joints that they do not span and body segments to which they are not attached. Thus to determine a muscles contribution to movement required a novel approach driven by the use of a unique set of tools to accomplish this task.

Muscle-actuated dynamic simulations provide a scientific framework, in combination with complementing experimental approaches for estimating important variables and identifying cause-and-effect relationships. In this study, muscle-actuated dynamic simulations, data mining and motion capture analysis were used to bridge the gap in our understanding of human movement.

130

This work advanced basic knowledge and understanding in this arena. It meshed the experimental capabilities of physicians, physical therapist, and rehabilitation scientists with the computer simulation capabilities of engineers, mathematicians, and computer scientist to address important (biomechanical) research questions. An added benefit of this research was that the development of subject-specific models was done using freely available open source software. Such results that are readily shared will hopefully accelerate the understanding of the underlying mechanisms behind injuries and movement disorders.

6.3 Fundamental Contributions

The objective of this research was to determine individual muscle force contribution to single-leg jump landing, assess how muscles function to support the knee against elevated abduction moment, identify individuals at risk for ACL injury and their associated muscle function to develop a muscle-targeted training ACL injury prevention program to mitigate ACL injury risk. The work presented here was able to accomplish all of these objectives.

Computed muscle control and induced acceleration analysis are techniques that have been previously used to study muscle contribution to walking and running. However, the novelty of their use in this work was in the development of the subject-specific models and application of these tools to investigate ACL injury risk. Models have to be tailored based on the research question being asked. Because ACL injuries are often the result of the combined loading of the ligament in all three planes, the model had to include a knee that allowed for such movement. Significant thought and time was spent adjusting this knee model to account for frontal plane knee rotation while also including torque actuators to represent the ligament and muscle forces that eliminated unrealistic joint motion in that plane. In addition, the decision to increase the models muscle forces uniformly by 60% was significant because all too often muscle forces are

131

increased at random per the researcher's discretion. This makes cross study comparisons of muscle force generation results difficult. This is a legitimate problem in this research and highlights a need for the development of an agreed upon standard for modifying maximum isometric muscle force. Furthermore, the use of both CMC and IAA to investigate muscle contributions in single-leg jump landings is relatively new; despite the fact that decades of research has shown that nearly half of all non-contact injuries are the result of single-leg jump landing (Cochrane et al., 2007; Laughlin et al., 2011; Mokhtarzadeh et al., 2013). The implementation of these tools for investigating single-leg jump landing with respect to ACL injury is an important step in ACL research. The results showed that greater emphasis should be placed on gastrocnemii muscles for their role in supporting the knee during single-leg jump landing and working to counterbalance the force produced by the quadriceps. More specifically, IAA quantified that the medial gastrocnemii was the greatest contributor to resisting knee abduction and internal rotation during single-leg jump landing while both the medial and lateral gastrocnemii have the potential to increase knee flexion during landing all of which can reduce ACL injury risk. These results suggest that the gastrocnemii play a significant role in stabilizing and supporting the knee and help oppose the quadriceps. Such results may affect how researchers develop ACL injury prevention programs and could potentially change the direction of ACL research.

Data mining is a technique that draws from many different fields to detect patterns within large datasets. Its name denotes the exploratory nature of this research area and it was used in this work to explore and discover patterns within biomechanical data. Principal component and wavelet analyses were used to identify critical features in surface EMG data associated with

potential ACL injury risk. PCA identified the gastrocnemii muscle activation as a source of variability between stable and unstable individuals while wavelet analysis found that strong muscle patterns between the gastrocnemii muscles were associated with individuals with stable frontal plane joint kinetics. Neither of these findings would have been obtained without the implementation of the Nyquist and Bode stability criteria. Drawing from control theory, these techniques were able to effectively classify individuals as exhibiting stable, marginally stable and unstable joint biomechanics with the potential to characterize these individuals as being at low-, moderate- and high risk for ACL injury. The significance of using stability for this application is that it provides researchers with a robust metric for classifying ACL injury risk that is independent of others' joint biomechanics. Thus a researcher could bring one individual into their laboratory and after running a few trials could assess their risk for ACL injury that day without having to perform the same test on a larger cohort of individuals to gain insight about their risk for injury. This application of stability in this context has not been previously explored. A seminal benefit of this work was that the classification of individuals into the stable, marginally stable and unstable populations and its impact on devising muscle activation strategies and/or patterns within these groups using PCA and wavelet analysis.

Musculoskeletal models and computational tools are critical in biomechanics research as they allow researchers to evaluate the causal relationship between joint movement and muscle function. The key contributions of this work was the creation of subject-specific dynamic simulations that assessed individual muscles contribution to ACL injury while developing unique methodologies for classifying joint stability and identifying muscle activation patterns distinct to individuals at varying levels of ACL injury risk. Both of these contributions can be used to

develop more effective muscle-targeted ACL injury intervention and prescreening tools to help reduce ACL injury rates.

6.4 Summary

All four studies found that the gastrocnemii muscles played a greater role in joint stability than previously believed. The CMC analysis indicated that the gastrocnemii generated forces comparable to the quadriceps muscles to help resist excessive sagittal plane motion while IAA results found the medial gastrocnemii was the strongest contributor to flex and adduct the knee which could help reduce the load exerted on the ACL. Similarly, the results of the data mining studies concluded that gastrocnemii muscle activation variability was associated with joint stability while the gastrocnemii muscles displayed comparable activation patterns in the stable trials.

The results of these studies can be used to develop muscle-targeted ACL training intervention and prescreening programs. The results of the dynamic simulation based studies (Chapters II and III) can be used for the muscle targeted ACL training intervention program. And the findings from the data mining studies (Chapters IV and V) could be used to develop an ACL injury prescreening tool. The findings of the latter studies are more preliminary. The development of an effective ACL injury prescreening could have a significant impact on reducing ACL injury rates. The methodologies developed in this work have been successful in quantifying joint stability and have begun to identify critical patterns within the muscles via the Hurst exponent and ORPs. Additional work is still needed to define the exact combination of Hurst exponents and/or exact pattern in the ORP that signals potential ACL injury. Future work should focus on analyzing sEMG data using ORPs with a moving window to detect time dependent ORP changes and their connection with muscle activations and joint stability.

This work was successful in investigating the relationship between joint biomechanics and muscle function with respect to ACL injury and how these findings may have a significant impact on ACL research.

6.5 Glossary

Abduction	Movement where the limb moves away from the midline of the body.
Acceleration	The rate of change of velocity. Measure of the change in a body's velocity.
Adduction	Movement where the limb moves toward the midline of the body
Anterior	Refers to the front of the body.
Anterior cruciate ligament	It is one of four ligaments in the knee that connects the femur to the tibia. It attaches from the anterior surface of the midtibial plateau to the distal notch on the femur.
Biceps femoris longus	One of the lateral hamstring muscles. It functions to flex the knee.
Bode stability criterion	A technique used to assess the stability of a system. Stable systems have positive gain and phase margins while unstable systems have negative gain and phase margins.
Center of mass	The point about which a body's mass is equally distributed.
Computed muscle control	An algorithm that uses optimization to estimate individual muscle excitation during dynamic movements.
Condyle	The round projection or prominence on a bone.
Daubechies wavelet	A wavelet transform similar to the Haar wavelet that is generated by calculating the scalar product of the running averages and differences with the scaling signals and wavelets, respectively.
Degree of freedom	A single coordinate of relative motion between two bodies. Such a coordinate responds without constraint or imposed motion to externally applied forces or torques. For translational motion, a DOF is a linear coordinate along a single direction. For rotational motion, a DOF is an angular coordinate about a single, fixed axis.
Distal	The more distant of two or more objects with respect to the origin or point of reference.
Dorsiflexion	The motion that occurs when the toes move up toward the tibia.
Extension	Movement that moves two limbs farther apart, increasing the angle between them, which occurs in the sagittal plane.
External Rotation	Motion that rotates away from the midline of the body.
Femur	The bone that is located between the hip and knee joints.

Flexion	Movement that moves two limbs closer together, reducing the angle between them, which occurs in the sagittal plane.
Force	An action or effect applied to the body that tends to produce acceleration.
Force plate	A transducer that is set in the floor to measure about some specified point, the force and torque applied by the foot to the ground. These devices provide measures of the three components of the resultant ground reaction force vector and the three components of the resultant torque vector.
Forward dynamics	Utilizes know known forces and torques to calculate motion.
Frontal plane	This is one of three planes used to divide and describe the body. This plane separates the anterior and posterior sections of the body. Knee adduction-abduction occurs in this plane.
Generalized coordinates	A set of coordinates (or parameters) that uniquely describes the geometric position and orientation of a body or system of bodies. Any set of coordinates that are used to describe the motion of a physical system.
Ground reaction force	The force exerted by the ground that is equal and opposite to a force applied to the ground by an impacting object (e.g. foot).
Haar wavelet	A simple wavelet that is used to transform the data into two wavelets that are half of the original signal called the trend and fluctuation to analyze these wavelets for hidden patterns in the data.
Hurst exponent	A metric for calculating the 'self-similarity' property of a time series.
Induced acceleration analysis	Determines the accelerations caused or "induced" by individual muscle forces acting on a model (e.g., contribution of muscle forces to knee accelerations).
Inferior	Refers to the lower or bottom half of a structure or body.
Injury	Describes damage to the tissue caused by physical trauma.
Internal rotation	Motion that rotates toward the midline of the body.
Inverse kinematics	A process that derives joint angles from experimental marker data.
Joint stability	The ability of a joint to resist dislocation and maintain an appropriate functional position throughout its range of motion.
Kinematics	Describes movement without regard to the forces involved.
Kinetics	Describes movement with regard to the forces involved.

Knee adduction-abduction	Motion of the long axis of the shank within the frontal plane as seen by an observer positioned along the anterior-posterior axis of the thigh.
Knee flexion-extension	Motion of the long axis of the shank within the sagittal plane as seen by an observer positioned along the medial-lateral axis of the thigh.
Knee internal-external rotation	Motion of the medial-lateral axis of the shank with respect to the medial-lateral axis of the thigh within the transverse plane as viewed by an observer positioned along the longitudinal axis of the shank.
Laplace Transform	Technique that converts a signal from the time to frequency domain.
Lateral	Located away from the midline or center of the body.
Lateral gastrocnemius	One of the muscles that makes up the calf muscle complex. It lies on the lateral side of the posterior portion of the tibia. It functions to plantarflex the foot and flex the knee.
Medial	Refers to the midline or center of the body.
Medial gastrocnemius	One of the muscles that makes up the calf muscle complex. It lies on the medial side of the posterior portion of the tibia. It functions to plantarflex the foot and flex the knee.
Moment	The effect of a force that tends to rotate or bend a body or segment.
Newton	Unit of force (N).
Nyquist stability criterion	A technique used to assess the stability of a system. When there are no poles in the right half plane systems are stable if (-1, 0) is not encircled and unstable if (-1,0) is encircled.
Order recurrence plot	Is a unique plot that displays the underlying behavior of a dynamical system in phase space.
Plantarflexion	The motion that occurs when the toes away from the tibia.
Posterior	Refers to the back plane of the body.
Principal component analysis	A statistical technique that reduces large high-dimensional datasets to a smaller subset of orthogonal vectors called principal components to identify patterns within the data.
Proximal	The closer of two or more objects with respect to the origin or point of reference.
Rectus femoris	It is one of the quadriceps muscles that resides in the middle of the thigh functions to extend the knee.

Residual reduction analysis	A process that employs forward dynamics to create a simulation that recreates the inverse kinematic motion using torques actuators acting at/on the joints to create dynamically consistent models.
Sagittal plane	One of three planes used to divide and describe the body. This plane divides the right and left halves of the body. Knee flexion-extension occurs in this plane.
Semimembranosus	A medial muscle located in the hamstring. It is more medial than the semitendinosus muscle. It functions to flex the knee.
Semitendinosus	A medial muscle located next to the semimembranosus in the hamstring. It functions to flex the knee.
Single-leg jump landing	Describes when an individual lands solely on one leg after an initial jump or hop.
Soleus	It is one of the muscles that makes up the calf muscle. It functions to plantarflex the foot.
Superior	Refers to the upper or top half of a structure or body.
Tibia	One of two bones located between the knee and ankle joint.
Transverse plane	One of three planes used to divide and describe the body. This plane dives the superior and inferior halves of the body. Knee internal-external rotation occurs in this plane.
Torque	The effect of a force that tends to cause a rotation or twisting about an axis.
Valgus	Medial deviation of a joint (e.g., knock-kneed).
Varus	Lateral deviation of a joint (e.g., bowlegged).
Vastus Intermedius	It is one of the quadriceps muscles. It stretches from the front to lateral portion of the femur. It functions to extend the knee.
Vastus Lateralis	It is the largest of the quadriceps (i.e. thigh) muscles. It is the most lateral of the quadriceps muscles and functions to extend the knee.
Vastus Medialis	It is the medial quadriceps muscle and functions to extend the knee.
Velocity	The rate of change of position of an object.
Wavelets	They are waveforms of varying duration, extracted from an original signal, that retains hidden information or patterns that may not be apparent in the original signal.
Weight-acceptance phase	Defined as the time from the initial heel strike to the first trough in the ground reaction force profile.

VITA

Kristin Denise Morgan was born March 19, 1985 in Albany, New York. She graduated from Hampton Roads Academy, Newport News, Virginia in 2003. She received her Bachelors of Science in Biomedical Engineering from Duke University, Durham, North Carolina in 2007, a Master's in Biomedical Engineering from Virginia Commonwealth University, Richmond, Virginia in 2009, before pursuing her PhD at the University of Tennessee in 2010.